

**Proteome studies on leaf peroxisomes from  
*Spinacia oleracea* L. and *Arabidopsis thaliana* (L.) Heynh.**

Dissertation  
zur Erlangung des Doktorgrades  
der Mathematisch-Naturwissenschaftlichen Fachbereiche  
der Georg-August-Universität zu Göttingen

vorgelegt von  
Lavanya Babujee  
aus Chennai, Indien

Göttingen 2004

D7

Referent: Prof. Dr. Hans-Walter Heldt

Korreferent: Prof. Dr. Ivo Feussner

Tag der mündlichen Prüfung:

1. INTRODUCTION	
1. Introduction	1
1.1. The role of peroxisomes in plant metabolism	1
1.1.1. Photorespiration	1
1.1.2. Fatty acid degradation	3
1.1.3. Metabolism of reactive oxygen species	4
1.2. Targeting of proteins to peroxisomes	7
1.3. Analysis of the protein content of peroxisomes	8
1.3.1. Resolution of peroxisomal proteins	9
1.3.2. Identification of individual peroxisomal proteins	10
1.3.2.1. Peptide mass fingerprinting (PMF)	11
1.3.2.2. Protein identification based on peptide sequences	12
1.4. The peroxisomal proteome and the choice of the model plant	13
1.5. Objectives of the present investigation	14
2. Material and methods	15
2.1. Plant material	15
2.1.1. <i>Spinacia oleracea</i> L.	15
2.1.1.1. Normal growth conditions	15
2.1.1.2. Stress treatments	15
2.1.1.2.1. Light stress	15
2.1.1.2.2. Oxidative stress	16
2.1.2. <i>Arabidopsis thaliana</i> (L.) Heynh.	16
2.1.2.1. Normal growth	16
2.1.2.2. Stress treatment: Cold treatment of <i>Arabidopsis</i> plants	16
2.2. Isolation of leaf peroxisomes	17
2.2.1. Isolation of leaf peroxisomes from <i>Spinacia oleracea</i> L.	17
2.2.1.1. Preparative method	17
2.2.1.2. Analytical method	20
2.2.2. Isolation of leaf peroxisomes from <i>Arabidopsis</i>	21
2.3. Estimation of intactness of the isolated peroxisomes by sedimentation	23
2.4. Enrichment of core particles	23
2.5. Biochemical analysis of subcellular fractionation	24
2.5.1. Determination of enzyme activities	24
2.5.1.1. Hydroxypyruvate reductase (HPR) ( <i>adapted from Titus et al., 1983</i> )	24
2.5.1.2. Fumarase ( <i>adapted from Titus et al., 1983</i> )	25
2.5.1.3. NADP <sup>+</sup> -dependent glyceraldehyde-3-phosphate dehydrogenase ( <i>Wirtz et al., 1983</i> )	25
2.5.2. Chlorophyll ( <i>Arnon, 1949</i> )	26
2.6. Protein determination	27
2.6.1. The Lowry Method ( <i>Lowry et al., 1951</i> )	27
2.6.2. Protein determination using Bradford's reagent ( <i>Bradford, 1976</i> )	28
2.7. Protein precipitation ( <i>Wessel and Fluegge, 1984</i> )	28
2.8. Two-dimensional gel electrophoresis	29
2.8.1. Solubilization of proteins	29
2.8.2. Removal of insoluble material	30
2.8.3. Rehydration of immobiline pH gradient (IPG) gel strips	30
2.8.4. Isoelectric Focusing	30
2.8.5. Equilibration of focused IPG strips	31

2.8.6. Second dimension sodium dodecylsulfate polyacrylamide gel electrophoresis .....	32
2.8.7. Electrophoresis conditions .....	33
2.9. Sodium dodecyl sulphate polyacrylamide gel electrophoresis (SDS-PAGE)....	34
2.10. Post-electrophoretic staining of proteins in acrylamide gels .....	36
2.10.1. Silver Staining.....	36
2.10.1.1. Method 1: Analytical purposes ( <i>Blum et al., 1987</i> ):.....	37
2.10.1.2. Method 2: Compatible with mass spectrometric analyses .....	38
2.10.2. Coomassie staining .....	39
2.10.2.1. Normal method .....	39
2.10.2.2. Colloidal Coomassie ( <i>Herbert et al., 2001</i> ).....	39
2.11. Documentation .....	40
2.12. Gel Drying.....	40
2.13. Preparation of samples for Mass Spectrometric Analysis.....	41
2.13.1. Excision of protein spots from gels .....	41
2.13.2. Destaining silver stained spots .....	41
2.13.3. In-gel tryptic digestion ( <i>adapted from Shevchenko et al. 1996</i> ) .....	41
2.13.4. Extraction of peptides .....	42
2.13.5. A modified in-gel digestion protocol for automated application .....	42
2.13.6. Zip-Tip purification prior to mass spectrometry .....	43
2.14. Mass Spectrometric Analysis.....	43
2.14.1. Matrix-assisted laser desorption ionization mass spectrometry (MALDI-MS)	43
2.14.2. Liquid chromatography tandem mass spectrometry (LC-MS/MS) .....	44
2.15. Phosphoprotein enrichment by phosphate metal affinity chromatography (PMAC) .....	45
2.15.1. Equilibration of the phosphoprotein enrichment column .....	45
2.15.2. Solubilization of proteins.....	45
2.15.3. Clarification of sample .....	46
2.15.4. Binding of phosphorylated proteins .....	46
2.15.5. Removal of non-phosphorylated proteins .....	46
2.15.6. Elution of phosphorylated proteins .....	46
2.16. Methods used for molecular biology .....	47
2.16.1. RNA isolation .....	47
2.16.2. Estimation of nucleic acids .....	47
2.16.2.1. Photometric method .....	47
2.16.2.2. Gel-electrophoretic method .....	47
2.16.3. Agarose gel electrophoresis .....	48
2.16.4. Staining.....	49
2.16.5. Documentation .....	49
2.16.6. Synthesis of cDNA by RT reaction.....	49
2.16.7. Oligonucleotide primers.....	49
2.16.8. Polymerase Chain Reaction (PCR) .....	50
2.16.9. Elution of resolved nucleic acid fragments from agarose gel.....	52
2.16.10. Ligation into pGEM®-T Easy vector .....	52
2.16.11. Transformation of <i>E. coli</i> competent cells .....	53
2.16.12. Colony PCR.....	54
2.16.13. Isolation of plasmid DNA .....	55
2.16.14. Restriction digest .....	55

2.16.15. Sequencing.....	55
2.16.16. Precipitation of DNA .....	56
2.17. Biochemicals .....	57
2.18. Kits.....	57
2.19. Bacterial strain.....	57
3. Results.....	58
3.1. Isolation of leaf peroxisomes from <i>Spinacia oleracea</i> L. and <i>Arabidopsis thaliana</i> (L.) Heynh.....	58
3.1.1. Improvement of the purity of leaf peroxisomes from <i>Spinacia oleracea</i> L... 59	
3.1.1.1. A preparative method for isolating leaf peroxisomes for proteome analyses .....	59
3.1.1.2. An analytical method for isolating leaf peroxisomes for proteome analyses .....	62
3.1.2. Development of a method for the enrichment of leaf peroxisomes from <i>Arabidopsis thaliana</i> (L.) Heynh.....	65
3.1.2.1. Composition of a stabilizing buffer .....	66
3.1.2.2. Enrichment of leaf peroxisomes from <i>A. thaliana</i> by sucrose density gradient centrifugation .....	67
3.2. Resolution of soluble matrix proteins of leaf peroxisomes by two-dimensional electrophoresis.....	69
3.2.1. Optimization of chaotrope composition.....	70
3.2.2. Optimization of detergent composition.....	74
3.2.3. Optimization for two-dimensional electrophoresis of alkaline proteins.....	76
3.2.4. Optimization of other variables .....	79
3.2.5. Leaf peroxisomal proteome coverage .....	79
3.2.5.1. Proteome coverage of leaf peroxisomes from <i>Spinacia oleracea</i> L. achieved by two-dimensional electrophoresis .....	79
3.2.5.2. Increasing proteome coverage by narrow range immobilized pH gradient (IPG) strips .....	81
3.2.5.3. Increasing proteome coverage by subfractionation.....	84
3.2.5.4. Increasing proteome coverage by induction of gene expression ....	85
3.3. Peroxisomal proteins identified by mass spectrometry .....	86
3.3.1. Known proteins of leaf peroxisomes .....	87
3.3.2. Novel proteins of leaf peroxisomes.....	91
3.3.2.1. Putative naphthoate synthase (At1g60550).....	91
3.3.2.2. Short chain dehydrogenase/reductase family protein.....	94
3.3.2.3. Small heat shock protein (At1g06460) .....	96
3.3.2.2. Monofunctional enoyl-CoA hydratase (At4g16210) .....	97
3.3.3. Stress inducible proteins of leaf peroxisomes from <i>Spinacia oleracea</i> L. ...	98
3.3.4 Evidence for peroxisomal localization of novel proteins.....	101
3.3.4.1. Differential profiling .....	101
3.3.4.2. Cloning of genes encoding novel peroxisomal proteins .....	103
3.4. Post-translational modifications of peroxisomal proteins from spinach.....	104
3.4.1. Detection of post translational modifications of spinach leaf peroxisomal proteins by two-dimensional electrophoresis .....	105
3.4.2. Studies on protein phosphorylation in leaf peroxisomes.....	106
3.4.2.1. Phosphate metal affinity enrichment of phosphorylated proteins from leaf peroxisomes of <i>Spinacia oleracea</i> L.....	107

3.4.2.2. Resolution of phosphorylated proteins from leaf peroxisomes of <i>Spinacia oleracea</i> L. by two-dimensional gel electrophoresis.....	109
4. Discussion .....	112
4.1. Isolation of leaf peroxisomes from <i>Spinacia oleracea</i> L. and <i>Arabidopsis thaliana</i> (L.) Heynh. for proteome analyses .....	112
4.1.1. On the improvement of purification of leaf peroxisomes from <i>Spinacia oleracea</i> L. for proteome analyses .....	113
4.1.2. Establishment of an analytical method for the isolation of leaf peroxisomes from <i>Spinacia oleracea</i> L. for proteome analysis.....	117
4.1.3. On the development of a method to enrich leaf peroxisomes from <i>Arabidopsis thaliana</i> .....	118
4.2. Two-dimensional electrophoresis for resolving soluble proteins from leaf peroxisomes.....	121
4.2.1. On the optimization of the method for two-dimensional electrophoresis.....	121
4.2.2. On the proteome coverage achieved by two-dimensional electrophoresis for leaf peroxisomes .....	123
4.3. A comparison of the peroxisomal proteome of <i>Spinacia oleracea</i> with the recently published <i>Arabidopsis thaliana</i> peroxisomal proteome .....	125
4.4. Novel proteins identified in the present proteomic investigation of leaf peroxisomes.....	128
4.5. On the occurrence of post-translational modifications of proteins in leaf peroxisomes of <i>Spinacia oleracea</i> L. ....	134
4.5.1. On the analysis of protein phosphorylation in leaf peroxisomes .....	135
4.6. On stress-inducible proteins of leaf peroxisomes from <i>S. oleracea</i> .....	137
5. Summary .....	141
6. List of figures and Tables.....	145
6.1. List of figures .....	145
6.2. List of tables.....	146
7. List of abbreviations .....	147
8. Appendices.....	149
9. REFERENCES .....	153
ACKNOWLEDGEMENT	

## **1. Introduction**

### **1.1. The role of peroxisomes in plant metabolism**

Peroxisomes are globular, single membraned, intracellular entities of approximately 1  $\mu\text{m}$  diameter and found ubiquitously in eukaryotic cells. A characteristic property of peroxisomes is their functional flexibility as their protein complement can vary depending on the organism, cell/tissue-type and environmental conditions. Largely due to their functional differentiation, the peroxisomes found in plants are broadly sub-divided as glyoxysomes, leaf peroxisomes, and unspecialized peroxisomes (Beevers, 1979). Additionally the peroxisomes present in a cell during senescence have been, sometimes, referred to as gerontosomes (Vicentini and Matile, 1993).

#### **1.1.1. Photorespiration**

In leaves, peroxisomes are mainly involved in the recycling of 2-phosphoglycolate produced by the oxygenase activity of RubisCO during photorespiration. A constant flux of metabolites occurs in this process, which involves the coordinated functioning of sixteen enzymes and at least six translocators distributed over chloroplasts, peroxisomes and the mitochondria (Douce and Heldt, 2000; Reumann, 2002, Fig. 1.1). The peroxisomal enzymes that are involved in photorespiration include the flavin-dependent glycolate oxidase, the serine-glyoxylate aminotransferase, glutamate-glyoxylate aminotransferase, hydroxypyruvate reductase, malate dehydrogenase and aspartate aminotransferase. Catalase is involved in the detoxification of hydrogen peroxide formed as a result of glycolate oxidation during photorespiration. The photorespiratory enzymes alanine-glyoxylate aminotransferase and glutamate-glyoxylate aminotransferase have been cloned recently (Liepman and Olsen, 2001, 2003; Igarashi *et al.*, 2003).

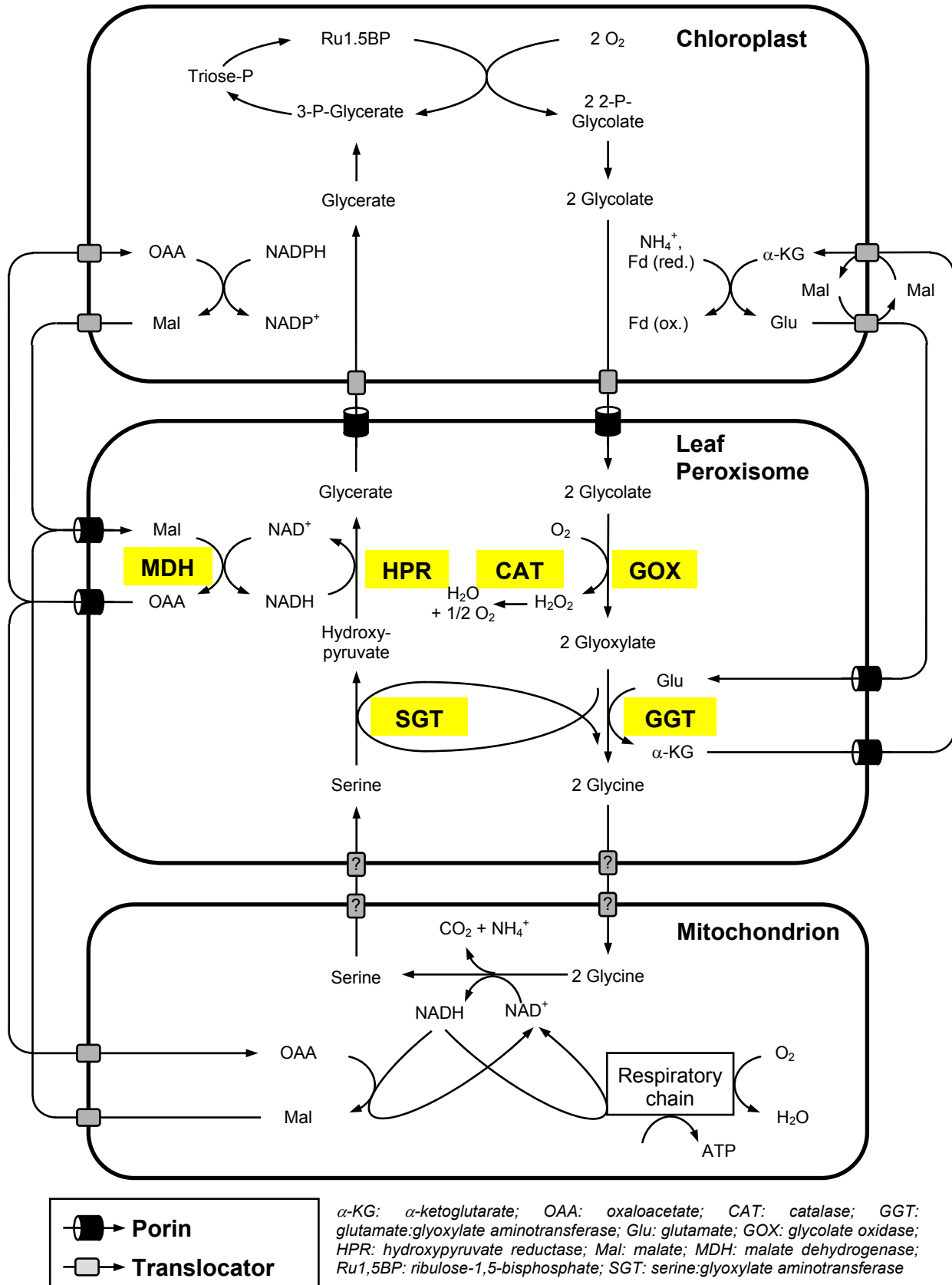


Fig. 1.1: Reactions and transport of intermediates of the photorespiratory C<sub>2</sub> cycle (taken from Reumann, 2002)



Photorespiration is inevitable due to the reaction mechanism of RubisCO and is counterproductive since it results in the release of up to 25% of CO<sub>2</sub> that is fixed during light (Sharkey, 1988). However, photorespiration is thought to protect the plant from photoinhibition in a low CO<sub>2</sub> environment by consuming ATP and NADPH and limiting the amount of toxic oxygen species (Heber and Krause, 1980; Ogren, 1984).

Within the peroxisome, the photorespiratory metabolism is compartmentalized by an organized arrangement of matrix enzymes in a multi-enzyme complex, rather than by the surrounding membrane (Heupel *et al.*, 1991, 1994). Instead of forming a strict permeability barrier, the membrane of plant peroxisomes is equipped with a porin-like channel that is well-suited to facilitate diffusion of a broad range of small negatively charged metabolites across the membrane (Reumann *et al.*, 1995, 1998; Reumann, 2000).

### **1.1.2. Fatty acid degradation**

Glyoxysomes are present in germinating seeds, and especially abundant in seeds that are rich in lipids. They contain enzymes that are involved in the complete degradation of fatty acid to produce acetyl-CoA via  $\beta$ -oxidation. This process consists of four enzymatic reactions involving the activities of acyl-CoA synthetase, acyl-CoA oxidase, the multifunctional protein (with enoyl-CoA hydratase and 3-hydroxyacyl-CoA dehydrogenase activities), and ketoacyl-CoA thiolase (Fig.1.2). The role of the glyoxylate cycle is primarily in the conversion of acetyl-CoA into succinate accomplished through the activities of peroxisomal citrate synthase, isocitrate lyase, malate synthase and malate dehydrogenase, supplemented by cytosolic aconitase.

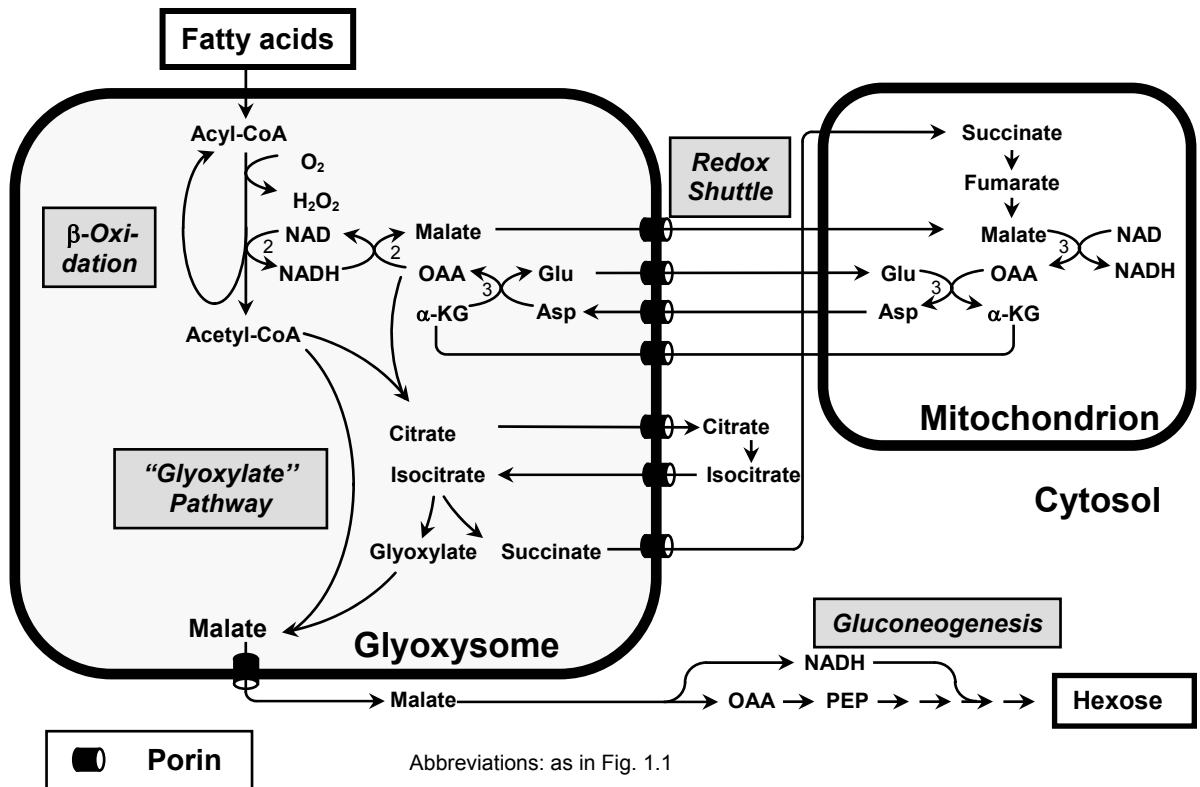


Fig. 1.2: Reactions of fatty acid  $\beta$ -oxidation cycle

### 1.1.3. Metabolism of reactive oxygen species

Reactive oxygen species (ROS) is the collective term used to include radicals such as, superoxide radicals ( $O_2^-$ ), hydroxyl radicals ( $\cdot OH$ ), hydroperoxyl radicals ( $HO_2\cdot$ ), and also some non-radical derivatives of  $O_2$ , such as, hydrogen peroxide ( $H_2O_2$ ) and singlet oxygen. ROS play a dual role in metabolism. On the one hand, they are highly toxic and must be kept under tight control (Noctor and Foyer, 1998). On the other hand, they serve as substrates in metabolism and as signals for regulation (Foyer and Noctor, 2000). Peroxisomes are involved in a predominantly oxidative type of metabolism. For example, both the metabolism of glycolate and of fatty acid begins with oxidation reactions that generate copious amounts of  $H_2O_2$  as hydrogen atoms are extracted from the incoming substrates such as fatty acyl-CoA and glycolate. The xanthine oxidase present within the peroxisomal matrix can also generate superoxide (Fig. 1.3, del Rio *et al.*, 2002). Superoxide radicals can also be produced in the peroxisomal membrane as a consequence of NAD(P)H oxidation. Thus, there is a considerable potential for oxidative

damage to proteins and lipids in the peroxisomal matrix and membranes. Under normal conditions of metabolism, peroxisomes have a multiplicity of protective mechanisms to detoxify oxygen radicals. Catalase is abundant in the matrix and catalyzes the dismutation of hydrogen peroxide to water and molecular oxygen at high  $H_2O_2$  concentrations. Superoxide dismutases are present in the membranes and in the matrix and catalyze the disproportionation of superoxide radicals to hydrogen peroxide and molecular oxygen. The membrane may also possess enzymes of the ascorbate-glutathione cycle that can efficiently dispose of hydrogen peroxide by making use of the nonenzymic antioxidants, ascorbate and glutathione in a series of reactions catalyzed by four enzymes namely, ascorbate peroxidase, monodehydroascorbate reductase, dehydroascorbate reductase, and glutathione reductase (del Rio *et al.*, 1998).

Under conditions of stress such as, high light, high and low temperature, pathogen attack etc., an oxidative burst is induced in plants. Adaptation to such stress conditions is multifactorial and involves a complicated antioxidant network composed of non-enzymatic as well as enzymatic processes and antioxidants such as, ascorbate, glutathione to detoxify reactive oxygen species and to quench radicals. While increases in antioxidative enzymatic activity have been shown to follow stress stimuli, their true physiological significance in the natural stress-tolerance mechanism remains largely hypothetical. Because plants sustain growth and development amidst a wide variety of environmental fluctuations and during invasion by pathogens, by employing a flexible metabolic network that allows dynamic changes to the prevailing conditions, an understanding of the mechanisms underlying such metabolic shifts is essential and may contribute significantly towards enhancing stress tolerance in plants.

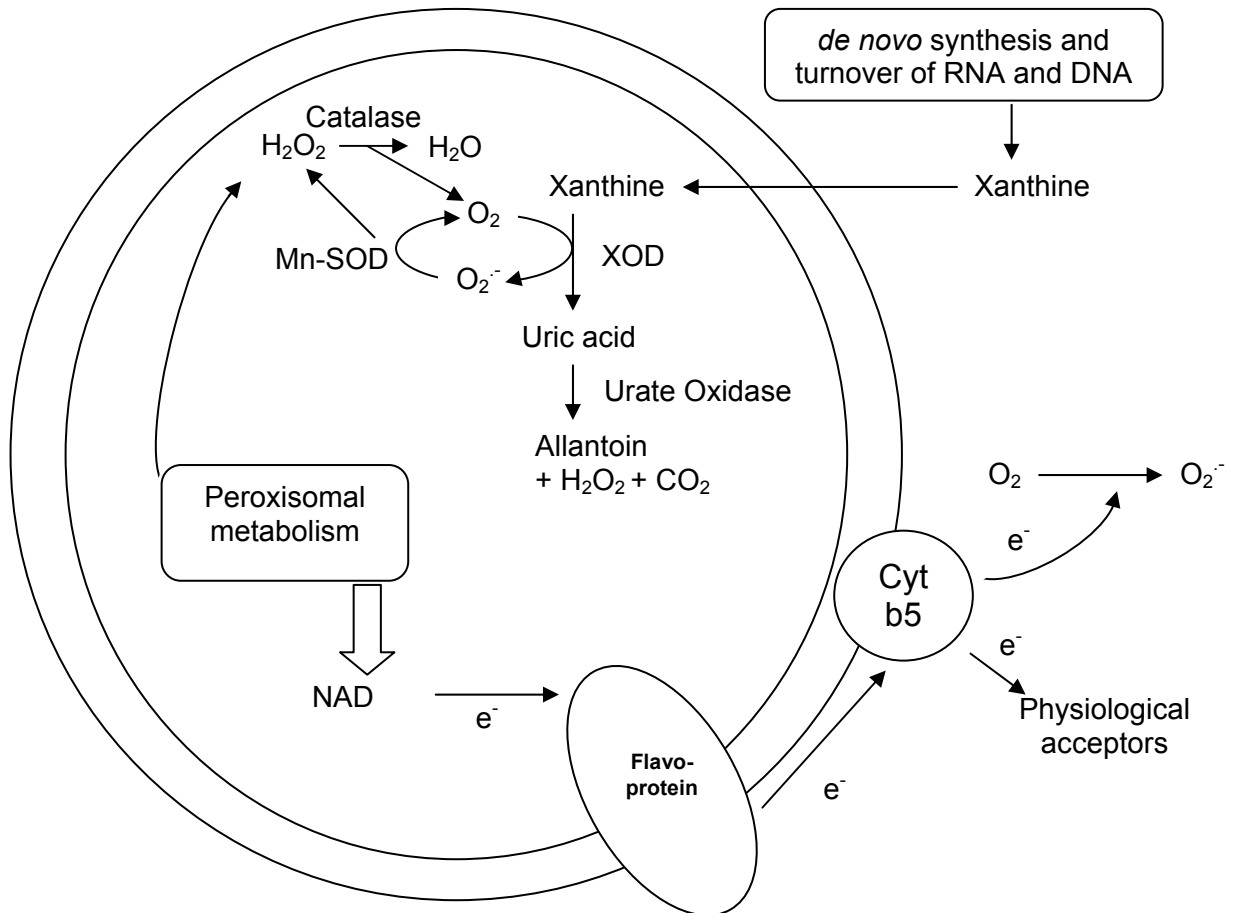


**Fig. 1.3: Model proposed to explain the production of  $O_2^{\cdot-}$  radicals by peroxisomes from pea leaves (del Rio et al., 1992; Lopez-Huertas et al., 1996) (taken from del Rio et al., 1998).**

In the soluble fraction (matrix) of pea leaf peroxisomes, xanthine oxidase (XOD) is responsible for the generation of superoxide radicals. The Mn-SOD present in the matrix can scavenge  $O_2^{\cdot-}$  radicals and convert them into  $H_2O_2$  which can be decomposed by catalase. In the peroxisomal membranes there is an NADH-dependent site of superoxide production, which could be due to a small electron transport chain similar to that reported in peroxisomal membranes from castor bean endosperm, which is composed of a flavoprotein NADH:ferricyanide reductase and cytochrome b<sub>5</sub> (Fang et al., 1987), and could perhaps use  $O_2$  as an electron acceptor with the production of  $O_2^{\cdot-}$  radicals.

In the recent past, an increasing number of novel proteins and novel isoforms of proteins also found in other subcellular compartments have been reported from plant peroxisomes. These point towards a role for plant peroxisomes in sulfur metabolism (Eilers et al., 2001; Nakamura et al., 2002), generation of nitric oxide (Barrosso et al., 1999), biosynthesis of jasmonic acid (Stintzi and Browse, 2000; Sanders et al., 2000; Strassner et al., 2002) and valine catabolism (Zolman et al., 2001). Besides, the presence of novel proteins strongly indicates that plant peroxisomes may possess as yet unrevealed

extended metabolic capacities. Hooks (2002) has assigned six functions to  $\beta$ -oxidation based on literature including its proven role in the provision of respiratory and biosynthetic substrates during stages of lipid mobilization. These include maintenance of cellular homeostasis leading to reproductive fitness, regulation of acyl-CoA pools, removal of potentially harmful fatty acids and contribution to hormone production and generation of reactive oxygen species (ROS) in response to abiotic stress. This lends indirect support to the view that there may be several more proteins in plant peroxisomes than in their fungal, yeast and mammalian counterparts as proposed earlier (Emanuelsson *et al.*, 2003).

## 1.2. Targeting of proteins to peroxisomes

Peroxisomes do not possess any genetic material and are therefore not capable of protein synthesis. Thus, proteins synthesized on free cytosolic ribosomes are imported into them post-translationally, mediated, in most cases, by recognizable targeting sequences called the peroxisome targeting signals (PTS) (Fig. 1.4; Lazarow and Fujiki, 1985; de Hoop and Ab, 1992; Subramani, 1993). Such sequences comprise a non-cleaved C-terminal tripeptide of the prototype SKL>, the PTS type 1 (PTS1), or conservative variations thereof (Gould *et al.*, 1987; 1989) or a conserved, cleavable nonapeptide embedded in a longer N-terminal presequence (e.g., RL(X)<sub>5</sub>HL, Swinkels *et al.*, 1991; Glover *et al.*, 1994) that is termed PTS2. The proteins are recognized in the cytosol by the soluble receptors Pex5 (van der Leij *et al.*, 1993; Kragler *et al.*, 1998) and Pex7 (Marzioch *et al.*, 1994; Rehling *et al.*, 1996), respectively, and directed towards a single protein import complex at the peroxisomal membrane. Some peroxisomal matrix proteins do not contain either of the two PTS (Karpichev and Small, 2000) and are thought to be targeted to the organelle by internal sequences that are yet to be specified. In rare cases, both PTS1 and PTS2 have been found within the same protein (Fulda *et al.*, 2002, Waterham *et al.*, 1994; Karpichev and Small, 2000)

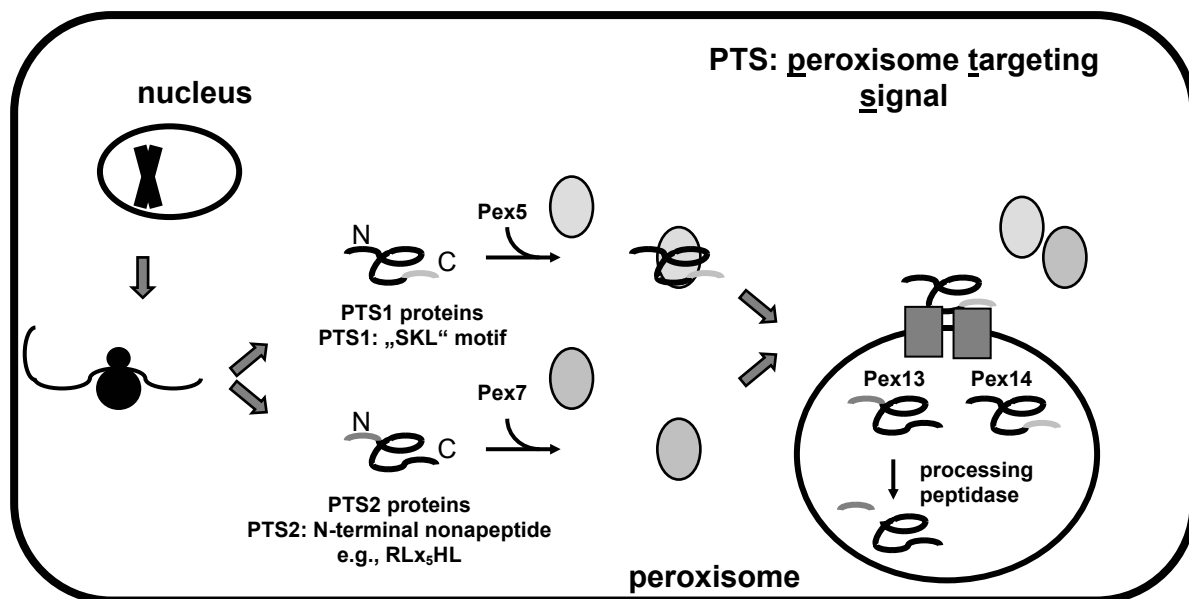


Fig.1.4. Targeting of proteins to peroxisomes

### 1.3. Analysis of the protein content of peroxisomes

A thorough understanding of the different aspects of peroxisomal metabolism may contribute towards manipulation of plants to increase productivity, to increase their resistance towards hostile environments (Wang *et al.*, 1999; Taler *et al.*, 2004) as well as their exploitation for commercial applications such as, production of novel fatty acids (Rylot and Larson, 2002) and synthesis of biodegradable plastics (Poirier, 2000).

‘Proteomics’, aptly defined as the analysis of “the functional complement of the genome”, is conceptually attractive because of its potential to determine properties of biological systems including the level of protein synthesis, the subcellular location, the state of modification, and the association with ligands as well as the rate of change with time of such properties that are not apparent by DNA or mRNA sequence analysis alone. In this respect, classic biochemical fractionation techniques for the enrichment of particular subcellular structures in combination with the large-scale identification of proteins by mass spectrometry and bioinformatics provides an approach that interfaces cell biology and proteomics, and thus is termed ‘subcellular proteomics’. It is a powerful strategy for the initial identification of previously unknown protein components and for their assignment to

particular subcellular structures. The targeting of proteins to particular subcellular sites is an important principle of the functional organization of cells at the molecular level. In turn, knowledge about the subcellular localization of a protein is a characteristic that may provide a hint as to the function of the protein. For example, the peroxisomal confinement of the  $\beta$ -oxidation pathway in plants was suggested (Cooper, 1971; Hutton and Stumpf, 1969) following the discovery of several enzymes involved in the pathway. The operation of an ascorbate-glutathione cycle in the membrane of plant peroxisomes was postulated, also, based on the discovery of proteins (del Rio *et al.*, 1998). In addition to its exceptional power for the identification of previously unknown gene products, the analysis of proteins at the subcellular level is the basis for monitoring important aspects of dynamic changes in the proteome such as protein translocation and organelle biogenesis.

### 1.3.1. Resolution of peroxisomal proteins

The proteome is amenable to analysis by gel-based methods, such as, isoelectric focusing sodium dodecyl sulphate polyacrylamide gel electrophoresis (IEF-SDS/PAGE) or two-dimensional electrophoresis (2-DE), non-equilibrium pH gel electrophoresis (NEPHGE), 16-benzyl dimethyl hexadecyl ammonium chloride (16-BAC) gel electrophoresis as well as by non-gel-based methods such as capillary isoelectric focusing (CIEF). The applications of these methods have been reviewed elsewhere (Wu and Yates, 2003). The choice of the method is, to a large extent, dictated by the kind of sample being analyzed and the scale of information.

Two-dimensional gel electrophoresis first described by O'Farrell (1975) is, by far, the most widely used method and involves the separation of proteins in two dimensions, namely in the first dimension according to their isoelectric point and in the second dimension according to their molecular mass. One key advantage of this technique is that it provides a global snapshot of a cell or subcellular compartment. Over the past few years, several improvements have enabled this technique to be integrated into a number of laboratories for varied applications. (Majoul *et al.*, 2004; Perez-Bueno *et al.*, 2004; Campo *et al.*, 2004; Corpillo *et al.*, 2004; Consoli *et al.*, 2001; Blee *et al.*, 2001; Finne *et al.*, 2002; Gallardo *et al.*, 2001; Gomez *et al.*, 2002). These improvements have been targeted

towards enhancing the reproducibility of the pH gradient (Georg *et al.*, 1997, 1998, 1999, 2000), development of novel chemicals, especially detergents, and methods for improved solubilization of proteins (Chevallet *et al.*, 1998; Rabilloud, 1998), advances in two-dimensional electrophoresis of membrane proteins (Molloy, 2000; Wu and Yates, 2003) and alkaline proteins (Goerg *et al.*, 1997, 1999). Proteomics based on two-dimensional electrophoresis is often biased towards particular classes of proteins, especially since biological mixtures are inherently heterogeneous and include a wide dynamic range of protein solubilities, molecular masses, isoelectric points and abundances. For example, highly hydrophobic membrane proteins are biologically designed to be insoluble in solution, therefore they remain nearly impossible to solubilize for electrophoretic purposes. Similarly, many low abundance proteins are present on 2-D gels, but they cannot be visualized due to the overwhelming presence of abundant 'house-keeping' proteins. Strategies to overcome such limitations are numerous and have been reviewed (Huber *et al.*, 2003).

### 1.3.2. Identification of individual peroxisomal proteins

Two-dimensional electrophoresis (2-DE) is descriptive and bears much information, for instance, on the expression level and post-translational regulation of proteins but identification of proteins is only possible when 2-DE is used in conjunction with sensitive analytical techniques such as, by immunodetection using antibodies and by mass spectrometry.

In principle, there are two major approaches to identify and characterize proteins by mass spectrometry. When working with an organism whose genome is sequenced, proteins can be identified using peptide mass fingerprinting (PMF). For organisms that are poorly represented in databases, partial peptide sequences have to be determined. In both cases, mass spectrometry (MS) is applied to determine the mass-to-charge ratios ( $m/z$ ) of gas-phase ions. Today MS is the most sensitive method for the analysis of biomolecules like pure proteins or very simple mixtures. The spots excised from two-dimensional gels are thus ideal. Sensitivity is so high that analysis of proteins at picomole, femtomole and even zeptomole level is possible (Shevchenko *et al.*, 1996; Andren *et al.*, 1994).



A mass spectrometer has three components: a source of ions, a mass analyzer and a detector. In MS for the determination of mass-to-charge ( $m/z$ ) ratio of gas-phase ions is measured for which the sample must first be ionized and vaporized in a vacuum and exposed to a high voltage. Special soft-ionization techniques are required for proteins because they have a low volatility. The ions thus produced are accelerated through the mass analyzer that separates the ions according to their mass-to-charge ratio. The detector records the impact of individual ions, producing peaks on a mass spectrum. The mass of a molecule can be calculated from the  $m/z$  ratio of its derivative ions.

### 1.3.2.1. Peptide mass fingerprinting (PMF)

This method involves digestion a sample with trypsin and determination of the masses of the intact peptides, producing a 'peptide mass fingerprint' of a sample. This fingerprint can be used to search protein databases. A search algorithm such as Peptide Sequence Tags (Mann and Wilm, 1994) or Mascot (Perkins *et al.*, 1999) is used that carries out virtual digests of protein sequences based on the sequence-specificity of trypsin and then calculates the masses of the predicted peptides (for example, by adding up the masses of the individual atoms). The search algorithm then theoretically digests all proteins of the organism of interest in the database with the specified enzyme and matches the theoretical and experimental peptide masses. Thus, the more accurate the experimentally determined peptide masses are, the more likely the protein will be correctly identified. This is of particular importance when the peptide mass map is a composite for a number of proteins.

Two MS methods can be used to determine peptide masses.

**Matrix-assisted laser desorption ionization (MALDI):** MALDI, first described by Karas and Hillenkamp (1988) is an efficient method of ionizing peptides using laser light directed at a co-crystallization product of sample and a light-absorbing matrix such as  $\alpha$ -hydroxycinnamic acid. Analysis by MALDI-TOF is used for peptide mass mapping, where proteins are digested by a suitable enzyme and the mass-to-charge ratio is determined for the resulting peptides. MALDI is limited in the low-mass range by matrix-associated chemical noise.

**Electron-spray ionization (ESI):** While MALDI is the most efficient method for ionizing peptides, electron-spray is the optimum method of ionization/vaporization for the widest range of polar biomolecules. In this method initially the sample of interest is dissolved in a solvent and pumped through a thin capillary which is raised to a high potential. The result is a beam of ions, which are sampled by the mass spectrometer. Electron-spray is a concentration- rather than a mass-dependent process, and improved sensitivity is obtained for high-concentration low-volume samples such as micro-ES and nano-ES (Wilm *et al.*, 1996) both of which are widely used in biological mass spectrometry.

### 1.3.2.2. Protein identification based on peptide sequences

When working with an organism whose genome is not sequenced, peptide mass fingerprints will not lead to protein identification since amino acid substitutions affect mass of tryptic peptides. In this case, partial amino acid sequences have to be determined to identify homologous sequences in the databases. For sequence determination, the method of tandem mass spectrometry is applied. In tandem mass spectrometry (MS/MS), a series of ions termed 'mass spectrum' is obtained by the random fragmentation of the peptides along the peptide bond. The masses of these shorter fragments can be searched against further databases containing short sequences, such as expressed sequence tags. Alternatively, the fragment ions can also be ordered by size and the masses of sequential fragments used to establish which amino acids have been cleaved off.

The time required for processing a single polypeptide to obtain useful information limits the application of ESI-MS/MS to a small number of proteins. For analysis on a larger scale an alternative approach known as on-line liquid chromatography coupled to tandem mass spectrometry (LC-MS/MS) is widely employed. In this method, the tryptic peptides are separated by a reversed-phase chromatograph whose effluent is directly coupled to the mass spectrometer for analysis. Peptides are sequenced on-line as they elute from the column. Database searching is then performed by correlating tandem mass spectra against the calculated mass spectra of all the peptides in the database.

## 1.4. The peroxisomal proteome and the choice of the model plant

Mass spectrometry-based methods that are widely used to establish subcellular proteomes influence the choice of a suitable model organism for proteome analyses. Ideal model plants should offer the possibility to prepare highly pure organelle fractions from them and should possess sufficient genome information in databases to process the data generated to 'extract' desirable information.

As far as leaf peroxisomes are concerned, the real bottleneck seems to be obtaining pure fractions in sufficient quantities from a suitable model plant. This is, perhaps the most likely reason why, even four years after the genome information of *Arabidopsis* had been made publicly available (The *Arabidopsis* Genome Initiative, 2000), no comprehensive data are available on the leaf peroxisomal proteome. An effective method to isolate very pure leaf peroxisomes from this model plant will be an indispensable tool to understand the different aspects of peroxisomal metabolism. *Spinacia oleracea* L. yields leaf peroxisomes of good quality and thereby helps to overcome the problem of low yield mentioned above. However, there are some disadvantages. The potential of mass spectrometric analyses may be fully realized when complete genome sequences are available. In this context, genetic information is indispensable not only to curtail the laborious experimental procedures but also more importantly, to unambiguously identify isoforms of specific proteins and to identify post-translational modifications that occur in different proteins. This is especially important in the case of enzymes whose different isoforms play a role in different metabolic processes. However, fragmentary genome information does not substantially hinder proteomic analyses, particularly, if novel strategies are devised to address problems in a specific manner to overcome such handicaps.

## 1.5. Objectives of the present investigation

The following were the objectives of this study:

- Establishment of a method to obtain highly pure peroxisomes from spinach for proteome analysis of soluble matrix proteins
- Establishment of a method to enrich leaf peroxisomes from *Arabidopsis* that would enable proteome analysis
- Establishment of two-dimensional electrophoresis techniques for the proteome analysis of soluble leaf peroxisomal proteins
- Analysis of the leaf peroxisomal proteome to identify novel proteins
- Analysis of the leaf peroxisomal proteome to identify novel isoforms of proteins (from *Arabidopsis*)
- Cloning of genes encoding interesting proteins
- Analysis of post-translational modifications occurring in leaf peroxisomes
- Analysis of protein phosphorylation in leaf peroxisomes

## 2. Material and methods

### 2.1. Plant material

*Spinacia oleracea* L. and *Arabidopsis thaliana* (L.) Heynh. were used in this investigation for the isolation of leaf peroxisomes.

#### 2.1.1. *Spinacia oleracea* L.

##### 2.1.1.1. Normal growth conditions

For routine isolation of leaf peroxisomes, plants were cultivated under normal growth conditions. Seeds of *Spinacia oleracea* L. cv. Monorpa or Matador were obtained from Carl Spering & Co. GmbH, (Lueneburg, Germany), and germinated in the dark on vermiculite. After one week the seedlings were transferred to a climate chamber and grown further for a week (8/16 h light/dark period). Subsequently, plants were hydroponically grown in a nutrient solution (Randall and Bouma, 1983) for up to 8-12 weeks. Typical growth conditions were  $350 \mu\text{molm}^{-2}\text{s}^{-1}$  light intensity, 9/15 hour light dark cycle and 21°C/18°C day-night temperature.

##### 2.1.1.2. Stress treatments

For certain experiments, (e.g. for comparative proteome analyses of leaf peroxisomes from normal and stressed states), plants were subjected to different abiotic stresses.

###### 2.1.1.2.1. Light stress

In order to subject the spinach plants to a high light stress, the illumination was increased to  $700 \mu\text{molm}^{-2}\text{s}^{-1}$  during the 8 h light period. Plants were maintained thus for 3 days and harvested at the end of the light period for peroxisome isolation. Plants grown under a normal illumination of  $350 \mu\text{molm}^{-2}\text{s}^{-1}$  served as control.

### **2.1.1.2.2. Oxidative stress**

The catalase inhibitor 3-amino-1,2,4-triazole (3-AT) was used to induce oxidative stress symptoms in spinach plants. This compound binds to the active site of catalase and inhibits its activity irreversibly. Four plants were maintained in 2 L of nutrient solution supplemented with 10 mM 3-AT for 3 days, with normal illumination ( $\mu\text{molm}^{-2}\text{s}^{-1}$ ), until the onset of oxidative stress symptoms. Plants maintained similarly in a nutrient solution without any inhibitor served as control.

## **2.1.2. *Arabidopsis thaliana* (L.) Heynh.**

### **2.1.2.1. Normal growth**

*Arabidopsis thaliana* ecotype Col-0 seeds were obtained from The Arabidopsis Stock Resource Centre (Nottingham, England). The seeds were sown on a mixture of commercial soil (Balster Einheitserdewerk GmbH, Froendenberg, Germany) and vermiculite (4:1) and grown at 22°C with a light intensity of 130  $\mu\text{molm}^{-2}\text{s}^{-1}$  in a 8/16 light dark cycle (short-day) or a 16/8 h dark cycle (long-day). Between five and seven plants were maintained per pot (9 x 9 x 9 cm: 15 pots/tray). The soil was supplemented with the commercial fertilizer Wuxan (2-3 mL/ L) every week.

### **2.1.2.2. Stress treatment: Cold treatment of *Arabidopsis* plants**

Cold stress was induced in 8 weeks old *Arabidopsis* plants by subjecting the plants to a low-temperature for 1 h. The plants were kept in refrigerator (between 6 and 10 °C). Leaves from cold-treated plants were used for the isolation of total RNA for molecular biological analyses.

## 2.2. Isolation of leaf peroxisomes

For the isolation of leaf peroxisomes from spinach, a protocol described by Yu and Huang (1986) and involving a Percoll density gradient separation of leaf peroxisomes was used with adaptations for large scale isolation as described by Reumann (1996).

### 2.2.1. Isolation of leaf peroxisomes from *Spinacia oleracea* L.

In the present study, for preparative purposes, the purity of leaf peroxisomes obtained from an initial Percoll density gradient was further improved, by an additional purification step involving a sucrose density gradient centrifugation. For analytical purposes, a new method was developed which is described elsewhere (2.2.1.2).

#### 2.2.1.1. Preparative method

Eight to twelve weeks old apparently healthy spinach plants with fully expanded leaves were harvested on the day of preparation shortly after the end of the dark period. They were kept covered with aluminium foil with their roots dipping in water at 4 °C (for about 3 h) until the beginning of the preparation to reduce the amount of starch in chloroplasts.

All steps were carried out at 4 °C. About one kilogram of fresh deribbed mature leaves was finely chopped using a kitchen knife and ground in 2 L semi-frozen grinding buffer using a mortar and pestle. The homogenate was filtered through eight layers of gauze and one layer of Mira cloth. The filtered 'brei' was centrifuged (in polyallomer bottles) at 5,000  $xg$  using a GS3 rotor in a Sorvall high speed centrifuge (Sorvall RC-5B) for one min to remove cell debris and most of the plastids. The supernatant was again centrifuged using the same rotor at 12,000 rpm for 18 min to sediment the remaining organelles. The sediments were resuspended using a brush in Wash medium A and resedimented at 25,000  $xg$  using SS34 tubes (SS34 rotor, Sorvall RC-5B) to reduce the volume. Protease inhibitors (0.5 mM PMSF in isopropanol, 1 mM benzamidine in ethanol, 1  $\mu g/mL$  each leupeptin, antipain and pepstatin) were added to the 25,000  $xg$  sediments followed by gentle resuspension in Wash medium A using a soft paint brush and

homogenization in a tight fitting Potter-Elvehjem homogenizer (capacity: 50 mL) for 20 strokes of the plunger.

The suspension was layered over 8 preformed Percoll step gradients chilled on ice. The composition of the gradient was adapted from the original method as follows: a linear gradient of seven mL each 18 and 27% (v/v) Percoll was used instead of the discontinuous 15 + 27 % layers, the 14 mL 45% (v/v) Percoll layer was replaced with 16 mL 48% (v/v) Percoll and the volume of the 60% (v/v) Percoll cushion was reduced to three mL (earlier: five mL); all Percoll solutions were prepared in 0.25 M sucrose. The gradients were spun in an SS34 rotor for 12 min at 10,000  $xg$  with slow acceleration and deceleration. The peroxisome band above the 60% Percoll cushion was pooled from all the tubes, diluted with freshly prepared Wash medium B and centrifuged to sediment the organelles at 12,000  $xg$  for 12 min. The washing step was repeated (10 min, 5,000  $xg$ ) to remove Percoll. Protease inhibitors (concentrations as above) were added to the final peroxisome pellet. This pellet was gently homogenized in a tight fitting (capacity: 5 mL) Potter-Elvehjem homogenizer and layered on a discontinuous sucrose density gradient comprised of small layers of 2 mL each 18, 25 and 35% (w/w) sucrose over a linear 40-60% (w/w) sucrose density gradient. The gradients were spun for 2 h at 83,000  $xg$  in a Beckman Coulter ultracentrifuge using an SW28 rotor. The gradient was fractionated into 2 mL fractions from the top and saved as ready-to-use aliquots for the determination of the marker enzyme activities. For preparative purposes the gradient was slightly modified (40-50% w/w sucrose over a 60% cushion) and the peroxisome fraction above the sucrose cushion was saved after the addition of protease inhibitors. The activities of marker enzymes hydroxypyruvate reductase (peroxisomes), NADP-dependent GAPDH (plastids) and fumarase (mitochondria) and the chlorophyll content were determined as described (2.5). The typical yield of peroxisomes as determined by the activity of hydroxypyruvate reductase (HPR, marker enzyme peroxisomes, 2.5.1.1) was between 6 and 11% with respect to the activity in the crude extract. The leaf peroxisomes contained less than 0.5% mitochondria (determined by activity of fumarase, 2.5.1.2) and almost no detectable chlorophyll (2.5.2).



**Grinding buffer:**

Mannitol	350	mM
Mops - NaOH pH 7.5	30	mM
EDTA (Na <sup>2+</sup> )	1	mM
BSA	0.2	% (w/v)
PVP – 40	0.6	% (w/v)
Cystein	4	mM

**Wash medium A:**

Mannitol	300	mM
MOPS- NaOH pH 7.2	20	mM
EDTA (Na <sup>2+</sup> )	1	mM
BSA	0.2	% (w/v)

**Percoll density gradient medium:**

MOPS- NaOH pH 7.2	10	mM
Sucrose	250	mM
BSA	0.2	% (w/v)
Percoll	18, 27, 48, 60	% (v/v)

**Wash medium B:**

Sucrose	250	mM
Hepes –NaOH pH 7.5	2	mM

**Sucrose density gradient medium:**

Hepes- NaOH pH 7.5	10	mM
EDTA (Na <sup>2+</sup> )	1	mM
Sucrose	18, 25, 35, 40, 50, 60	% (w/v)

### 2.2.1.2. Analytical method

A new analytical method was developed in the present study that facilitated isolation of leaf peroxisomes from spinach within a very short time. This method was suitable for the comparison of peroxisomal proteomes from differently treated tissues. In this method, the 'post-plastidic' supernatant obtained after centrifugation of the filtered crude extract was directly applied on a Percoll density gradient.

- the leaf tissue was homogenized using a limited volume of grinding buffer (the ratio of leaf tissue to the grinding buffer was 1.5 g/ mL)
- the peroxisomes were not subjected to any kind of manual handling by way of sedimentation and resuspension
- the separation and purification of peroxisomes occurred within a single Percoll density gradient which was shortened to accommodate a larger volume of sample. It constituted a linear gradient of 18-27% (v/v) (2 x 6 mL) over a 55% (v/v) Percoll layer (12 mL) that formed a density barrier and prevented further migration of contaminants, yet, allowed the peroxisomes to sediment. The former (18 and 27% (v/v) Percoll) was prepared in 250 mM sucrose and the latter (55% (v/v)) in 250 mM raffinose. (Propane 1, 2-diol was omitted from the Percoll density gradient solutions).

All steps were carried out at 4 °C. Freshly harvested leaves were washed, deribbed, cut into small pieces and homogenized in a limited volume of grinding buffer using a mortar and pestle. The protease inhibitor 0.5 mM PMSF was included during homogenization. The homogenate was filtered through a layer of Mira cloth and centrifuged at 5,000  $xg$  for 1 min. About 10 to 12 mL of the supernatant was applied on preformed Percoll density gradients and spun for 12 min at 10,000  $xg$  in a Sorvall SS34 rotor. After centrifugation, the upper layers were aspirated away and the pale white peroxisome pellets were quickly aliquoted after transferring then to clean tubes. Aliquots were immediately frozen for later determination of enzyme activities and protease inhibitors (see 2.2.1.1) were added to the remaining peroxisome fraction which was saved as larger aliquots for 2-DE. It was not possible to concentrate the peroxisome fraction by

washing away the Percoll because of a significant loss of protein (<10% recovered after washing). Peroxisomes obtained by this method were of high purity with no detectable chlorophyll. Fumarase activity could not be detected. The contamination with pro-plastid like organelles was about 0.2 to 0.6%.

### **Grinding buffer:**

The composition of the grinding buffer was the same as that used for the preparative method.

### **Percoll density gradient medium:**

MOPS- NaOH pH 7.2	10	mM
Osmoticum*	250	mM
Percoll	18, 27, 55	% (v/v)

\* The 18 and 27% (v/v) Percoll solutions were prepared with sucrose and the 55% (v/v) Percoll solution was prepared with raffinose as the osmoticum

### **2.2.2. Isolation of leaf peroxisomes from *Arabidopsis***

All steps were performed at 4 °C. About 40 g of fresh leaf material from eight to ten weeks old plants were ground thoroughly in 250 ml grinding buffer using a mortar and pestle. The homogenate was filtered through six layers of gauze and one layer of Mira cloth. Cell debris and chloroplasts were removed by differential centrifugation of the homogenate at 5,000  $xg$  for 1 min in a Sorvall SS34 rotor (Sorvall RC5B). Peroxisomes were sedimented by centrifugation at 25,000  $xg$  for 5 min. The pellets were immersed in about 0.5 ml fresh grinding buffer and gently resuspended using a soft paint brush and homogenized for 10 strokes in a loose fitting Potter-Elvehjem homogenizer (capacity: 5 mL). The suspension was equally layered over 2 preformed discontinuous sucrose density gradients (2 mL each 18, 25 and 35% (w/w) sucrose over 12 mL each 41-50% (w/w) sucrose over a 2 mL 60% (w/w) sucrose cushion in 5 mM Tricine–KOH, pH 7.5, 1 mM

EDTA). The gradients were spun for 2 h at 83,000  $xg$  in a Beckman Coulter Ultracentrifuge using an SW28 rotor.

The peroxisome band at the 50-60% interface was pooled from the two gradients and homogenized as described before. The peroxisome suspension (about 52% (w/w) sucrose) was gradually diluted using a solution of 25% (w/w) sucrose to a density of 48% (w/w) sucrose and equally dispensed into two SW28 centrifugation tubes and underlaid with 2 mL 60% (w/w) sucrose solution. The peroxisome suspension was overlaid with 5 mL 45% (w/w) sucrose and the remaining space was filled with a 35% (w/w) sucrose solution. The gradients were centrifuged for 18 h at 83,000  $xg$  in an ultracentrifuge. The peroxisomes were visible as a pale green band at the interface of the 48 and 60% (w/w) sucrose layers. Chloroplasts and mitochondria 'floated' away from the 48% (w/w) sucrose layer. The peroxisome band above the 60% cushion was frozen in convenient aliquots after the addition of 1 mM PMSF. The activity of hydroxypyruvate reductase and fumarase and the chlorophyll content were determined in the crude extract and the peroxisome fractions obtained after each density gradient centrifugation step. Peroxisomes obtained by this method were of good purity as indicated by the content of mitochondria which was about 2%, chlorophyll content was less than 1% and the contamination with pro-plastid like organelles was about 0.2%. For analysis of peroxisomal protein by two-dimensional gel electrophoresis, the fraction obtained after the 2<sup>nd</sup> sucrose density gradient centrifugation was used.

**Grinding buffer:**

Tricine KOH pH 7.5	50	mM
Sucrose	450	mM
EDTA (Na <sup>2+</sup> )	1	mM
KCl	10	mM
MgCl <sub>2</sub>	1	mM
BSA	0.1	% (w/v)
PVP-40	1	% (w/v)
DTT (freshly added)	5	mM

**Sucrose density gradient medium:**

Tricine KOH pH 7.5	10	mM
EDTA (Na <sup>2+</sup> )	1	mM
Sucrose	18, 25, 35, 41, 50, 60	% (w/v)

### 2.3. Estimation of intactness of the isolated peroxisomes by sedimentation

Determination of the intactness of the peroxisomes was based on their sedimentation behaviour. Intactness was usually determined in the organelle suspension that was applied on the density gradient. An aliquot of the peroxisome suspension was diluted in grinding buffer (1:5) and centrifuged at 15,000 *xg* for 5 min in a Sorvall SS34 rotor (using adapters for eppendorf tubes) in order to sediment only the intact organelles. The activity of hydroxypyruvate reductase (HPR, marker enzyme of peroxisomes, 2.1.1) was determined in the supernatant and in the pellet. Intactness was calculated as the percentage of HPR activity retained in the pellet with respect to total activity in the sample.

$$\text{Intactness [\%]} = \frac{\text{Activity of HPR in the pellet}}{\text{Total activity the aliquot}} * 100$$

### 2.4. Enrichment of core particles

Core particles were enriched from freshly isolated leaf peroxisomes essentially as described by Heupel *et al.* (1991). Leaf peroxisome fractions in wash medium B, obtained after Percoll density gradient centrifugation, were diluted ten-fold with water and the detergent Triton X-100 was added to a final concentration of 0.05% (v/v) and mixed by drawing the sample gently through a 1 mL disposable pipette tip. After incubation on ice for 10 min, the concentration of the sample was adjusted to the initial concentration of wash medium B (with 10x Wash medium B) and centrifuged at 25,000 *xg* for 5 min. The

sediment enriched in the core particles and the supernatant containing the soluble fraction were saved separately for further analysis.

## 2.5. Biochemical analysis of subcellular fractionation

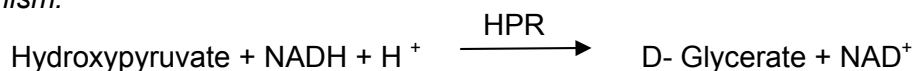
The activities of the following enzymes were determined spectrophotometrically at 25 °C using a spectrophotometer (Uvikon 932, Kontron Instruments). Enzyme containing samples were frozen as ready-to-use aliquots that were freshly thawed prior to measurement to avoid loss of activity due to frequent freezing and thawing.

### 2.5.1. Determination of enzyme activities

#### 2.5.1.1. Hydroxypyruvate reductase (HPR) (*adapted from Titus et al., 1983*)

(D-Glycerate:NAD<sup>+</sup> oxidoreductase; E.C. 1.1.1.81)

*Reaction mechanism:*



Molar extinction coefficient at 334 nm  $\epsilon = 6.18 \text{ mM}^{-1}\text{cm}^{-1}$

*Assay mixture* (1 ml)

Sucrose	300	mM
KH <sub>2</sub> PO <sub>4</sub> -KOH, pH 6.5	50	mM
NADH	400	μM
Triton X-100	0.1	% (v/v)

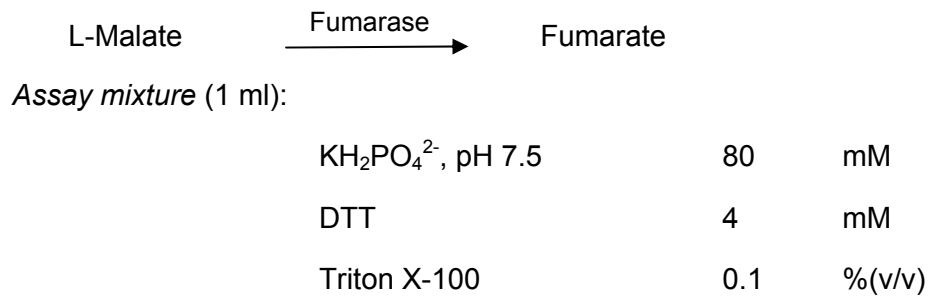
About 20 μl of the enzyme containing sample were added to a final volume of 1000 μl in plastic cuvettes. The reaction was started with 4 mM hydroxypyruvate (lithium salt) and the decrease in extinction at 334 nm at 25 °C was measured using a spectrophotometer (Kontron Instruments) against an air blank. The activity of HPR was routinely measured to determine the yield and intactness of leaf peroxisome preparations.

**2.5.1.2. Fumarase** (*adapted from Titus et al., 1983*)

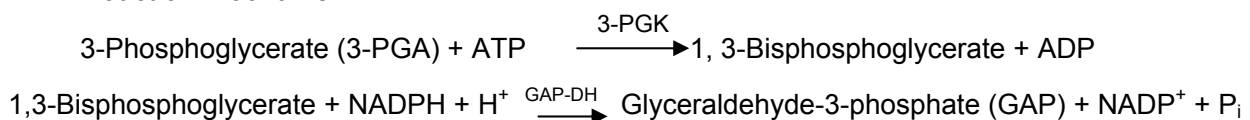
(Fumarate hydratase; E.C. 4.2.1.2)

*Reaction mechanism:*

Fumarase catalyzes the trans hydration of malate and fumarate.



About 10-50  $\mu\text{l}$  of the sample was incubated in the assay mixture for 15 minutes at room temperature. The reaction was started by the addition of 8 mM L-malate. The activity of fumarase was determined photometrically against air via the time-dependent formation of fumarate which resulted in an absorption of UV light by the double bond of fumarate at a wave length of 240 nm (extinction coefficient  $\epsilon = 2.57 \text{ mM}^{-1}\text{cm}^{-1}$ ).

**2.5.1.3. NADP<sup>+</sup>-dependent glyceraldehyde-3-phosphate dehydrogenase** (*Wirtz et al., 1983*)(NADP<sup>+</sup>-GAPDH; E.C. 1.2.1.13)*Reaction mechanism:*

*Assay mixture (700 µL)*

HEPES-KOH,pH 8.0	100	mM
KCl	20	mM
EDTA	2	mM
MgCl <sub>2</sub>	30	mM
Triton X-100	0.1	% (v/v)
DTT	6.7	mM
ATP	6.7	mM
NADPH	0.3	mM
Phosphoglycerate kinase (3-PGK)	600	nkat

The reaction was started by the addition of 5.7 mM 3-phosphoglycerate. The activity of NADP-GAPDH was determined by the time-dependent decrease of the extinction at 340 nm ( $\epsilon = 6.18 \text{ mM}^{-1}\text{cm}^{-1}$ ) due to the oxidation of NADPH against an air blank.

### 2.5.2. Chlorophyll (*Arnon, 1949*)

Aliquots from fractions were diluted with 96% ethanol to a volume of 1 mL and vortexed vigorously. The samples were incubated at room temperature for 5-10 minutes and spun in a microfuge at maximum speed for 10 minutes to remove insoluble particles. The extinction was measured in a spectrophotometer (Kontron) at 652 nm against an appropriate blank. The chlorophyll content was determined using the following formula:

$$\text{Chlorophyll (mg)} = [E_{652}/\epsilon \cdot d^2] \cdot [V_c/V_a] \cdot \text{Total Volume} \cdot \text{Dilution factor}$$

where  $E_{652}$  = extinction at 652 nm

$\epsilon$  is the extinction coefficient for chlorophyll in ethanol viz .,  $36 \text{ cm}^2\text{mg}^{-1}$   $d$ = thickness of the cuvette;  $V_c$ = volume in the cuvette ( $\mu\text{L}$ );  $V_a$ = volume of the aliquot used ( $\mu\text{L}$ )



## 2.6. Protein determination

### 2.6.1. The Lowry Method (Lowry *et al.*, 1951)

A widely used quantitative assay for determining protein content in a solution is the Lowry method (Lowry *et al.*, 1951) which is based on the formation of a Biuret complex formed between  $\text{Cu}^{2+}$  and the peptide bonds of proteins. The  $\text{Cu}^{2+}$  as well as the alkyl groups of tyrosine, tryptophan and cysteine residues of the Biuret complex react with the folin reagent resulting in the reduction of the phosphomolybdate/tungsten to molybdenum/tungsten blue under alkaline conditions. The assay is reliable for solutions with a protein concentration from 5  $\mu\text{g/mL}$  to 100  $\mu\text{g/mL}$ . This method was used to estimate protein concentration in fractions derived from sucrose density gradients.

A sample volume containing between 1 and 20  $\mu\text{g}$  protein was mixed with 800  $\mu\text{l}$  of the ABC mixture by vortexing and incubated for 15 min. Afterwards, 32  $\mu\text{l}$  of Folin-Ciocalteu's phenol reagent were added, mixed rapidly by vortexing and the samples were incubated for 10 min and the extinction was measured at 578 nm. From each sample, two aliquots were analyzed. For samples with a high concentration of chlorophyll, blank samples were run in parallel, in which the protein samples were added last (i.e. solution ABC, Folin reagent, and finally the sample). This was done to determine the background absorbance of chlorophyll. For each analysis, a calibration curve was made using bovine serum albumin (BSA). The calibration curve points corresponded usually to 2.5, 5, 7.5, 10, 15, 20, and 25  $\mu\text{g}$  protein in the sample. Typically, a calibration curve with an equation of  $y = 0.115x + 0.005$  was obtained.

#### Stock solutions:

Solution A	2% (w/v) $\text{Na}_2\text{CO}_3$ in 0.1 M NaOH
Solution B	1% (w/v) $\text{CuSO}_4 \cdot 5\text{H}_2\text{O}$
Solution C	2% (w/v) Na-K-tartarate

Just prior to use, the stock solutions A, B and C were mixed in the ratio 20:1:1

### 2.6.2. Protein determination using Bradford's reagent (*Bradford, 1976*)

The Bradford protein assay is one of several simple methods commonly used to determine the total protein concentration of a sample. The method is based on the proportional binding of the dye Coomassie to proteins. The assay is linear in the range of ~5-25 mg/mL protein concentration. The assay is colorimetric; as the protein concentration increases, the color of the test sample becomes darker. Coomassie absorbs at 595 nm. The protein concentration of a test sample is determined by comparison to that of a series of protein standards, usually bovine serum albumin (BSA), known to reproducibly exhibit a linear absorbance profile in this assay.

An aliquot of the protein sample was added to 950  $\mu$ l of Bradford's reagent and filled up with water to a final volume of 1 ml. After incubation for at least 10 min at room temperature, the absorption at 595 nm was read against a suitable blank sample. The protein content was calculated using a standard curve made with BSA. The extinction coefficient was around  $0.04 \text{ mL} \cdot \mu\text{g}^{-1} \text{ cm}^{-1}$ .

#### Bradford's reagent:

Serva Blue G	0.07	mg/mL
Ethanol	4.8	% (v/v)
Phosphoric acid	8.8	% (v/v)

### 2.7. Protein precipitation (*Wessel and Fluegge, 1984*)

Precipitation of proteins is one of the methods to concentrate them. The method of Wessel and Fluegge (1984) based on precipitation using chloroform-methanol results in nearly 100% recovery of proteins from very diluted solutions (0.02 mg/mL).

The entire procedure was performed at 4 °C. The diluted protein sample was mixed successively first with a four fold volume of methanol, an equal volume of chloroform and three volumes of water and briefly spun at 12,000 xg for a minute for phase separation. The upper phase was carefully removed using a finely drawn capillary followed by

precipitation of the proteins with three volumes of methanol. The protein pellet was air-dried at room temperature or was dried at 37 °C using a heat block.

## 2.8. Two-dimensional gel electrophoresis

The separation of proteins in two-dimensions, first by isoelectric focusing followed by SDS-PAGE is based on the method described by O'Farrell. The IPG-phor instrument (Amersham Biosciences) was used for the two-dimensional resolution of peroxisomal proteins during the present study. Immobilized pH gradient (IPG) strips that offer separation of proteins in different ranges e.g. 3 to 10 (non-linear), 6 to 11 and 6 to 9 (linear) and 4 to 7 (linear) over a length of 18 cm were used in this study. They were obtained from the same manufacturer. For the second dimension, home-made acrylamide gels were used.

### 2.8.1. Solubilization of proteins

Proteins were precipitated by the method of Wessel and Fluegge (1984, 2.7) prior to their solubilization. For analytical purposes 40 to 60 µg protein were used. For preparative purposes, 100 to 600 µg proteins were precipitated. The precipitated proteins were solubilized in 350 µL of the 2-DE solubilization buffer by rocking the samples for 2 h on a laboratory shaker (HLC HTM 130) set to speed level 9.

#### Solubilization buffer

Urea*	7	M
Thiourea*	2	M
CHAPS §	4	% (w/v)
IPG buffer	0.5	% (v/v)
DTT added fresh	3	mg/mL
Bromophenol blue	trace	mM

The buffer was prepared fresh or stored as 500 µL aliquots at -20 °C.

\*For some experiments 9 M urea was used as the only chaotrope instead of a mixture of 7 M urea and 2 M thiourea

§To test the efficiency of detergents the following variations were tested instead of 4% (w/v) CHAPS

(i) CHAPS (2% w/v) + N-octylglucoside (2% w/v)

(ii) CHAPS (2% w/v) + NP-40 (2% w/v)

(iii) ASB14 (2% w/v)

(iv) ASB14 (2% w/v) + N-octylglucoside (2% w/v)

The following additives to the buffer were tested for their efficiency to improve alkaline two-dimensional electrophoresis:

glycerol, isopropanol, isobutanol, each at 5% (v/v)

### **2.8.2. Removal of insoluble material**

The solubilized sample was centrifuged at 13,000 rpm in a microfuge for 20 min at room temperature to remove insoluble material.

### **2.8.3. Rehydration of immobiline pH gradient (IPG) gel strips**

The clarified supernatant was pipetted into a ceramic strip holder (18 cm). The plastic cover was removed from a frozen IPG strip with a pair of forceps. The strip was lowered, gel side down over the protein solution. After about 2-3 minutes, the strip was overlaid with silicone oil (DryStrip cover fluid, Amersham Pharmacia) to prevent evaporation. The lid was put on the strip holder. The dry strips were rehydrated in the protein solution for at least 10 h at 30 V (active rehydration). The isoelectric focusing (IEF) protocol was programmed accordingly.

### **2.8.4. Isoelectric Focusing**

The following protocol was used for isoelectric focusing. The first step of the IEF protocol was programmed for sample entry.

Step	Voltage (V)		Time (h)	Volt.hours (Vh)
1	30	step-n-hold	10	300
2	200	step-n-hold	1	200
3	1000	step-n-hold	1	1000
4	2000	step-n-hold	1	1000
5	8000	gradient	2	16000
6	8000	step-n-hold	5	40000

### 2.8.5. Equilibration of focused IPG strips

After IEF, the IPG strip was removed from the strip holder and briefly washed with distilled water to remove the silicone oil and stored at -80 °C if required. The focused proteins were treated with DTT for their complete reduction. To do this, the strip was placed in a 50 mL Duran tube, containing 5 mL equilibration buffer with DTT. The tube was sealed with parafilm and placed in a horizontal position so that the strip was fully immersed in the buffer. The tubes were rocked for 12 min at room temperature. Alkylation of the reduced proteins was carried out similarly but with equilibration buffer that contained iodoacetamide. The equilibration step also allowed for an exchange of detergent (with SDS) so as to facilitate migration of proteins to the 2<sup>nd</sup> dimension. After equilibration, the strip was rinsed for a few seconds with distilled water to remove excess buffer and left on pre-wetted paper towels until the following step.

**Equilibration buffer**

Urea	6	M
Tris-HCl pH 8.8	50	mM
Glycerol	30	% (v/v)
SDS	2	% (w/v)
Bromophenol blue	trace	mM

The buffer was stored as 15 mL aliquots at -20 °C. Prior to use the equilibration buffer was thawed and supplemented with DTT and iodoacetamide as follows.

- A. 10 mg DTT/ mL equilibration buffer
- B. 25 mg Iodoacetamide/ mL equilibration buffer

**Agarose sealing solution**

(in electrophoresis buffer)

Agarose	1% (w/v)
Bromophenol blue	trace

**2.8.6. Second dimension sodium dodecylsulfate polyacrylamide gel electrophoresis**

The 2<sup>nd</sup> dimension polyacrylamide gel consisted of the resolving gel of desired concentration which was prepared a day in advance and stored at 4 °C. This was done to prevent modification of proteins by acrylamide monomers and was preferred when proteins needed to be analyzed by mass spectrometry. The isopropanol overlay was washed away with distilled water. The IPG strip with the proteins was positioned over the surface of the gel such that the plastic backing rested against the larger glass plate. A piece of comb was placed at the side to make a well for the molecular weight marker. The gel and the comb were sealed in place with an agarose sealing solution. This layer also served to stack the proteins. The piece of comb was removed after the agarose had solidified. Protein molecular weight standard was applied into the well.

**Protein molecular weight standard** (Amersham Biosciences)

Phosphorylase b	97 kDa
Albumin	66 kDa
Ovalbumin	45 kDa
Carbonic anhydrase	30 kDa
Trypsin inhibitor	20.1 kDa
$\alpha$ -Lactalbumin	14.4 kDa

The contents of the vial were reconstituted in SDS sample buffer to a protein concentration of 1  $\mu\text{g}/\mu\text{l}$  and heated to 95°C for 5 min. Aliquots of 50  $\mu\text{l}$  were stored at -20°C. For Coomassie gels about 10  $\mu\text{g}$  of marker protein was used per lane and for silver stained gels 1 – 2  $\mu\text{g}$  was used per lane.

**2.8.7. Electrophoresis conditions**

The gel was run first at constant current (10 mA/gel) for 20 min to stack the proteins. Resolution of proteins was carried out at a constant current of 40 mA/gel until the bromophenol blue had migrated nearly to the end of the gel. Post-electrophoretic staining of the gels was carried out in clean plastic boxes according to the protocols described (2.9).

## 2.9. Sodium dodecyl sulphate polyacrylamide gel electrophoresis (SDS-PAGE)

Standard procedures according to Laemmli (1970) were followed for the electrophoretic resolution of proteins by denaturing SDS-PAGE.

### Sodium dodecyl sulphate polyacrylamide gel electrophoresis (SDS-PAGE)

#### Stacking gel:

Tris-HCl pH 6.8	0.13	M
SDS	0.1	% (w/v)
Acrylamide	4.6	% (w/v)
N,N-Methylenebisacrylamide	0.12	% (w/v)
APS	0.06	% (w/v)

#### Resolving gel:

Tris-HCl pH 8.8	0.38	M
SDS	0.1	% (w/v)
Acrylamide	12.5	% (w/v)
N,N-Methylenebisacrylamide	0.33	% (w/v)
APS	0.05	% (w/v)



**Stock solutions for SDS-PAGE****Acrylamide stock solution**

(30%T / 2.7% C):

Acrylamide	25	mM
N,N-Methylenebisacrylamide	0.8	% (w/v)

**Lower Gel Stock** (Resolving gel buffer):

Tris-HCl pH 8.8	1.5	M
SDS	0.4	% (w/v)

**Upper Gel Stock** (Stacking gel buffer)

Tris-HCl pH 6.8	0.5	M
SDS	0.4	% (w/v)
Ammonium peroxy disulfate (APS)	10	% (w/v)
N,N,N',N'-Tetramethylethylenediamine (TEMED)		

**Electrophoresis buffer:**

Tris-HCl (pH not adjusted)	25	mM
Glycine	192	mM
SDS	0.1	% (w/v)

**SDS-sample buffer (1x):**

Tris-HCl (pH 6.8)	60	mM
SDS	2	% (w/v)
2-Mercaptoethanol	5	% (w/v)
Glycerol	10	% (v/v)
Bromophenol blue	trace	

## 2.10. Post-electrophoretic staining of proteins in acrylamide gels

Following one-dimensional or two-dimensional gel electrophoresis of protein mixtures, the proteins are typically visualized by some kind of protein staining. By far, the most common protein staining solutions utilize the Coomassie Brilliant Blue R or Coomassie Brilliant Blue G dyes that can detect about 50 µg/band. Silver staining can increase the sensitivity from 10 to 100 fold.

### 2.10.1. Silver Staining

Staining protein with silver is more sensitive than with Coomassie. In silver staining the proteins are first fixed to insolubilize them in the gels, followed by sensitizing them with compounds that bind both the protein and silver ion. After this, silver is impregnated and finally developed. The use of sodium thiosulfate as the developing agent, introduced by Blum *et al.*, 1987 results in complete development of image with minimal background staining.

**2.10.1.1. Method 1: Analytical purposes (Blum et al., 1987):**

This protocol was routinely followed to visualize proteins on analytical gels with 40 to 60 µg protein load.

Step	Time	Solution	Final concentration	
Fixation	≥ 90 min	ethanol	50	% (v/v)
		acetic acid	12	% (v/v)
		formaldehyde (37%)	0.05	% (v/v)
Wash	3x 20 min	ethanol	50	% (v/v)
Sensitizing	60 sec	Na <sub>2</sub> S <sub>2</sub> O <sub>3</sub> ·5 H <sub>2</sub> O (sodium thiosulfate)	0.01	% (w/v)
Wash	3x 20 sec	dd H <sub>2</sub> O		
Impregnation	20 min	AgNO <sub>3</sub>	0.1	% (w/v)
		formaldehyde (37%)	0.075	% (v/v)
Wash	2x 20 sec	dd H <sub>2</sub> O		
Development	2-10 min	Na <sub>2</sub> CO <sub>3</sub>	3	% (w/v)
		formaldehyde (37%)	0.05	% (v/v)
		Na <sub>2</sub> S <sub>2</sub> O <sub>3</sub> ·5 H <sub>2</sub> O	2·10 <sup>-4</sup>	% (w/v)
		(Sodium thiosulfate)		
Stop	ca. 10 min	Na <sub>2</sub> EDTA	10	mM
Storage		dd H <sub>2</sub> O		

### 2.10.1.2. Method 2: Compatible with mass spectrometric analyses

(Blum et al., 1987, with modifications as in Soerensen et al., 2002)

This protocol was used when silver stained proteins were analyzed by mass spectrometry at the Max-Planck-Institut für Experimentelle Medizin, Goettingen, Germany.

Step	Time	Solution	Final concentration	
Fixation	≥ 90 min	methanol	50	% (v/v)
		acetic acid	12	% (v/v)
Wash	3x 20 min	ethanol	30	% (v/v)
Sensitizing	60 sec	sodium thiosulfate (Na <sub>2</sub> S <sub>2</sub> O <sub>3</sub> ·5 H <sub>2</sub> O)	0.8	mM
Wash	3x 20 sec	dd H <sub>2</sub> O		
Impregnation	20 min	AgNO <sub>3</sub>	11.8	mM
		formaldehyde (37%)	0.02	% (v/v)
Wash	2x 20 sec	dd H <sub>2</sub> O		
Development	2-10 min	Na <sub>2</sub> CO <sub>3</sub>	566	mM
		formaldehyde (37%)	0.02	% (v/v)
		sodium thiosulfate	0.02	0.02
		(Na <sub>2</sub> S <sub>2</sub> O <sub>3</sub> ·5 H <sub>2</sub> O)		
Wash	2x2 min	dd H <sub>2</sub> O		
Stop	10 min	methanol	50	% (v/v)
		acetic acid	12	% (v/v)
Wash	> 20 min	methanol	50	% (v/v)

## 2.10.2. Coomassie staining

Coomassie Brilliant Blue R 250 is the most commonly used staining procedure for the detection of proteins. It is the method of choice if SDS is used in the electrophoresis of proteins, and is sensitive for a range of 0.5 to 20  $\mu\text{g}$  of protein. Within this range, it also follows the Beer-Lambert law and thus can be quantitative as well as qualitative.

### 2.10.2.1. Normal method

The normal method was used for routine purposes. The gels were stained overnight with the staining solution. Destaining was carried out with frequent changes of the destaining solution until desired contrast was obtained for the protein spots/bands.

#### Staining solution:

Coomassie brilliant blue R-250	0.1	% (w/v)
Methanol	50	% (v/v)
Glacial acetic acid	10	% (v/v)

The Coomassie dye was first dissolved in the methanol and water component, and then the acetic acid was added. The solution was filtered through Whatman No.1 filter paper and stored at room temperature.

#### Destaining solution:

Methanol	10	% (v/v)
Glacial acetic acid	7	% (v/v)

### 2.10.2.2. Colloidal Coomassie (Herbert *et al.*, 2001)

The method was used when mass spectrometric analysis was desired for the proteins. The gels were stained for 24 h with one change of the staining solution after 12 h

to enhance dye deposition on low abundance proteins. The gel was placed in 1% (v/v) acetic acid for better contrast between the spots and the gel.

**Staining solution:**

Ammonium sulfate	17	% (w/v)
Phosphoric acid	3	% (w/v)
Coomassie G-250	0.1	% (w/v)
Methanol	34	% (v/v)

**Destaining solution:**

Glacial acetic acid	1	% (v/v)
---------------------	---	---------

## 2.11. Documentation

The stained gels were carefully placed inside transparent folders. Air bubbles were smoothed out and an image of the gel was acquired with the help of a scanner using Adobe Photoshop version 7.0 (Adobe Systems, USA).

## 2.12. Gel Drying

The Coomassie or silver-stained gels were soaked in 10% glycerol for at least 30 minutes. The gel was transferred carefully on Whatman filter paper (slightly larger than the gel) wetted with 10% glycerol. The gel was placed filter paper side down on the white plastic sheet of the gel drier and covered with gel drying foil (larger than the filter paper) also wetted with 10% glycerol. Air bubbles trapped between the drier and the filter paper and between the gel and foil were removed. The gel was covered with the polythene sheet of the gel drier and vacuum was applied via opening the water outlet. The heater was turned on to quicken the process. A normal 1 mm thick gel was dried in less than 3 hours with the heater turned on. The gels were filed after and stored away from moisture.

## 2.13. Preparation of samples for Mass Spectrometric Analysis

### 2.13.1. Excision of protein spots from gels

Excision of protein spots from the gels was carried out within a closed hood to avoid contamination by dust particles. Gloves were used indispensably to avoid contamination with keratin.

The gel was placed on a scrupulously clean glass plate and the protein spots were pressed out of the gel using a 1 mL disposable pipette tip which was cut at the end up to a diameter of about 2 mm. Each gel 'circle' was transferred into an eppendorf tube.

### 2.13.2. Destaining silver stained spots

The excised gel pieces were incubated in the destaining solution until they were completely decolorized after which they were washed with several changes of water until the yellow color was no longer visible.

#### Destaining solution:

The destaining solution was freshly prepared by mixing equal volumes of the following solutions.

#### Stock solution 1:

Potassium hexacyanoferrate ( $K_3Fe(CN)_6$ )	30	mM
--	----	----

#### Stock solution 2:

Sodium thiosulfate ( $Na_2S_2O_3$ )	100	mM
-------------------------------------	-----	----

### 2.13.3. In-gel tryptic digestion (*adapted from Shevchenko et al. 1996*)

A protocol compatible with mass spectrometric analysis was used for the proteolytic in-gel digestion by trypsin. The entire procedure was completed in two days. On the first

day samples were prepared for overnight digestion. The following day samples were lyophilized and then reconstituted in a solution for MS analysis.

The protein spot was excised and dehydrated in acetonitrile (CH<sub>3</sub>CN) for approximately 10 min. The acetonitrile was removed and the gel piece was dried in a speedvac. The dried gel pieces were rehydrated at 4°C for 45 min in a buffer containing trypsin and 50 mM ammonium bicarbonate (NH<sub>4</sub>HCO<sub>3</sub>). About 5 µL of the trypsin (Promega, Madison, WI, USA; 10µL at 12.5 ng/µL in 25 mM ammonium hydrogen carbonate) solution were used per mm<sup>2</sup> of the gel so that the gel pieces were just covered. Digestion was performed overnight at 37°C.

#### **2.13.4. Extraction of peptides**

The gel pieces were centrifuged to collect the supernatant. Further extraction of peptides was carried out by one change of 20 mM NH<sub>4</sub>HCO<sub>3</sub>, and 3 changes of 5% formic acid in 50% CH<sub>3</sub>CN (20 min between changes) at room temperature. The solution containing the extracted peptides was dried down in a speedvac until the desired volume had been reached or if needed for transportation they were completely dried down.

#### **2.13.5. A modified in-gel digestion protocol for automated application**

Protocol followed for the analysis of proteins from spinach leaf peroxisomes at the LSMBO, Strasbourg, France

In gel digestion with trypsin was performed according to published methods (Jeno *et al.*, 1995; Wilm *et al.*, 1996) modified for use with a robotic digestion system (MassPREP, Micromass, Manchester, UK). Each gel slice was decolorized by washing with 50 µL of 25 mM ammonium hydrogen carbonate followed by washing with 50 µL of acetonitrile. This step was repeated twice. Cysteine residues were reduced with DTT and derivatized by treatment with iodoacetamide. The gel pieces were then dehydrated with acetonitrile and dried at 60°C, prior to the addition of modified trypsin (Promega, Madison, WI, USA; 10µL at 12.5 ng/µL in 25 mM ammonium hydrogen carbonate). The digestion



was performed at 35°C overnight followed by extraction in 5 µL of 30% (v/v) water / 65% (v/v) acetonitrile / 5% (v/v) formic acid.

### 2.13.6. Zip-Tip purification prior to mass spectrometry

Zip Tip<sup>®</sup> Pipette Tips (Millipore Corporation) were used for the rapid purification and concentration of peptides prior to mass spectrometry.

The C18 columns (ZipTips) were pre-wetted by washing (3x 10 µL) with 10 µL acetonitrile. The tips were equilibrated with 1% (v/v) formic acid (3x 10 µL). Ten µL of 1% formic acid were added to the peptide extract. The peptides were bound to the equilibrated C18 column by drawing the sample slowly through it. The columns were washed with (3 x 10 µL) the loading solvent to remove the non-peptide impurities. The desalted peptides were concentrated by eluting in 2 to 5 µL of solvent 3.

#### Solvents:

Solvent 1 (wash)	Acetonitrile (CH <sub>3</sub> CN)	50% (v/v)
Solvent 2 (Equilibrating/loading)	Formic acid (HCOOH)	1% (v/v)
Solvent 3 (Eluting)	Acetonitrile (CH <sub>3</sub> CN)	60% (v/v)
	Formic acid (HCOOH)	1% (v/v)

## 2.14. Mass Spectrometric Analysis

### 2.14.1. Matrix-assisted laser desorption ionization mass spectrometry (MALDI-MS)

Protocol followed for the analysis of proteins from spinach leaf peroxisomes at the LSMBO, Strasbourg, France.

Mass measurements were carried out on a Biflex (Bruker, Wissenbourg, Germany) matrix assisted laser desorption time of flight mass spectrometer (MALDI-TOF). A saturated solution of  $\alpha$ -cyano-4-hydroxycinnamic acid in acetone was used as the matrix. The first layer of fine matrix crystals was obtained by spreading and fast evaporation of 0.5

$\mu\text{L}$  of matrix solution. On this fine layer of crystals, a droplet of 0.5  $\mu\text{L}$  of aqueous formic acid (5% v/v) was deposited. Afterwards, 0.5  $\mu\text{L}$  of the peptide sample was added and a second 0.25  $\mu\text{L}$  droplet of saturated matrix solution (in 50% water / 50% acetonitrile) was added. The preparation was dried under vacuum and washed in 1  $\mu\text{L}$  of 5% (v/v) formic acid.

All mass spectra were internally calibrated with trypsin autolysis peaks. The resulting peptide mass fingerprints (PMFs) were searched against a local copy of the non redundant database SWISS-PROT (<http://www.expasy.ch/sprot>) using MASCOT (Perkins *et al.*, 1999) search program. The parameters used in the search were as follows: peptide mass tolerance 50 ppm, 1 missed cleavage, carboxymethylated cysteine, methionine oxidation and N-terminal acetylation.

### **2.14.2. Liquid chromatography tandem mass spectrometry (LC-MS/MS)**

Protocol followed for the analysis of proteins from spinach leaf peroxisomes at the LSMBO, Strasbourg, France

Samples were injected into a CapLC (Waters, Milford, MA, USA) System equipped with an autosampler, gradient and auxiliary pump. A volume of 6.4  $\mu\text{L}$  was injected via “microliter pickup” mode and desalted on-line through a 300  $\mu\text{m}$  x 5 mm  $\text{C}_{18}$  trapping cartridge (LC Packings, San Francisco, CA, USA). The samples were desalted at a high flow rate of 30  $\mu\text{L}/\text{min}$  for 3 min. The peptides were separated on a 75  $\mu\text{m}$  x 15 cm 3  $\mu\text{m}$   $\text{C}_{18}$  100 Å PepMap<sup>TM</sup> column (LC Packings, CA, USA) prior to introduction into the mass spectrometer. A typical reversed-phase was used from low to high organic over about 35 min. Mobile phase A was 0.1% formic acid and B was 95% acetonitrile, 0.1% formic acid. The flow rate was 5  $\mu\text{L}/\text{min}$ . The system utilized a split flow resulting in a column flow rate of approximately 400-500  $\mu\text{L}/\text{min}$ .

MS/MS data were obtained using a Q-ToF 2 (Micromass, Manchester, UK) fitted with a Z-spray nanoflow electrospray ion source. The mass spectrometer was operated in positive ion mode with a potential of 3500 V applied to the nanoflow probe body. The collision energy was determined on the fly based on the mass and charge state of peptide.

Charge state recognition was used to switch into MS/MS mode only for double and triple charged ions. Several trypsin autolysis ions were excluded. The data were processed by Protein Lynx Version (Micromass, Manchester, UK) to generate searchable peak lists. Initial protein identifications were made by the correlation of uninterpreted tandem mass spectra to entries in SWISS-PROT using Global Server (Version 1.1, Micromass).

## **2.15. Phosphoprotein enrichment by phosphate metal affinity chromatography (PMAC)**

Enrichment of phosphoproteins is necessary because of their low-abundance. Immobilized metal affinity chromatography (IMAC) uses affinity resins that can be charged with different metal ions such as Al (III), Fe (III), Ga (III) and Zn (II). Adsorption in IMAC is based on a reversible complex between the phosphate and metal ion formed under acidic conditions, and dissociated at alkaline pH. The sample containing both unphosphorylated and phosphorylated proteins is passed over the column at an acid pH. The column is washed to remove unbound proteins and the phosphorylated proteins are eluted by displacement with phosphate buffer.

### **2.15.1. Equilibration of the phosphoprotein enrichment column**

The phosphoprotein enrichment column was pre-treated according to the manufacturer's instructions. The storage solution (ethanol) was allowed to flow out of the column. The column was washed twice with distilled water and further washed with lysis/equilibration/loading buffer until the pH of the wash was less than 6.

### **2.15.2. Solubilization of proteins**

Peroxisome fractions (derived from preparative sucrose density gradients) containing 3 mg total protein were enriched for phosphorylated proteins using the phosphoprotein enrichment kit (BD Biosciences, San Jose, USA). The peroxisomal proteins were diluted to a concentration of 0.1 mg/mL with the solubilization/lysis buffer

provided with the kit. The sample was incubated on ice for 45 min with frequent vigorous vortexing every 5 min to facilitate solubilization.

### **2.15.3. Clarification of sample**

The sample was clarified by sedimenting the insoluble material in eppendorf tubes at 10,000 *xg* for 20 min at 4 °C.

### **2.15.4. Binding of phosphorylated proteins**

Phosphorylated proteins were batch-bound to the equilibrated affinity resin of the column at 4 °C as follows. The clarified sample was incubated with the phosphoprotein enrichment resin at 4°C in a 50 mL Falcon tube with gentle shaking for 30 min. After incubation, the slurry was transferred back to the column support and the unbound proteins were allowed to flow through. The flow-through was collected on ice and aliquots were frozen immediately at -20 °C for later analysis (protein estimation and SDS-PAGE analysis).

### **2.15.5. Removal of non-phosphorylated proteins**

The column was washed with 8 mL solubilization/lysis buffer to remove residual non-phosphorylated proteins. The wash was collected as 1 mL fractions separately and aliquots were frozen from each fraction to evaluate the specificity of the PMAC procedure.

### **2.15.6. Elution of phosphorylated proteins**

Complete elution of phosphorylated proteins was achieved using 5 mL phosphate buffer. The buffer was applied 1 mL at a time (5x 1 mL). The eluted fractions were subdivided into aliquots and stored at -20 °C.

## 2.16. Methods used for molecular biology

For these methods only sterilized pipette tips and reaction tubes were used. All media were made with ddH<sub>2</sub>O and either autoclaved or sterile filtered (unless specified different).

### 2.16.1. RNA isolation

Total RNA was isolated from leaves of cold-treated (section 2.1.2.2) *Arabidopsis* plants using the Invisorb® Spin Plant RNA Mini Kit (Invitex, Berlin, Germany) according to the manufacturer's protocol.

### 2.16.2. Estimation of nucleic acids

#### 2.16.2.1. Photometric method

Nucleic acid was diluted with ddH<sub>2</sub>O (1:50) in a total volume of 100 µL and the extinction was measured at 260 and 280 nm against water blank using a spectrophotometer (Ultrospec 1100 pro, Amersham Bioscience, Freiburg, Germany). The concentration of the nucleic acid was automatically calculated using the following formula:

$$\text{RNA } [\mu\text{g/mL}] = E_{260} * 42 * V_{\text{cuvette}} * V_{\text{aliquot}}^{-1}$$

$$\text{DNA } [\mu\text{g/mL}] = E_{260} * 50 * V_{\text{cuvette}} * V_{\text{aliquot}}^{-1}$$

The extinction quotient (260/280 nm) reflects contamination by proteins and typical values should be between 1.8 and 2.0.

#### 2.16.2.2. Gel-electrophoretic method

Alternatively, the quality and concentration of nucleic acid was also estimated by agarose gel electrophoresis (2.15.3). A 1% agarose gel was prepared, and electrophoresis and UV detection were performed as described. Good RNA quality was indicated by a ratio

of band intensities between 28 S RNA and 18 S rRNA of  $\geq 1.5:1$ . The concentration of RNA was estimated by comparison against a size standard of known concentration (1  $\mu\text{g}$   $\lambda$ /PstI-Marker).

### 2.16.3. Agarose gel electrophoresis

For most analytical purposes, 1% agarose gels in 1 x TEA buffer were used. 1/6 volume of loading dye was added to DNA samples before loading them on a gel. Electrophoresis proceeded at 80 V with 1 x TEA as running buffer. Bacteriophage  $\lambda$  DNA restricted with *Pst*I, to which tracking dye had been added, was used as size marker (1  $\mu\text{g}$  per slot).

#### 50 x TEA buffer:

Tris-acetate pH 8.3	2	M
EDTA	100	mM

#### Loading dye:

Glycerol	50	% (v/v)
Tris-acetate pH 8.3	40	mM
EDTA	2	mM
Orange G	0.2	% (v/v)

#### Tracking dye:

Xylene cyanol	0.1	% (w/v)
Sucrose	20	% (w/v)
EDTA	250	mM
Bromphenol blue	50	% (w/v)

#### **2.16.4. Staining**

The gel-resolved nucleic acids were stained protected away from light for 20 min in an aqueous solution containing 0.25 µg/mL of the intercalating dye ethidium bromide. The gel was briefly rinsed with water to remove excess dye and the dye-molecules, bound to nucleic acids, were made visible under UV-light.

#### **2.16.5. Documentation**

DNA was photographed under UV light using a transilluminator (raytest IDA; Herolab, Wiesloch, Germany) connected to a printer.

#### **2.16.6. Synthesis of cDNA by RT reaction**

Reverse transcription (RT) of total RNA was carried out using oligo(dT)<sub>18</sub> as a primer. The transcriptase M-MuLV (Moloney Murine Leukemia Virus) Reverse Transcriptase (MBI Fermentas, Vilnius, Lithuania) was used according to specifications by the manufacturer. Each reaction contained 1-5 µg of total RNA with 500 ng of oligo(dT)<sub>18</sub>-primer and was incubated at 70°C for 5 min for denaturation of RNA. After addition of 10 mM 4 dNTPs, 5× reaction buffer and 40 units ribonuclease inhibitor an incubation for 5 min at 37°C followed and 20 units of M-MuLV RT (Fermentas) in a total reaction volume of 20 µL were added last. The reaction was incubated at 37°C for 60 min, and then inactivated at 70°C for 10 min.

#### **2.16.7. Oligonucleotide primers**

For amplification of specific DNA sequences by PCR, there are short, single-stranded DNA sequences (primers) necessary which anneal to a complementary DNA strand and provide a free 3'OH-end. The DNA polymerase can begin with DNA synthesis at those free 3'OH-ends in 3'-direction. A pair of primers (forward and reverse) is necessary for PCR. By choosing the primers, the beginning and the end of the amplified DNA strand can be defined. The deduced primers were 18-20 nucleotides long, had a GC-content of 40-60 % and contained in the last five nucleotides at the 3'-end at least three A

or T but did not end with a T. From the deduced sequence the melting temperature  $T_m$  was calculated, at which 50 % of the primers were annealing to the complementary strand. The melting temperature is an important criteria for selection of the annealing temperature in the PCR program to inhibit false annealing of the primers and amplification of undesired sequences. For one primer pair  $T_m$  should be close together. It was calculated via the following formula:

$$T_m [^{\circ}\text{C}] = 69,3 + 0,41 * [\text{GC-content in \%}] - 650/\text{no. of nucleotides}$$

The primers should not be complementary to each other or form secondary structures. This was checked with the program GeneWalker in the internet:

<http://www.cybergene.se/primerdesign/index.html>

Primers were obtained from Carl Roth GmbH & Co. KG (Karlsruhe, Germany).

Primer ID f=forward, r=reverse	Sequence (5'→3')	Application
<u>Primers for the amplification of cDNA</u>		
SR150f	ACTGCGGCCGCTATG GAGCATGAATCTATCAC	Small heat shock protein
SR151r	TCAAAGCTTTGG AATTACTATTCTCAG	Small heat shock protein
SR158f	CACCATGGCGGA TTCCAATGAGCTTG	Naphthoate Synthase-like protein
SR160r	GAGCTCCATGGAAGG TCGCCGGTGAAATTT A	Naphthoate Synthase-like protein
<u>Primers for sequencing</u>		
T7	TAATACGACTCACTATAGGG	pGEM <sup>®</sup> -T Easy
SP6	ATTTAGGTGACACTATAG	pGEM <sup>®</sup> -T Easy

### 2.16.8. Polymerase Chain Reaction (PCR)

Genes were amplified by Polymerase Chain Reaction (PCR, Mullis und Faloona, 1987). With this method specific DNA sequences can be amplified more than  $10^6$ -fold. The DNA is thermally denatured and hybridized with primers in order to result in an exponential



increase of the desired fragments which are elongated by a thermostable DNA-polymerase. A thermocycler with heated lid was used (Mastercycler personal, Eppendorf, Hamburg, Germany) and different DNA-polymerases, according to the purpose. *Taq* DNA-polymerase (Invitex, Berlin, Germany), which is isolated from *Thermophilus aquaticus*, was used for colony PCR (2.15.12). It is one of the cost-effective DNA-polymerase whose amplification rate is higher than the proofreading DNA-polymerases which were used for cloning. These have a 3'→5' exonuclease proofreading activity and thereby a tenfold increased accuracy (error rate about  $2 \times 10^{-3}$ ) than *Taq* polymerase. The proofreading polymerase which was used for amplification of the desired gene from cDNA was Expand High Fidelity (Roche, Penzberg, Germany) which is an enzyme mix and generates blunt-ended PCR products as well as PCR products with an overhanging A at the 3'-ends.

Standard reactions contained the following components:

	<b><u>Taq polymerase</u></b>	<b><u>proofreading polymerase</u></b>
10x reaction buffer (matching the enzyme)	2,5 µl	5 µl
50 mM MgCl <sub>2</sub>	1 µl	-
10 mM dNTP	0,5 µl	1 µl
10 µM 5'-primer	0,5 µl	1 µl
10 µM 3'-primer	0,5 µl	1 µl
DNA template	2 µl	2 µl
DNA polymerase	0,25 µl (1,25 U)	1 µl (1 U)
dd H <sub>2</sub> O	to 25 µl	to 50 µl

A standard program was as follows:

<b>cycles</b>	<b>temperature</b>	<b>duration</b>
1	95°C	2 min
35	95°C	30 sec
	annealing temperature	30 sec
	72°C	1:30 min
1	72°C	10 min

The annealing temperature was 5°C lower than the melting temperature which was specific for each primer pair. Of each of the two primers the lowest temperature was chosen. The amplification products were analysed by TEA agarose gelelectrophoresis.

### 2.16.9. Elution of resolved nucleic acid fragments from agarose gel

DNA fragments deriving from PCRs or restriction enzyme reactions were separated on 1% agarose gels (2.15.3). This step allowed the purification of DNA from proteins and the primers and the isolation of the DNA fragment of the desired size. The DNA bands were cut from the gel under long-waved UV light. The agarose was removed using Qiaquick® Gel Extraction Kit (Qiagen) according to the manufacturer's instructions. After dissolving the agarose at 50°C in a chaotropic reagent, DNA was bound to a silica gel filter in a spin column in the presence of high salt concentrations, washed and eluted from the filter with dd H<sub>2</sub>O.

### 2.16.10. Ligation into pGEM®-T Easy vector

In a ligation reaction a DNA fragment is inserted into a vector if they have corresponding overhanging ends. To achieve this, they usually have to be digested with the same restriction enzyme.

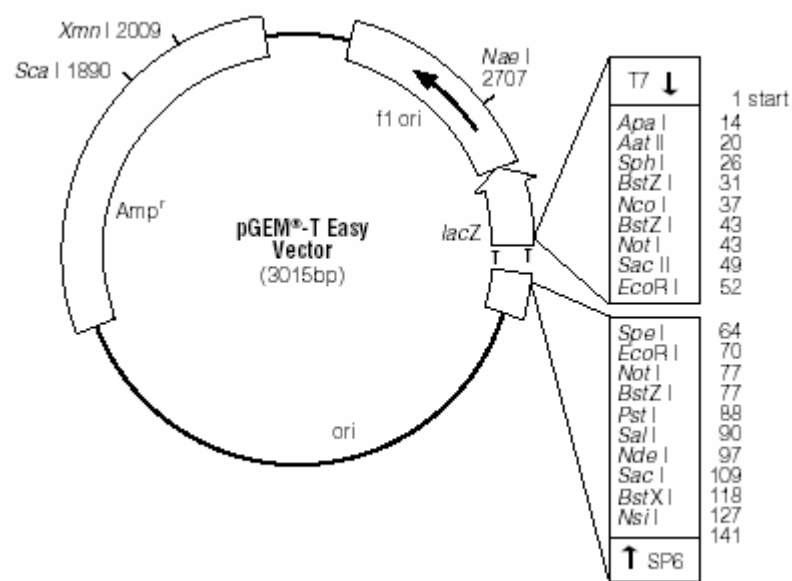
It is relatively easy to clone PCR products into pGEM-T Easy by the T/A-cloning method. PCR products amplified with *Taq* DNA-polymerase or with Expand High Fidelity DNA-polymerase (2.15.8) have an overhanging A at their 3'-ends. Corresponding to that, the vector pGEM-T Easy has an overhanging T at its 3'-ends so that such PCR products can be ligated into it without further modifications.

The ligation reaction (10 µl) contained 1 µl (1 U/µl) T4-DNA-ligase (Promega, Madison, USA), 1 µl 10 x ligase buffer, 25 ng vector and the insert in an amount suited to provide a molar vector:insert ratio in the range of 1:3 to 1:10.

$$ng\ insert = \frac{ng\ vector * size\ of\ insert\ (kb)}{size\ of\ vector\ (kb)} * molar\ ratio\ \frac{insert}{vector}$$

The reaction was performed at 16 °C overnight. The 10 x ligase buffer contained 300 mM Tris-HCl (pH 7.8 at 25°C), 100 mM MgCl<sub>2</sub>, 100 mM DTT and 10 mM ATP.

For cloning and analysis of PCR products, the vector pGEM<sup>®</sup>-T Easy (Amp<sup>r</sup>, Promega) was used.



### 2.16.11. Transformation of *E. coli* competent cells

The competent cells were thawed on ice. 5 µl ligation reaction or 50 – 200 ng plasmid DNA were added to the suspension of competent cells and mixed by pipetting. After incubation on ice for 20 min, the cells were incubated at 42°C for exactly 45 sec and transferred back to ice for a minute. 800 µl SOC medium were added to the cells under a laminar flow hood and the cells were incubated in a shaker at 37°C for an hour to allow the expression of antibiotic resistance genes. The cells were pipetted under a clean bench onto LB agar plates supplemented with the appropriate antibiotic(s) (2.15.13). If the cells were transformed with a ligation product in pGEM<sup>®</sup>-T Easy, the plates were supplemented with IPTG (40 µL 100 mM) and X-Gal (40 µL 2% (w/v) in DMF) that allowed for a blue-

white selection. The plates were dried and incubated at 37°C overnight. Single colonies were picked for analysis by colony-PCR (2.15.12), positive ones were grown overnight in LB with antibiotic(s) and plasmid-DNA was isolated (2.15.13). The DNA was characterized first by restriction enzyme digestion (2.15.14) and then by sequencing (2.15.15). In case of plates containing IPTG and X-Gal, blue colonies contained empty vector and only white colonies were picked for colony PCR.

**SOC medium:**

Select Pepton 140	2	% (w/v)
Yeast extract	0.5	% (w/v)
NaCl	10	mM
KCl	2.5	mM

The mixture was autoclaved for 10 min followed by the addition of filter-sterilized solutions of MgCl<sub>2</sub> (1 M), MgSO<sub>4</sub> (1 M) and glucose (2 M) under a clean bench to a final concentration of 10 mM, 10 mM and 20 mM, respectively.

**2.16.12. Colony PCR**

To identify positive clones of transformed bacteria, colony PCR was performed. A PCR master mix with gene-specific primers was prepared, containing all components except the DNA-template (2.15.8), and was distributed into 10-20 PCR-tubes, corresponding to the number of colonies to be analysed. Each colony was picked with a sterile toothpick. The toothpick was first dabbed into a PCR tube containing the mastermix and then streaked out on a correspondingly labelled patch of an LB-plate (2.15.13). The plate was incubated at 37°C. The PCR was performed using an appropriate program as described in 2.21 except that the first step at 94°C was extended (10 min) to break the cells. 10 µl of each PCR were run on 1% agarose gel to identify positive clones. These clones were used for the isolation of plasmid DNA.

### 2.16.13. Isolation of plasmid DNA

LB-medium (10 mL) supplemented with the appropriate antibiotic was inoculated with a single bacterial colony that was transformed with the gene of interest (verified by colony PCR, section 2.15.12). Cells were cultured overnight by incubating at 37°C in a shaker. The cultures were centrifuged at 4,000 xg for 10 min to obtain the cell pellets from which plasmid DNA was isolated using E.Z.N.A.<sup>®</sup> Plasmid Miniprep Kit II (Peqlab), according to the manufacturer's instructions. The plasmid-DNA was eluted with 50 µL ddH<sub>2</sub>O.

5 g/L Yeast extract  
10 g/L NaCl  
adjusted to pH 7.5 with NaOH  
for agar plates 1.5% (w/v) Select-Agar added before autoclaving

Antibiotics:	Stock solution	Final concentration
Ampicillin	100 mg/mL	100 µg/mL
Kanamycin	50 mg/mL	50 µg/mL

### 2.16.14. Restriction digest

Restriction digest was performed for further analysis of positive colonies. For a restriction digest, between 2 and 8.5 µL of plasmid-DNA (about 1 µg DNA) was mixed with 0.5 µL restriction enzyme and 1 µL of the appropriate 10x reaction buffer and made up to 10 µL with sterile ddH<sub>2</sub>O. The mixture was incubated for 1 h at 37°C followed by an electrophoretic analysis of the restricted fragments.

### 2.16.15. Sequencing

The method of Sanger *et al.* (1977) was followed for DNA-sequencing based on differential labelling of dideoxynucleotides using dRhodamine (ABI PRISM dRhodamine Terminator Cycle Sequencing Ready Reaction Kit, Perkin Elmer Applied Biosystems,

Weierstadt, Germany). The differentially labeled ddNTPs have absorption- and emission spectra at 450-650 nm. The PCR mix constituted the following:

Terminator Ready Reaction Mix	2 $\mu$ l
plasmid DNA	150-300 ng
sequencing primer	10 pmol
H <sub>2</sub> O	to 10 $\mu$ l

Sequencing primers are sections of the vector which are adjacent to the insertion site (2.15.7).

Chain elongation proceeded under the following conditions in a Personal Mastercycler (Eppendorf, Hamburg, Germany):

Cycle	Temperature	Duration
25	96 °C	10 sec
	50 °C	5 sec
	60 °C	4 min

#### 2.16.16. Precipitation of DNA

The DNA was precipitated using EDTA-sodium acetate in order to remove dRhodamine-ddNTPs that interfere with the sequencing. To 10  $\mu$ L PCR-mixture 3 M sodium acetate containing 125 mM EDTA were added to obtain a final concentration of 0.3 and 12.5 mM respectively and mixed by vortexing. Then 25  $\mu$ L 99.6% (v/v) ethanol were added and mixed by inverting. The samples were incubated for 15 min at room temperature, followed by centrifugation for 15 min at 13,000 rpm at 4°C. After removing the supernatant, the pellet was washed twice in 35  $\mu$ L 70% (v/v) ethanol. The pellet was dried for 10 min at 37 °C and finally dissolved in 30  $\mu$ L sterile ddH<sub>2</sub>O. The sample was then ready to be sequenced using ABI Prism 3100 Genetic Analyzer (Perkin Elmer Applied Biosystems, Weiterstadt, Germany). Verification for the nucleotide sequence was done using bioinformatics tools.

## 2.17. Biochemicals

Most chemicals were purchased from Sigma Aldrich (Taufkirchen, Germany), Merck (Darmstadt, Germany) and Carl Roth (Karlsruhe, Germany). Enzymes used for biochemical analyses were obtained either from Sigma or Roche Molecular Biochemicals (Mannheim, Germany) unless otherwise indicated. The restriction enzymes used in molecular biological analyses were from MBI, Fermentas (Vilnius, Lithuania).

## 2.18. Kits

The following kits were used in this study

Low molecular weight calibration Kit	Amersham Biociences, Freiburg, Germany
PhosphoProtein Purification Kit	BD Biosciences, San Jose, USA
Invisorb <sup>®</sup> Spin Plant RNA Mini Kit	Invitek, Berlin, Germany
E.Z.N.A. <sup>®</sup> Plasmid Miniprep Kit II	Peqlab, Erlangen, Germany
Qiaquick Gel extraction kit	QIAGEN GmbH, Hilden, Germany
ABI PRISM dRhodamine Terminator Cycle Sequencing Ready Reaction Kit	Perkin Elmer Applied Biosystems, Weiterstadt, Germany

## 2.19. Bacterial strain

The following *Escherichia coli* strain was used:

Stock	Genotype	Reference	Application
DH5 $\alpha$	F <sup>-</sup> ( $\Phi$ 80d <i>lacZ</i> $\Delta$ M15) <i>recA1 end A1 gyrA96 thi-1 hsdR17</i> (r <sub>k</sub> <sup>-</sup> m <sub>k</sub> <sup>+</sup> ) <i>supE44 rel A1 deoR</i> $\Delta$ ( <i>lacZYA-argF</i> ) U169	Woodcock <i>et al.</i> 1989	Cloning of PCR-products

## 3. Results

### 3.1. Isolation of leaf peroxisomes from *Spinacia oleracea* L. and *Arabidopsis thaliana* (L.) Heynh.

Plant peroxisomes are specialized subcellular compartments whose well-known primary roles include photorespiration, breakdown of fatty acids and metabolism of reactive oxygen species (ROS). However, their metabolic capacity has, apparently, been largely underestimated. This is underscored by the increasing recognition of a role for plant peroxisomes in diverse aspects of cell function, such as, sulfur metabolism (Eilers *et al.*, 2001; Nakamura *et al.*, 2002), generation of nitric oxide (Barroso *et al.*, 1999), biosynthesis of plant hormones like jasmonic acid (Stintzi and Browse, 2000; Sanders *et al.*, 2000; Strassner *et al.*, 2002), auxin metabolism (Zolman *et al.*, 2001) and catabolism of branched amino acids (Gerhardt 1993; Zolman *et al.*, 2001). The rationale for a proteomic study of the plant peroxisome is that the establishment of the plant peroxisomal proteome, which catalogues nearly all the proteins present within this organelle, may provide the key towards a better understanding of its full metabolic potential. The term 'proteome' is used to denote the functional complement of the genome. The ideal choice of a model plant for proteomic investigations would be *Arabidopsis thaliana* (L.) Heynh., owing to its fully sequenced genome that facilitates downstream applications (The Arabidopsis Genome Initiative, 2000). The small size of this plant, however, renders this organism far less suited for biochemical studies and especially 'notorious' for organelle preparations. Therefore *Spinacia oleracea* L. was initially chosen as the model plant to carry out proteome studies on leaf peroxisomes because of the relative ease with which these organelles can be obtained. In this study, an established protocol (Yu and Huang, 1986) that yields large quantities of leaf peroxisomes from this plant was further improved to significantly increase purity so as to make it more suitable for proteome investigations. The leaf peroxisomal proteins were used to optimize the method for two-dimensional electrophoresis (2-DE) and to generate a proteome map of the organelle. In parallel, a method was developed to enrich leaf peroxisomes from *A. thaliana*. Although being apparently far from optimal



(especially in comparison with the yield and purity from spinach), this method yielded good qualities of leaf peroxisomes which were suitable to generate two-dimensional maps.

### **3.1.1. Improvement of the purity of leaf peroxisomes from *Spinacia oleracea* L.**

An important pre-requisite for correct interpretation of the results by a proteomic approach is the purity of samples to be analyzed. For instance, proteins that are known to have a certain subcellular location may have novel isoforms in different locations. Isoforms of superoxide dismutase (SOD), for instance, have been shown to be present in chloroplasts, mitochondria and peroxisomes (Srivalli and Chopra, 2001). Also, NADP-dependent glucose-6-phosphate dehydrogenase of the oxidative pentose phosphate pathway, located in the plastids and the cytosol, was reported from plant peroxisomes (Corpas *et al.*, 1998). If the purity of the organelles analyzed is questionable such 'novel' proteins may be dismissed as artefacts resulting from the contaminants. Thus, the significance of the purity in proteome studies cannot be overemphasized.

#### **3.1.1.1. A preparative method for isolating leaf peroxisomes for proteome analyses**

Leaf peroxisomes of good purity can be isolated from spinach leaf tissue and purified via Percoll density gradient centrifugation (2.2.1.1.). This method is based on a procedure described by Yu and Huang (1986) and was adapted by Reumann (1996) for the large-scale analysis of membrane proteins. For peroxisome isolation, 8 to 12 weeks old apparently healthy plants were used. These were cultivated hydroponically with a 9/15 h light-dark cycle. The extent of contamination of the leaf peroxisomes with mitochondria and chloroplasts, obtained using this method, estimated on the basis of marker enzyme activities, fumarase and NADP-dependent glyceraldehyde-3-phosphate dehydrogenase (NADP-GAPDH), was about 1% and 4%, respectively (Table 3.1). To increase their purity, a method was established in this study, in which peroxisomes obtained from the Percoll density gradient were first washed, homogenized to reduce aggregation of organelles, and further purified on a continuous 40-60% (w/v) sucrose density gradient (Fig. 3.1).

Following sucrose density gradient centrifugation the peroxisomes formed an intense band half-way into the gradient and were well separated from residual mitochondria and chloroplasts which were located at the upper third of the gradient (data not shown). Peroxisomes (marker enzyme: hydroxypyruvate reductase, HPR) equilibrated roughly at 52.5% (w/w) sucrose while mitochondria (marker enzyme: fumarase) and chloroplasts (marker: chlorophyll) equilibrated roughly at 48% (w/w) and 45% (w/w) sucrose, respectively. The intense white band, constituting the peroxisomes was harvested (using a Pasteur pipette, after aspiration of the upper layers) and used for two-dimensional electrophoresis. This fraction contained between 65 and 95% of HPR activity loaded on the gradient. Following this step, the mitochondrial contamination was estimated as  $0.5 \pm 0.3\%$ , which is less than half of what was normally achieved with the Percoll density gradient purification alone (Reumann, 1996) and the chloroplast contamination was reduced to the detection limit at much less than 0.03% (Table 3.1).

However, plastid contamination of leaf peroxisomes was serendipitously discovered following mass spectrometric analysis of two-dimensionally resolved protein spots from the sucrose density gradient fractions. Proteins identified included aldolase, NADP-dependent glyceraldehyde-3-phosphate dehydrogenase (NADP-GAPDH), transketolase and phosphoglycerate kinase, among others (Appendix 1). Subsequently, the activity of NADP-GAPDH was determined and the level of contamination was estimated to be more than 25% in these samples. Because of the very low chlorophyll content (below detection limit) in these samples, the general term 'proplastid-like' organelle is used to refer to the contaminant. Also, these organelles equilibrated between 50 and 52% (w/w) sucrose, a density typical for proplastids in sucrose solutions.

Different methods were employed to reduce the contamination by the 'proplastid-like' organelles. The initial co-migration of NADP-GAPDH activity with HPR in linear sucrose density gradients of high resolution suggested an artificial adherence of these organelles to peroxisomes that probably occurred during their sedimentation. This association could partly be disrupted by mechanical means. By intensifying the extent of homogenization of the peroxisome suspension prior to density gradient centrifugation, the level of contamination by the proplastid-like organelles was reduced to a certain extent, and in some preparations, well resolved peaks could be obtained for hydroxypyruvate

reductase and NADP-dependent glyceraldehyde-3-phosphate dehydrogenase (NADP-GAPDH, marker for 'proplastid-like' organelles) (Fig. 3.1). Fairly consistent partial separation between the organelles could be achieved when a tight fitting Potter-Elvehjem homogenizer was used to carefully homogenize the peroxisome suspension.

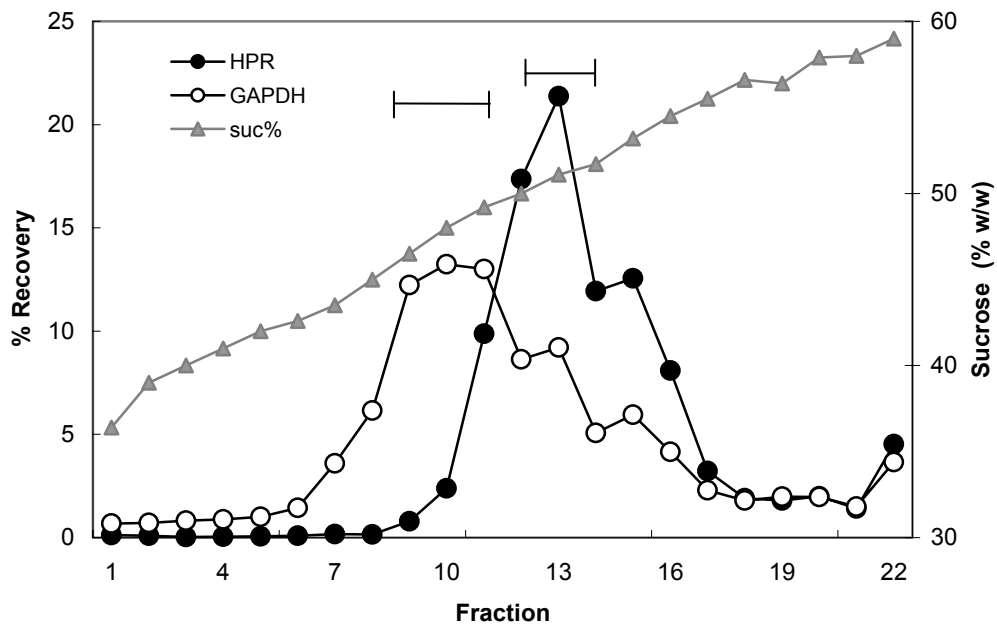


**Fig. 3.1: Separation of leaf peroxisomes and proplastid-like organelles from *Spinacia oleracea* L. by a second density gradient**

A fraction enriched for peroxisomes derived after Percoll density gradient centrifugation was homogenized in a tight fitting Potter-Elvehjem homogenizer and applied on a linear 40-60 % (w/w) sucrose density gradient and centrifuged at 83,000  $xg$  for 2 h. The enzyme activities of HPR (peroxisome marker) and NADP-GAPDH (proplastid-like organelles) were measured. Peroxisomes equilibrated at their typical equilibrium density of 52.5 % (w/w) sucrose in the gradient. The fractions 12-14 were significantly purified over the proplastid-like organelles (Table 3.1) which had an almost similar density although a broader peak (fr. 8-13) was obtained for NADP-GAPDH activity. Complete separation of the two organelles could not be achieved. A representative gradient from three independent experiments is shown ( $n=3$ ). 100% = activity loaded on the gradient (HPR and NADP-GAPDH)

For proteome studies, a subtractive-gel technique based on differential profiling was employed in order to differentiate the peroxisomal proteins from those originating

probably from the 'proplastid-like' organelles. Essentially, the 2-D pattern from the peroxisomal fractions (for example, Fig. 3.1: fr. 12 to 14) was compared with that of the fractions enriched in the proplastid-like organelles (fr. 9 to 11) in order to 'subtract' the contaminant proteins (Fig. 3.18, 3.3.4.1.).

### **3.1.1.2. An analytical method for isolating leaf peroxisomes for proteome analyses**

The method described above was suitable as a preparative process for obtaining good yields of leaf peroxisomes. However, it is imperative that subcellular fractionation for comparison of the peroxisomal proteome among different physiological states be done simultaneously. Some peroxisomal proteins are known to be regulated by diurnal rhythm (e.g., catalase, Zhong *et al.*, 1994; Polidoros and Scandalios, 1998) and by light (e.g., HPR, Mano *et al.*, 1999; Greenler *et al.*, 1990). This implies that it would be incorrect to compare proteomes of peroxisomes that have not been prepared at the same point of time. Keeping this in view, a shorter method was developed to isolate leaf peroxisomes for such analytical purposes. This method was based on the simultaneous separation of peroxisomes from the 'post-plastidic' supernatant and their purification within a single Percoll density gradient (see 2.2.1.2. for a description of the method). The important factors that contributed to the success of this method were the exclusion of artificial adherence enabled by separating an 'unsedimented' organelle fraction, and, the replacement of sucrose with raffinose as the osmoticum. The rationale for the replacement along with the elaborate preliminary processes involved in the development of this method is discussed elsewhere (4.1.2.).

The distribution of the various organelle markers in this density gradient is shown in Fig. 3.2. The activity peak for hydroxypyruvate reductase (HPR, peroxisomal marker enzyme) was detected at the bottom of the gradient (fr. 17 and fr. 18) and corresponded to the activity associated with intact peroxisomes. The activities of fumarase (mitochondrial marker) and NADP-dependent glyceraldehyde-3-phosphate dehydrogenase (NADP-GAPDH, marker for 'proplastid-like' organelles) were negligible in these fractions. They were well separated from the peroxisomes and effectively concentrated at the interface of

the 27% and 55% (v/v) Percoll layers (fr. 12). The large activity peak for HPR measured at the top of the gradient originated from broken organelles, which is to be expected since the 5,000  $xg$  supernatant contained a large proportion of broken peroxisomes. The yield of peroxisomes from this method was comparable to the yield obtained from other methods (Table 3.1).

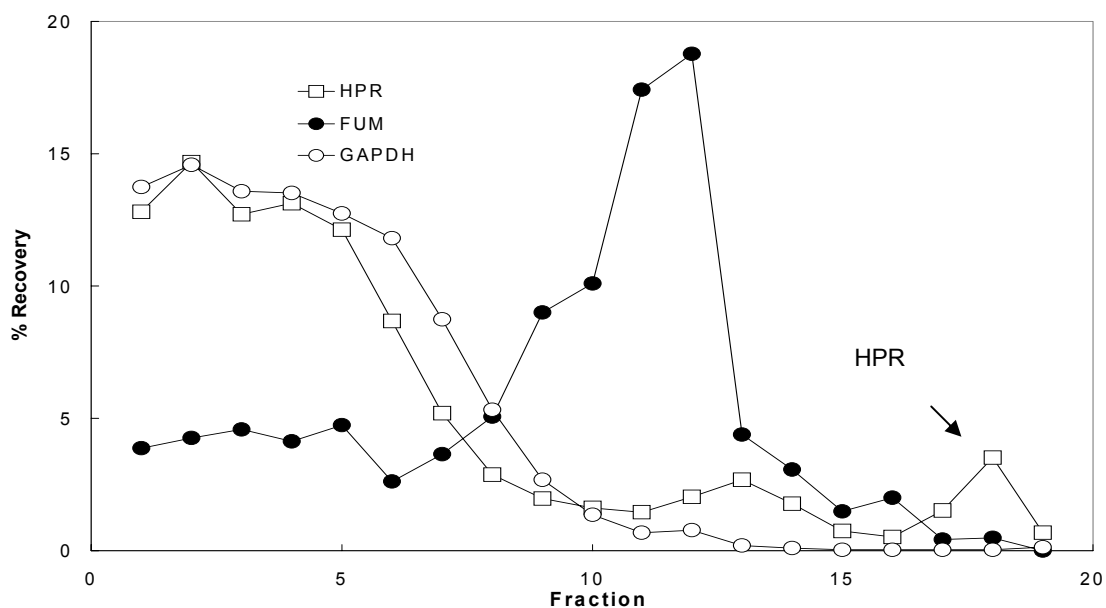


**Fig. 3.2: Analytical method to purify leaf peroxisomes from *Spinacia oleracea* L. by a single Percoll density gradient using raffinose**

The 5,000  $xg$  supernatant ('post-plastidic' fraction) derived from spinach leaf tissue harvested at the end of the light period was applied on a discontinuous (18-27% + 55% (v/v)) Percoll density gradient. The gradient was centrifuged at 10,000  $xg$  for 12 min. The distributions of HPR, fumarase and NADP-GAPDH were measured. The yield was comparable to that from other methods (Table 3.1). The apparently small peak (arrow head) of HPR activity at the bottom of the gradient is due to the lack of preselection for intact peroxisomes in the sample loaded on the gradient. Fractions 1-6 correspond to the loaded supernatant. The NADP-GAPDH activity was below the detection limit in the fractions (13-19) that constitute the 55% (v/v) Percoll layer. A major portion of mitochondria remained withheld by 55% (v/v) Percoll, although some migration into this layer is apparent. The 2<sup>nd</sup> peak for HPR (fr.11-15) may be due to peroxisomes that remained associated with the mitochondria. A representative gradient from three independent experiments is shown (n=3).

**Table 3.1: Comparison of methods for the purification of leaf peroxisomes isolated from *Spinacia oleracea* L. and *Arabidopsis thaliana* (L.) Heynh.**

(Yield of organelles was calculated as the percentage of marker recovered in the final peroxisome fraction with respect to the crude extract. The purification factor of peroxisomes was multiplied by the yield of other organelles to calculate the percentage of contamination)

Method of isolation of leaf peroxisomes	Yield (%)		% Contamination of peroxisomes	
	Peroxisomes (HPR)	Mitochondria (Fumarase)	Chloroplasts (chlorophyll)	Proplastid-like organelles (NADP-GAPDH)
<b><u>Spinach</u></b>				
Reported method *	5 to 11	ca. 1	not determined	ca. 4
Optimized method**	6 ± 1	0.5 ± 0.3	0.03 ± 0.03	>25
New analytical method §	5 ± 2	not detectable	not detectable	0.6 ± 0.2
<b><u>Arabidopsis</u></b>				
New preparative method§	4.2 ± 0.25	56 ± 25	6.5 ± 0.6	not determined
New analytical method§§	2 ± 0.2	2 ± 0.2	0.5 ± 0.2	0.2

\*Percoll density gradient method; \*\*Percoll density gradient enrichment followed by sucrose density gradient purification; § Post-plastidic-supernatant loading method using Percoll density gradient with raffinose; § Single sucrose density gradient method; §§ Two successive sucrose density gradient centrifugation method. Data are mean values of three experiments (n=3) ± SD.

Thus, to enable comparative proteome analysis, an efficient one-step purification method was developed for the preparation of leaf peroxisomes from *S. oleracea*. Further increase of Percoll concentration, to avoid sedimentation of peroxisomes was not possible because of crystallization of such highly concentrated Percoll-raffinose solutions at the low temperatures used during centrifugation.

### **3.1.2. Development of a method for the enrichment of leaf peroxisomes from *Arabidopsis thaliana* (L.) Heynh.**

Because of the distinct advantages of the fully sequenced genome (The Arabidopsis Genome Initiative, 2000), *Arabidopsis* is the model plant of choice for studies aimed at proteome analyses. Plant species that are close phylogenetic relatives of *A. thaliana*, such as members of Brassicaceae (e.g. *Brassica napus*) and those for which large collections of expressed sequenced tags (ESTs) libraries have been constructed such as, *Lycopersicon esculentum*, *Nicotiana tabacum* may also be lucrative alternatives. Until recently, no protocol has been published for the isolation of relatively pure peroxisomes from *Arabidopsis*. Although an enrichment of leaf peroxisomes from *Arabidopsis* has been reported earlier (Tugal *et al.*, 1999), these reports focused on an immunological characterization of peroxisomal proteins and therefore were not suitable for proteomic studies that demand high purity. Other cell organelles, such as, mitochondria (Millar *et al.*, 2001; Millar and Heazlewood, 2003) and endoplasmic reticulum (Prime *et al.*, 2000) have been isolated from heterotrophic cell suspension cultures of *Arabidopsis thaliana* and their proteome characterized successfully. However, an understanding of the diverse roles of peroxisomes in photosynthetic tissues can only be realized when the organelles are isolated directly from mesophyll cells. Thus, a method suitable for preparing reasonably pure peroxisomes from leaf tissues of *Arabidopsis* is, as yet, lacking. One of the important goals of this study was, therefore, to establish an efficient procedure for isolating leaf peroxisomes from *Arabidopsis*.

In preliminary experiments, the influence of several factors such as the age of the plants, and the illumination conditions, were investigated and optimum conditions were standardized within the limits of available resources (data not shown). For instance, the

effect of the size of the leaves on peroxisome yield and purity was investigated. Surprisingly, the size of the leaves did not seem to affect peroxisome purity and yield which were similar for a large-leaved *Arabidopsis* cultivar C24 and the smaller-leaved, most widely used cultivar Columbia (results not shown); the latter has been used for isolating leaf peroxisomes in this study.

### 3.1.2.1. Composition of a stabilizing buffer

The first step towards establishing an efficient protocol for the isolation of leaf peroxisomes from *Arabidopsis thaliana* was the choice of a homogenization buffer with optimum properties to stabilize peroxisomes. The 'intactness' of the isolated organelles was used to monitor their stability over a time-course. Intactness was calculated as the percentage enzyme activity of hydroxypyruvate reductase recovered in the pellet after sedimentation (25,000 *xg*) of a peroxisome fraction, relative to the total activity present in the unsedimented fraction.

The essential first step for any subcellular fractionation procedure is tissue disruption. The organelles are thereby liberated into a non-physiological environment and are vulnerable to the activities of the paraphernalia of proteases that are liberated from the vacuole and from disrupted organelles. Therefore, the capacity of the homogenizing buffer to maintain the integrity of the organelles during the time period between disintegration of tissues and density gradient centrifugation is a crucial factor that directly influences their final yield and consequently their purity.

Six buffers were chosen that differed in their composition with respect to either the osmoticum or the buffering substance. These have been reported as suitable for isolating peroxisomes from a variety of plants including *Arabidopsis* (Tugal *et al.*, 1999), castor bean (Mettler and Beevers, 1980), cucumber (Kindl and Kruse, 1983), pea (Lopez-Huertas *et al.*, 1995), spinach (Yu and Huang, 1986) and from yeast (Erdmann and Blobel, 1995). Of these, leaf peroxisomes from *Arabidopsis* were most stable in one that contained 1.0 M sucrose and 150 mM tricine, and was originally used for isolating pea leaf peroxisomes (Lopez-Huertas *et al.*, 1995). The intactness of freshly isolated *Arabidopsis* leaf peroxisomes in this buffer was  $67 \pm 8\%$ , immediately after homogenization ( $n > 10$ ) and  $53 \pm 7\%$  after 3 hours, indicating that the organelles maintained a relatively good integrity



(data not shown). In the other buffers, including that used for spinach, the intactness differed between 15 and 80% immediately following isolation but fell, in the case of the latter, below 10% within 3 h of standing on ice (data not shown).

The grinding buffer was further adapted for the isolation of *Arabidopsis* leaf peroxisomes. By reducing the sucrose concentration to 0.45 M and the tricine concentration to 50 mM, the peroxisome yield after sucrose density gradient centrifugation could be increased by nearly 18%. Addition of salts such as 10 mM KCl and 1 mM MgCl<sub>2</sub> and of 0.6% (w/v) polyvinylpyrrolidone-40 (PVP-40) to the medium also improved yield although the beneficial effect of these individual components was not investigated quantitatively. The addition of the protease inhibitor phenyl methyl sulfonyl fluoride (1 mM) however, led to a decrease in the stability of peroxisomes by about 16%. The addition of glycerol (5% (v/v)) did not have a beneficial effect either on the yield or on the purity of peroxisome preparations from *Arabidopsis* (data not shown). With the optimized buffer, between 15 and 20% of hydroxypyruvate reductase activity could be recovered in the fraction enriched for peroxisomes by differential centrifugation which was further purified by isopycnic centrifugation using a discontinuous sucrose density gradient.

### **3.1.2.2. Enrichment of leaf peroxisomes from *A. thaliana* by sucrose density gradient centrifugation**

Prior to sucrose, a number of different commercially available density gradient media, such as, the iso-osmotic chemicals Percoll, Nycodenz and Ficoll, were evaluated for their efficiency to enrich leaf peroxisomes from *Arabidopsis*. Rather surprisingly, the best yield and purity were, by far, obtained in a sucrose density gradient that comprised of short layers of 18, 25 and 35% (w/w) sucrose to provide a gradual increase of osmotic pressure over a 40-50% (w/w) linear part for optimal separation of peroxisomes from chloroplasts and mitochondria. A layer of 60% (w/w) sucrose was used underneath to cushion the sedimenting peroxisomes. The distribution profile of the different organelle markers in one representative gradient is shown in Fig. 3.3.

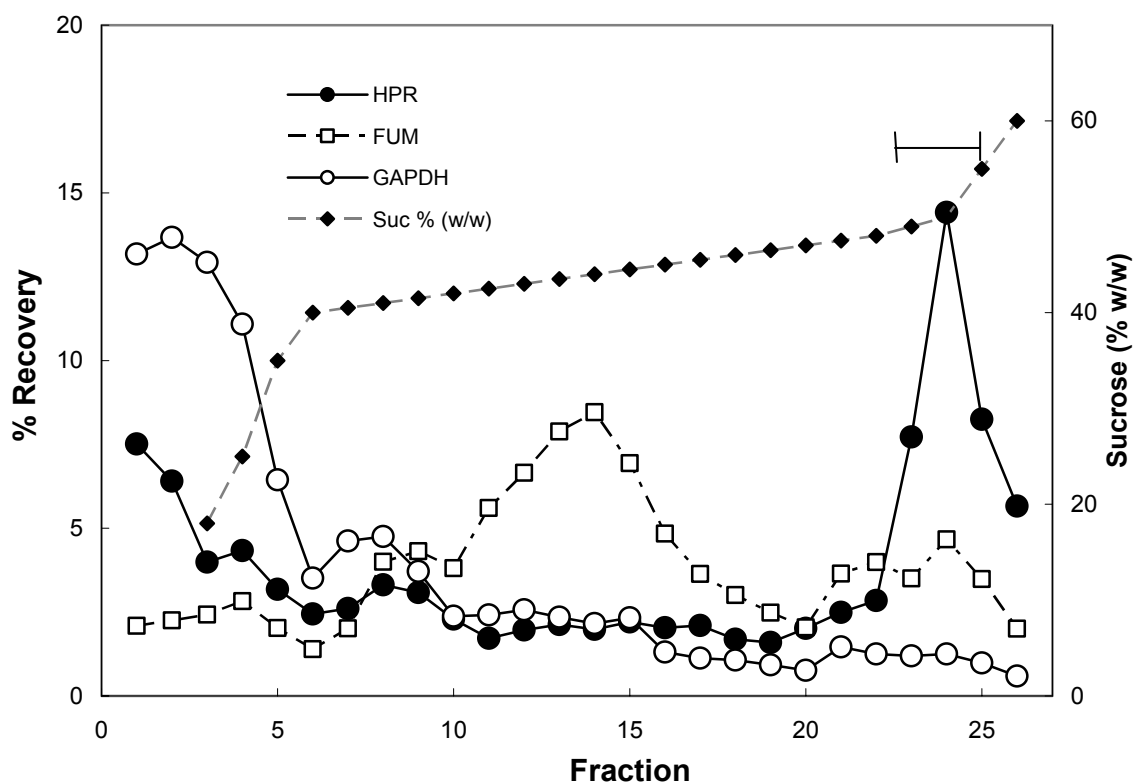


**Fig. 3.3: Distribution of marker enzyme activities in a linear sucrose density gradient used to enrich leaf peroxisomes from *Arabidopsis thaliana* (L.) Heynh.**

A peroxisome fraction (25,000  $xg$  pellet) derived from *Arabidopsis* leaf tissue was applied to a discontinuous sucrose density gradient (18, 25, 35% (w/w) over a linear gradient of 40-50% (w/w) on a 60% (w/w) sucrose cushion). The gradient was centrifuged at 83,000  $xg$  for 2 h in an ultracentrifuge. The distributions of HPR, fumarase and NADP-GAPDH were measured. Fraction 1 is at the top of the gradient. Peroxisomes were enriched at the interface of 50 and 60% sucrose layers (23 to 25, horizontal bar), and were well separated from the mitochondrial peak (Fr. 11-16). Some mitochondria were also present in the peroxisome fraction, probably due to adherence. The NADP-GAPDH activity was relatively low in the peroxisome fraction (Table 3.1). High peroxisome integrity in the applied sample was indicated by the low activity of HPR at the top of the gradient. One representative gradient from three independent experiments is shown ( $n=3$ ). 100%= activity loaded on gradient.

After sucrose density gradient centrifugation the peroxisomes formed a light green band above the 60% (w/w) sucrose cushion. The average yield of leaf peroxisomes from the sucrose density gradients was about 4% with respect to the activity in the crude extract (Table 3.1). The mitochondria and chloroplasts were located roughly at 48% and 45% (w/w) sucrose, respectively. Despite the good separation of mitochondria and peroxisomes, the contamination by mitochondria was relatively high ( $56 \pm 25\%$ ) due to the higher stability of mitochondria in the homogenization buffer (Fig. 3.3, Table 3.1). The

chloroplast contamination was about 7% (Table 3.1). The presence of additives such as KCl, MgCl<sub>2</sub>, EDTA, PVP-40 and glycerol in the density gradient (at concentrations as optimized for the homogenization buffer) did not result in a better yield or separation of peroxisomes (data not shown).

In order to enhance purity, the peroxisome fraction (fr. 23 to 25) was further purified via a second density gradient. In this method peroxisomes were further purified by floatation of mitochondria and chloroplasts and migration of peroxisomes to the bottom of the gradient. The concentration of sucrose in the peroxisome fraction was reduced from 52.5% (w/w) to 48% (w/w) by a gradual and careful dilution using 25% (w/w) sucrose and the diluted sample was transferred to ultracentrifuge tubes. A cushion of 60% (w/w) sucrose was laid beneath and a layer of 45% (w/w) sucrose was applied over the organelle fraction. The contaminating organelles were separated via floatation by a high-speed centrifugation for 16 to 18 h. This step reduced the contamination, especially with respect to mitochondria, to significantly lower levels (Table 3.1). The peroxisomes thus obtained were contaminated with mitochondria only by about 2%. The level of chloroplast contamination was about 0.5%. Exceptionally pure preparations were used for two-dimensional electrophoresis.

In summary, it was possible to enrich leaf peroxisomes from *A. thaliana* using an appropriate combination of methods. The purity of the organelles, thus obtained, allowed for their use in proteome studies.

### **3.2. Resolution of soluble matrix proteins of leaf peroxisomes by two-dimensional electrophoresis**

For proteome analysis of leaf peroxisomes, a two-dimensional gel based mass spectrometry approach was employed. By this method, the proteins were first separated in the first dimension according to their isoelectric point. Commercially available immobilized pH gradient (IPG) strips (Amersham Biosciences) were used for the first dimension isoelectric focusing. In the second dimension, proteins were resolved based on their mobility in polyacrylamide gels.

Efficient solubilization of proteins during the first-dimensional immobilized pH gradient (IPG) separation has a direct impact on their successive transfer to the second-dimension gel. Proteins that are insoluble or poorly soluble in the solubilization buffer will remain excluded further downstream. In a standard procedure for the preparation of two-dimensional gels, the proteins are usually solubilized in a buffer containing high concentrations of a chaotrope (up to 9.5 M urea), a surfactant (up to 4% (w/v) non-ionic or zwitterionic detergents), and a reducing agent such as dithiothreitol or tributyl phosphine. However, a universal buffer is not available that has the capacity to completely solubilize the wide variety of complex protein mixtures obtained from biological samples. The most suitable one for an individual sample has to be empirically determined according to the specific needs of the experiment. In an attempt to get a true 'snapshot' of the diverse protein components of the leaf peroxisome, the chaotrope and surfactant compositions of the 2-D solubilization buffer were manipulated to maximize protein recovery and spot resolution.

### 3.2.1. Optimization of chaotrope composition

The demonstration of the usefulness of thiourea in conjunction with urea for enhanced recovery of hydrophobic proteins and proteins with neutral isoelectric points was a breakthrough in two-dimensional electrophoresis (2-DE) with respect to sample solubilization (Rabilloud *et al.*, 1998a). Thiourea ( $\text{NH}_2\text{C}(\text{S})\text{NH}_2$ ) is derived from urea ( $\text{NH}_2\text{C}(\text{O})\text{NH}_2$ ) by the substitution of the oxo-group for a thio-group, within the carbonyl function. While several reports in general favoured the use of thiourea in 2-DE solubilization buffers, a high concentration can have an undesirable effect on protein resolution (Musante *et al.*, 1998). Therefore, the effect of thiourea in the 2-DE solubilization buffer used to solubilize leaf peroxisomal proteins was investigated.

Leaf peroxisomal proteins from spinach purified by two successive density gradients were solubilized in a 2-DE solubilization buffer that contained either 9 M urea or a mixture of 7 M urea and 2 M thiourea. The samples were clarified by centrifugation to separate soluble and insoluble proteins. The pattern of proteins recovered in these fractions was analyzed by one-dimensional sodium dodecylsulfate polyacrylamide gel

electrophoresis (1-D SDS-PAGE). Different concentrations of protein were tested in order to ascertain the influence of protein concentration on the efficiency of solubilization. The results are shown in Fig. 3.4 and in Table 3.2.

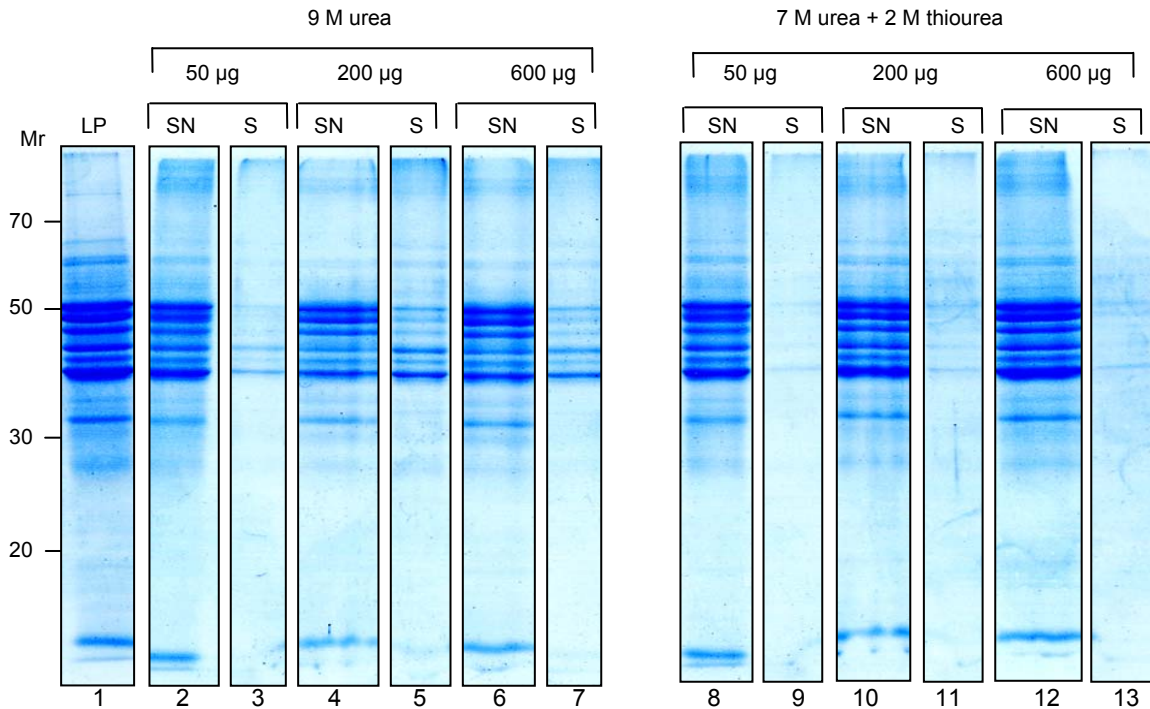


Fig. 3.4: Effect of thiourea on protein recovery demonstrated by one-dimensional SDS-PAGE

Spinach leaf peroxisomal proteins were precipitated with chloroform methanol (Wessel and Flügge, 1984) and solubilized in 350  $\mu$ L 2-DE solubilization buffer containing either 9 M urea or 7 M urea + 2 M thiourea. Three different quantities of protein were used (50, 200 and 600  $\mu$ g). Both buffers contained 4% w/v CHAPS as detergent, 3 mg/mL DTT as reducing agent and 0.5% (v/v) IPG buffer. Proteins were solubilized in a laboratory shaker for 2 h at RT after which the samples were clarified by centrifugation at 13,000 rpm for 20 min. Assuming complete solubilization, a sample volume corresponding to 10  $\mu$ g protein in the supernatants was mixed with an equal volume of 2xSDS-sample buffer and loaded in each lane of a 12.5% SDS-polyacrylamide gel (lanes indicated as SN). The sediments were dissolved in SDS sample buffer and a volume equivalent to the supernatant analyzed (lanes indicated as S). Lane 1 (LP) represents the unfractionated sample directly solubilized in SDS sample buffer. After SDS-PAGE, proteins were visualized by Coomassie staining. The presence of thiourea enhanced qualitative and quantitative protein recovery. Solubilization of some high molecular mass proteins (> 70 kDa) required the presence of thiourea. Adequate representation of low molecular mass proteins (< 20 kDa) required higher protein concentrations. (results shown here represent one of two independent experiments)

**Table 3.2: Summary of solubilization of proteins from leaf peroxisomes of *S. oleracea* in the presence or absence of thiourea as revealed by one-dimensional SDS-PAGE analysis**

Protein size (kDa)	LP	9 M urea						7 M urea + 2 M thiourea					
		50 µg		200 µg		600 µg		50 µg		200 µg		600 µg	
		SN	S	SN	S	SN	S	SN	S	SN	S	SN	S
above 70	++	+	-	-	+	-	+	+	-	+	-	+	-
50 to 30	++	++	+	++	+	++	+	++	-	++	-	++	-
30 to 20	++	+	-	+	-	+	-	++	-	++	-	++	-
below 20	++	-	-	-	-	-	-	-	-	-	-	+	-

Abb: SN: supernatant; S: sediment; LP: leaf peroxisome; ++: high recovery or 100%+; partial recovery; -: significantly low recovery or absent

Overall, the protein profile of solubilized proteins (lanes labelled as SN) represented a nearly true profile of the original sample (lane 1). After solubilization, proteins of molecular mass higher than 70 kDa appeared as less intense bands irrespective of the method of solubilization although in the presence of thiourea, their intensity was comparatively higher. The efficiency of solubilization with respect to the inclusion of thiourea in the buffer and in relation to increasing protein concentrations was reflected by the protein pattern and content obtained in the sediments. The amount of insoluble proteins recovered in the sediments (lanes labelled 'S') after solubilization exclusively with urea increased progressively with increasing protein concentration. By contrast, the recovery of proteins in the sediments was negligible when thiourea was included, indicating nearly complete solubilization. It appeared, however, that the loss of low molecular mass proteins was more pronounced. Small proteins (< 20 kDa) were recovered in the supernatant only when a relatively high protein concentration was used (600 µg, corresponding to 1.8 mg/mL) in conjunction with a buffer containing thiourea. These proteins were not present when lower concentrations were used or when thiourea was absent in the two-dimensional electrophoresis (2-DE) buffer. However, the absence of such proteins in the corresponding sediments suggested that the loss cannot be accounted entirely to the inefficiency of the 2-DE buffers alone.

For a more detailed analysis, the resolution of proteins following their solubilization with either of the buffers was examined using two-dimensional (2-D) gel electrophoresis.

An improved recovery was achieved for proteins both in the acidic and basic regions of the gel. As already indicated on the one-dimensional gel, the presence of thiourea was found to be necessary for enhanced recovery of some of the high molecular weight proteins, as estimated by the intensity of some of the spots on the 2-D gels. Results are shown in Fig. 3.5 and in Table 3.3.

In summary, the overall recovery of proteins, both qualitative and quantitative, was higher in the supernatants obtained in the presence of thiourea than in its absence. This suggested that the presence of thiourea in the 2-D solubilization buffer, by improving its solvating properties, increased the recovery of solubilized proteins in the supernatant. The effect was more pronounced for samples of higher protein concentration and is particularly valuable for preparative separations that require significantly higher protein loads. The overall resolution was not affected significantly by the presence of thiourea in the 2-D solubilization buffer.

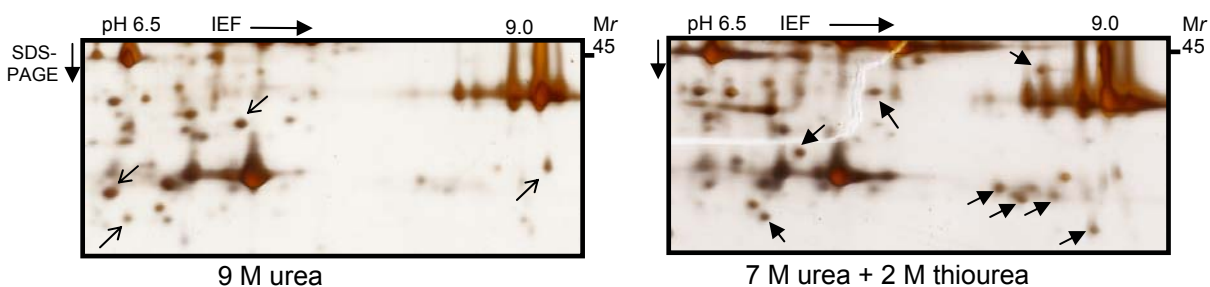


Fig. 3.5: Effect of thiourea on protein recovery and resolution in 2-DE

Equal protein amounts (50  $\mu$ g) extracted from spinach leaf peroxisomes (see Fig. 3.4) were solubilized with 2-DE solubilization buffer containing 9 M urea or with 7 M urea + 2 M thiourea. The remaining components of the buffer are as indicated in Fig. 3.4. The solubilized proteins were clarified by centrifugation and the supernatants were used to rehydrate IPG strips (pH 3-10 NL) at a constant voltage of 30 V for 10 h. Isoelectric focusing was performed up to a total of 57 kVh. After IEF, IPG strips were equilibrated and sealed on to 12.5% T second dimension gels. The resolved proteins were visualized by staining with silver. Thiourea improved the recovery of several proteins (closed arrowheads). The apparently lower resolution for proteins dissolved in thiourea-containing solubilization buffer is probably due to the higher protein recovery. A few other proteins, however, were more dominant in the presence of 9 M urea (open arrowheads). Representative results from  $n > 3$  experiments is shown.

### 3.2.2. Optimization of detergent composition

Detergents are included in the two-dimensional electrophoresis (2-DE) solubilization buffer to prevent interactions that may occur through chaotrope-generated exposure of hydrophobic domains. The detergents widely used for 2-DE have been classified structurally into three major types (Rabilloud, 1996). Detergents of type-1 contain a phenyl ring in the hydrophobic part and an oligooxyethylene polar head (e.g., Triton-X 100, Nonidet P-40). Type-2 detergents contain a linear alkyl tail and a hydrophilic sugar-based polar head (e.g. N-octylglucoside). Type-3 detergents carry sulfobetaines as polar head groups (e.g., CHAPS and ASB-14). These three types of detergents were tested either alone or as detergent cocktails for their efficiency to solubilize proteins from leaf peroxisomes. Protein recovery and resolution were the two main criteria considered for evaluating their performance. Results are presented in Fig. 3.6.

Two detergents of type-3 were tested, namely, CHAPS and ASB-14. Of these, CHAPS gave better results than ASB-14, as good spot resolution was obtained with only minimal streaking, indicating high protein solubility (Fig. 3.6 a). The solubilization was less effective when using ASB-14; while the dominant proteins were recovered, the overall amount of protein was lower, and many of the less abundant proteins were missing (Fig. 3.6 b). The detergent N-octylglucoside improved protein recovery when supplemented to CHAPS or ASB-14 (Fig. 3.6, compare (a) and (b) with (c) and (d), respectively). However, its presence in combination with either CHAPS or ASB-14 also led to a noticeable distortion of protein spots at the lower regions of the gel (Fig. 3.6 f). The performance of a solubilization buffer containing NP-40 and CHAPS was poor with respect to recovery of proteins (Fig. 3.6 e).

It was concluded on the basis of these comparative analyses that CHAPS allowed an efficient 2-DE analysis of leaf peroxisomal proteins at a concentration of 4% (w/v), and that a supplement of N-octylglucoside may have to be applied with caution (Table 3.2).



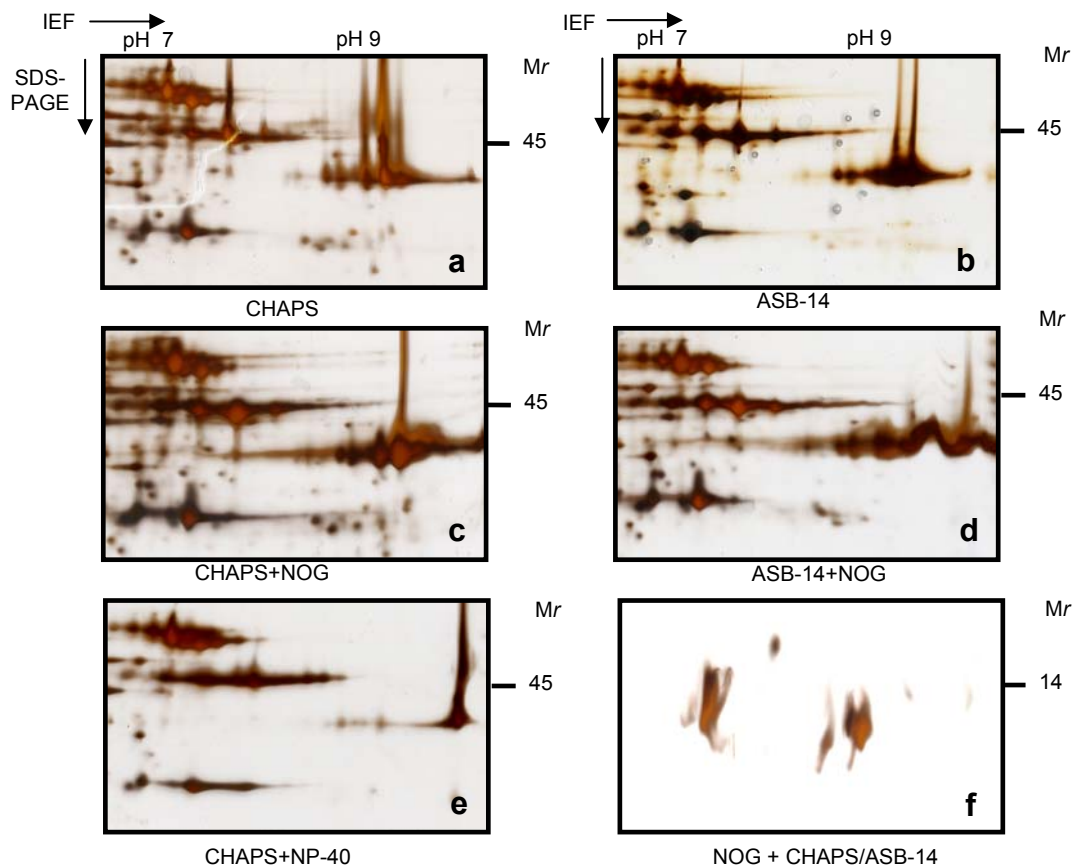


Fig. 3.6: Effect of different detergents on protein recovery and resolution in 2-DE

Proteins (50  $\mu$ g) extracted from spinach leaf peroxisomes were solubilized in the presence of different detergents (a) 4% (w/v) CHAPS (b) 2% (w/v) ASB-14, (c) 2% (w/v) CHAPS + 2% (w/v) N-octylglucoside, (d) 2% (w/v) ASB-14 + 2% (w/v) N-octylglucoside (NOG), (e) 2% (w/v) CHAPS + 2% (w/v) NP-40 and (f) represents region from either 2% (w/v) CHAPS or 2% (w/v) ASB-14 + 2% (w/v) N-octylglucoside. All buffers contained 7 M urea and 2 M thiourea, 3 mg/mL DTT and 0.5% (v/v) IPG buffer 3-10. Identical regions from the different gels are presented in (a) to (e) whereas is the region shown in (f) is from a lower part of the gel, as indicated on the right. CHAPS was the best performing detergent (a), and gave a much better recovery than the other sulfobetaine-based detergent ASB-14 (b). Supplementing CHAPS or ASB-14 with N-octylglucoside (c, d, respectively) significantly enhanced recovery of proteins but resulted in distortion of proteins at the lower region of the gel (f). Solubilization in the presence of NonidetP-40 reduced protein recovery (e). CHAPS: 3-[(3-cholamidopropyl)-dimethylammonio]-propanesulfonate, ASB-14: amidosulfobetaine-14; NOG: N-octylglucoside, NP-40: NonidetP-40. Results represent 2 independent experiments (n=2).

**Table 3.3: Summary of protein solubilization in the presence of different chaotropes and detergents**

Sample solubilization method	No. of spots detected			
	Acidic pI < 7	Basic pI > 7	Low mol mass (< 20 kDa)	High mol mass (>70 kDa)
U + CHAPS	70 to 90	35 to 40	10 to 14	25 to 30
UT + CHAPS	> 90	40 to 60	10 to 14	50 to 70
UT + CHAPS + NOG	> 90	45 to 60	distortion	50 to 70
UT + ASB-14	50 to 70	20 to 40	< 4	15 to 20
UT + ASB 14 + NOG	> 90	25 to 45	distortion	50 to 60
UT + CHAPS + NP-40	<50	10 to 15	< 6	3 to 5

Abbreviations: ASB-14: Amidosulfobetaine-14; CHAPS: 3-[(3-cholamidopropyl)-dimethylammonio]-propanesulfonate, NOG: N-octylglucoside, NP-40: NonidetP-40; U: Urea (9 M); UT: Urea + thiourea mixture (7 M urea + 2 M thiourea). See legend for Fig. 3.6

### 3.2.3. Optimization for two-dimensional electrophoresis of alkaline proteins

Alkaline proteins are technically challenging for two-dimensional electrophoresis (2-DE) for several reasons; this includes reverse electro-endosmosis resulting in sample loss due to aggregation and migration of DTT out of the gel, and consequently, a streaky two-dimensional pattern (Görg *et al.*, 2000; Leimgruber *et al.*, 2002). For plant peroxisomes, there is a specific need to address basic proteins since a large number of its proteins have isoelectric points that occur within the alkaline pH range of 7.5-9.5 (Reumann *et al.*, submitted) as determined for all proteins from *Arabidopsis* with a putative major and minor peroxisome targeting signal (PTS1 or PTS2) (Reumann, in press).

Preliminary experiments were performed in order to test the effect of alcohols that can counteract reverse-electro endosmosis during isoelectric focusing (Görg *et al.*, 2000; Leimgruber *et al.*, 2002). The optimized 2-DE solubilization buffer containing 7 M urea and 2 M thiourea 4% CHAPS, 3 mg/mL DTT and 0.5% (v/v) immobilized pH gradient (IPG) buffer (3.2.1 and 3.2.2) was supplemented with alcohols, like isopropanol, isobutanol and glycerol, to solubilize peroxisomal proteins. The samples were resolved by 2-DE using commercially manufactured IPG strips of a linear pH range from 6-9 for optimum resolution in this pH range of interest (Fig. 3.7). The 2-D gel patterns indicated that the presence of isopropanol did not result in an improved protein resolution; instead, it had a negative effect on protein recovery (Fig. 3.7 b). The presence of isobutanol was disadvantageous both in terms of protein recovery and resolution (data not shown).

The presence of glycerol served to reduce protein precipitation at the basic end but the resolution was compromised (Fig. 3.7 c). Additionally, it appeared that the protein recovery was poor when glycerol was present in the 2-D solubilization buffer. A 2-D buffer containing N-octylglucoside instead of CHAPS, included for comparison did not lead to better recovery or resolution of basic proteins (data not shown).

These results suggested that inclusion of alcohols was not necessary and actually disadvantageous for two-dimensional electrophoresis of leaf peroxisomal samples.

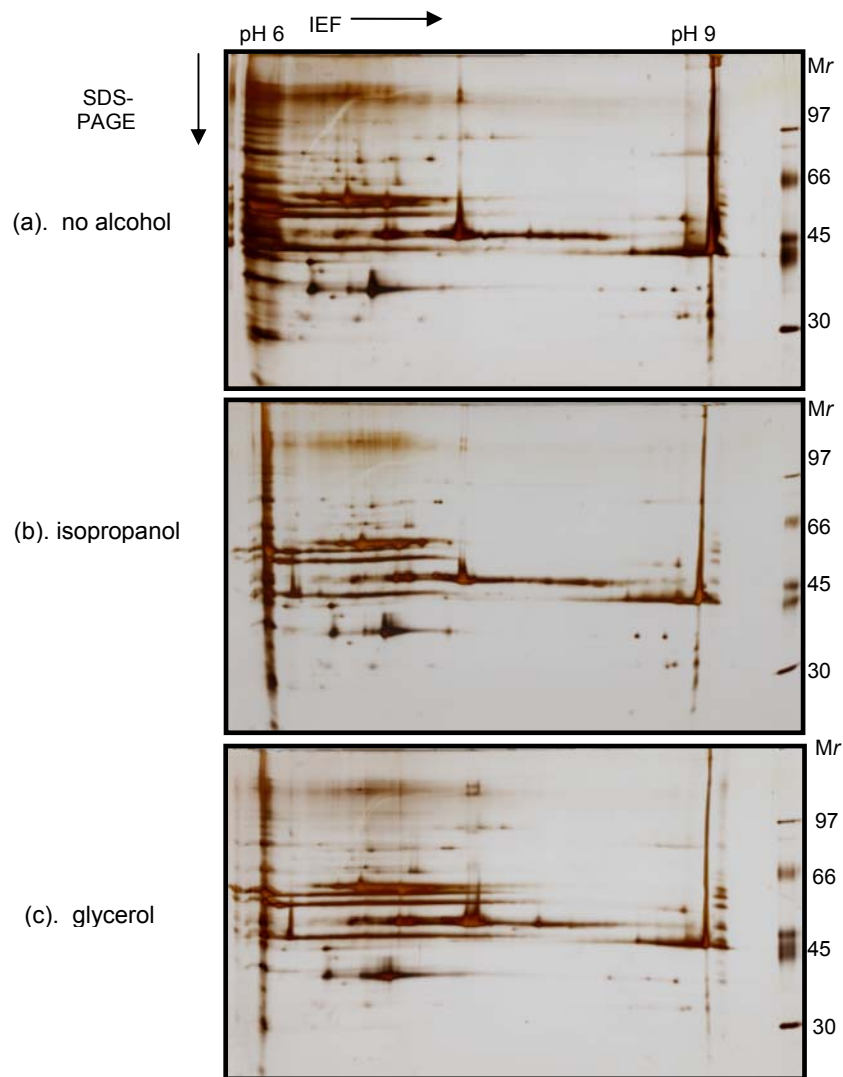


Fig. 3.7: Effect of alcohols on resolution of alkaline proteins in two-dimensional gels

Equal amounts of protein (50  $\mu$ g) extracted from spinach leaf peroxisomes were solubilized in the presence of 2-D solubilization buffer containing 7 M urea, 2 M thiourea, 3 mg/mL DTT and 0.5% (v/v) IPG buffer and analyzed in the absence of alcohols (a) or in the presence of 5% (v/v) isopropanol (b) or 5% (v/v) glycerol (c). Proteins were focused in IPG strips of a pH range from 6 to 9 for 80 kVh and subsequently resolved in the 2<sup>nd</sup> dimension by SDS-PAGE. Isopropanol did not improve protein resolution but had a negative effect on protein recovery (b). Glycerol reduced precipitation at the basic end (c) but protein resolution and recovery were poor. Results represent 2 independent experiments (n=2).

### 3.2.4. Optimization of other variables

Several other variables are known to contribute to the success of two-dimensional electrophoresis (2-DE). These include the type of sample entry into the immobilized pH gradient (IPG) strip, the duration of isoelectric focusing and the time for which the focused strips are equilibrated prior to the second dimension SDS-PAGE. In the present study, the proteins were incorporated into the IPG strip by an in-gel rehydration procedure. It was found that the application of a constant voltage of 30 V (active rehydration) during this process enhanced protein recovery as compared to an omission of voltage (passive rehydration). A focusing time between 45 and 80 kVh gave optimum recovery and resolution (data not shown), beyond which the spot patterns were either diffuse or showed increased streaking. Further, it was found that optimal protein recovery was obtained when IPG strips were equilibrated for a short time (12 min) in a small volume (5 mL) of equilibration solution (data not shown). A longer duration of incubation in larger volumes resulted in a considerable loss of proteins probably due to diffusion (data not shown).

### 3.2.5. Leaf peroxisomal proteome coverage

#### 3.2.5.1. Proteome coverage of leaf peroxisomes from *Spinacia oleracea* L. achieved by two-dimensional electrophoresis

Having optimized solubilization of leaf peroxisomal proteins with respect to recovery and resolution, the proteome of leaf peroxisomes was analyzed. Leaf peroxisomes from *S. oleracea* leaf tissue harvested shortly after the beginning of the light period were purified by sucrose density gradient centrifugation. The proteins were precipitated by the method of Wessel and Flügge (1984) and the resulting pellet was solubilized in the optimized two-dimensional electrophoresis (2-DE) solubilization buffer to resolve the complex protein mixture by 2-DE. Excellent resolution and reproducibility were achieved with an analytical protein load of 40 to 60 µg. The pattern of protein spots (Fig. 3.8) generated in a non-linear pH 3-10 gradient immobilized pH gradient (IPG) strip may be considered a general picture of the protein profile of matrix proteins of spinach leaf peroxisomes from apparently healthy tissue.

A total of more than 200 spots was reproducibly detected on an analytical gel. Taking into account that some non-peroxisomal proteins (originating mostly from

proplastid-like organelles) were also present, the actual number of 'truly' peroxisomal spots present on this map may be lower. The most abundant proteins had a pI greater than 6 (boxed area) while a considerable number of spots was also scattered over the pH range between 5 and 6. Highly acidic proteins (pI < 5) could not be detected on the 2-D gel. The region of the gel that corresponded to a molecular mass between 30 and 70 kDa had the highest spot density. Many known peroxisomal proteins are located in the same region (Fig. 3.8).

For the sake of convenience in description, the proteins are referred to by their identities (wherever identities are known) rather than as 'spots', in the forthcoming sections, although they may not have been identified from the gel that is being analyzed in the particular context; rather, identities may have been derived on the basis of 2-D parameters on analogous gels.

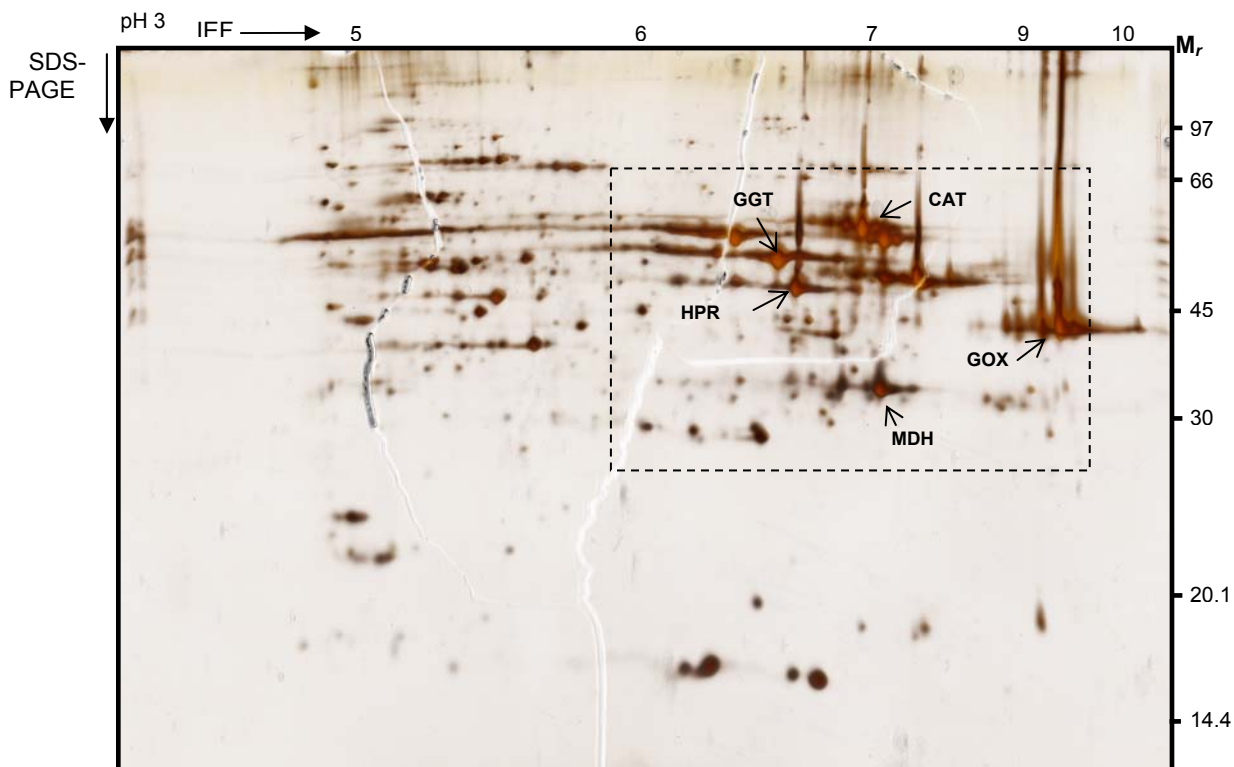


**Fig. 3.8: 2-D map of leaf peroxisomal proteins from *Spinacia oleracea* L. using a broad range IPG strip**

Peroxisomes were prepared from plants were harvested shortly after the beginning of the light period. About 50  $\mu\text{g}$  soluble leaf peroxisomal proteins (purified from two successive density gradients) were solubilized with 2-D solubilization buffer (7 M urea, 2 M thiourea, 4% (w/v) CHAPS, 3 mg/mL DTT, 0.5% (v/v) IPG buffer 3-10) for 2 h in a laboratory shaker and subjected to 2-DE using an IPG strip of a non-linear pH gradient from 3-10 for the 1<sup>st</sup> dimension IEF and a 12.5% acrylamide gel for the 2<sup>nd</sup> dimension SDS-PAGE. More than 200 protein spots were visualized after silver staining according to Blum *et al.* (1984). The boxed area (pH ca. 6.5 to 9.5; mol. mass 30-70 kDa) represents a region of the gel with high spot density in which most of the dominant peroxisomal proteins are present. The identity of the proteins was inferred based on their localization by analogy to those later on identified by MS. Such proteins are indicated. Abbreviations: GGT: glutamate-glyoxylate aminotransferase, CAT: Catalase, HPR: hydroxypyruvate reductase, GOX: glycolate oxidase, MDH: malate dehydrogenase.

### 3.2.5.2. Increasing proteome coverage by narrow range immobilized pH gradient (IPG) strips

One of the methods employed to increase proteome coverage on the 2-D maps was the use of narrow pH range immobilized pH gradient gels for the first dimension isoelectric focusing to 'zoom-in' on regions of high spot density. An IPG strip that offered resolution of proteins with isoelectric points between 6 and 11 was used to overcome the

lack of resolution due to spot overlap. This strip served to display the catalase (CAT) isoforms as distinct spots. A slightly better resolution was also evident for the isoforms of glycolate oxidase (GOX). Apparently, these zoom-in gels were also most advantageous to resolve the region that contained proteins such as ketothiolase, sulfite oxidase (SOX), 12-oxophytodienoate reductase (OPR3), etc. (boxed region, Fig. 3.9 a). Besides, some additional proteins were detected only on this map (arrowheads, Fig. 3.9 a). An IPG strip of the same size (18 cm) that offered a much greater linear separation range of 2 pH units (pH 6.3 to 8.3) was applied for IEF but it did not further enhance resolution, rather, increased streaking was observed leading to an obscured 2-D pattern (data not shown).

Acidic proteins (pI 4-7) were separated over a greater horizontal range using a 4-7 linear IPG strip (b). However, there was no specific advantage over the 3-10 non-linear IPG because the pH gradient of the latter is structured to offer a wider separation range for proteins with isoelectric points between 5 and 7. Some proteins whose isoelectric points were slightly above 4 were better resolved (Fig. 3.9 b, arrowheads).



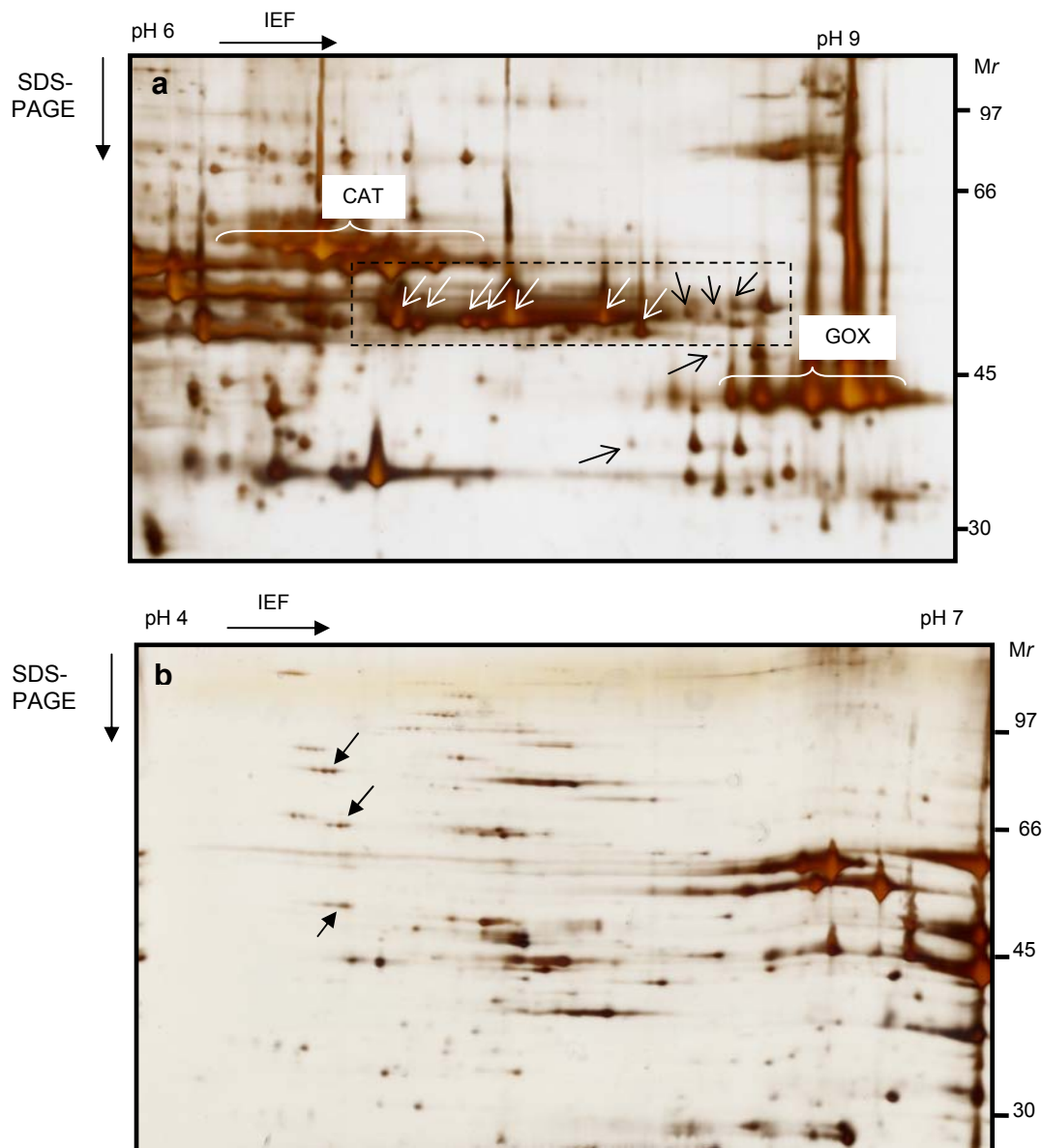


**Fig. 3.9: Two-dimensional electrophoresis of leaf peroxisomal proteins from *Spinacia oleracea* L. using narrow pH range immobilized pH gradient strips in the first dimension**

Peroxisomes were prepared from plants were harvested shortly after the beginning of the light period. About 50  $\mu\text{g}$  soluble leaf peroxisomal proteins (purified from two successive density gradients) were solubilized with 2-D solubilization buffer (7 M urea, 2 M thiourea, 4% (w/v) CHAPS, 3 mg/mL DTT, 0.5% (v/v) corresponding IPG buffer) for 2 h in a laboratory shaker and subjected to 2-DE using an IPG strip of a linear pH gradient from 6 to 11 (a) and 4 to 7 (b) for the 1<sup>st</sup> dimension IEF and a 10% acrylamide gel for the 2<sup>nd</sup> dimension SDS-PAGE. Arrows indicate spots that were better resolved on these gels as compared to previous gels. The box in gel (a) encloses region of better resolution.

### 3.2.5.3. Increasing proteome coverage by subfractionation

Peroxisomes are unique in that the compartmentation of their metabolism is not due to the boundary membrane as a permeability barrier, but is a function of the structural arrangement of enzymes in the peroxisomal matrix (Heupel *et al.*, 1991). An treatment of the peroxisomes with a mild detergent affected the various enzymes differently depending on their intra-peroxisomal localization. In the case of malate dehydrogenase (MDH), hydroxypyruvate reductase (HPR) and serine-glyoxylate aminotransferase (SGAT), a ready release of enzymes from the peroxisomes was indicated, but not in the case of catalase (Heupel *et al.*, 1991). Sub-fractionation of the leaf peroxisomes into the matrix and the core particles by treating freshly isolated intact leaf peroxisomes with a mild detergent was therefore explored to increase protein coverage on 2-D gels. Leaf peroxisomes contain a crystalline core that mostly contains catalase (CAT) and glycolate oxidase (GOX) as the major proteins. Therefore, it was decided to remove the abundant proteins by enriching for them by a treatment with a mild detergent. The idea was to indirectly enrich for low abundant proteins in the soluble fraction.

Following sedimentation of the core particles from Triton X-100 treated peroxisomes, the distribution of protein content was equal between the two fractions. Despite this, a selective enrichment of some low-abundant proteins, could still be achieved either in the core (Fig. 3.10 a, arrows) or in the soluble fraction (Fig. 3.10 b, arrows). A significant proportion of glycolate oxidase (GOX) was enriched in the core (Fig. 3.10 c) as compared to the soluble fraction. Besides, the reduction in GOX content in the fraction of soluble matrix proteins facilitated the detection of other proteins with similar molecular mass and pI that were previously unresolved due to spot overlap (arrow, Fig. 3.10 c). The total catalase content did not seem to differ significantly between the core and the matrix (Fig. 3.10 d). However, the relative proportions of the catalase polypeptides whose molecular masses have been reported to differ between the matrix and the core particles indeed seemed to differ. While the higher molecular mass catalase was more abundant in the matrix than the low molecular mass form, there was only a slight difference in their amounts in the core particles. Here, the former was slightly more abundant than the latter.

This procedure, when optimized to obtain reproducible results, may serve as a simple and useful prefractionation method to enrich for low-abundant proteins in leaf peroxisomes to further increase proteome coverage by two-dimensional electrophoresis.

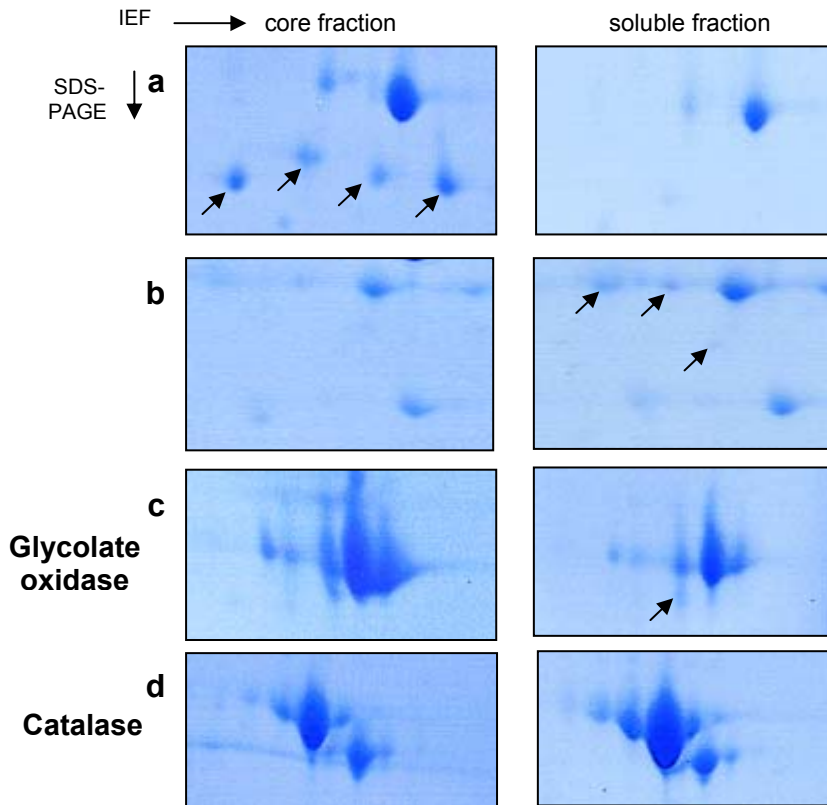


**Fig. 3.10: Sub-fractionation of leaf peroxisomes from *Spinacia oleracea* L. by Triton X-100 treatment for the selective enrichment of low-abundant proteins**

Freshly isolated spinach leaf peroxisomes (75  $\mu$ g protein) enriched by a single Percoll density gradient purification was incubated with 0.05% (v/v) Triton-X 100 for 10 min at 4  $^{\circ}$ C. The samples were centrifuged to separate the core particles (panels to the left) from the soluble fraction (panels to the right) and the proteins resolved by 2-DE. Selective enrichment of proteins could be achieved in the core (a) and in the soluble fraction (b). Glycolate oxidase (GOX) was significantly enriched in the cores (c, left) enabling the detection of previously unresolved proteins in the matrix (c, right), the content of catalase (CAT) was not significantly different (d). The identity of GOX and CAT were inferred based on analogy to 2-D pattern. Please see Fig. 3.11 for appropriate migration coordinates for the proteins indicated.

#### 3.2.5.4. Increasing proteome coverage by induction of gene expression

Yet another strategy to increase protein coverage is the induction of gene expression due to specific stress treatments, and has been applied for the analysis of

stress-inducible proteins. This is especially promising for leaf peroxisomes because this could enable the detection of proteins that are not present in normal tissues since several unknown proteins, from plants, with a peroxisome targeting signal (PTS) may be stress-induced (3.3.3).

### **3.3. Peroxisomal proteins identified by mass spectrometry**

The leaf peroxisomal proteins from spinach were analyzed by Dr. V. Wurtz, at the laboratory of Dr. Alain Van Dorsselaer, LSMBO, Strasbourg, France. In all, 120 spots were analysed from spinach leaf peroxisome two-dimensional gels. Out of these, 115 spots were analyzed by liquid chromatography coupled to tandem mass spectrometry (LC-MS/MS). A further five spots were analyzed by *de novo* sequencing by electrospray ionization-tandem mass spectrometry (ESI-MS/MS). For 15 samples, two or more proteins were identified from a single spot. This indicated a mixture of proteins due to spot overlap or a contamination of the less abundant protein by one of the more abundant proteins in its vicinity. Nineteen protein spots gave no interpretable spectra and require further analysis in the near future. Some proteins suspected as mixtures were resequenced by Dr. H. Urlaub, Max-Planck-Institut für Biophysikalische Chemie, Goettingen, Germany. The identity of a few of the proteins was confirmed by reanalyzing the corresponding spots. The analysis was performed by Dr. K. Mutenda, at the laboratory of Dr. B. Schmidt, The Department for Biochemistry, University of Goettingen, Germany. Eighteen spots turned out to be contaminants. Of these, thirteen were analyzed without any selection for peroxisomal spots (3.3.4.1), out of the remaining five contaminants, three derived from bovine serum albumin (BSA), an artefact from the component of the buffer used for isolating leaf peroxisomes and one came from keratin. Only one spot namely RubisCO, was thus a non-peroxisomal contaminant. Information on these spots is summarized in appendix 1.

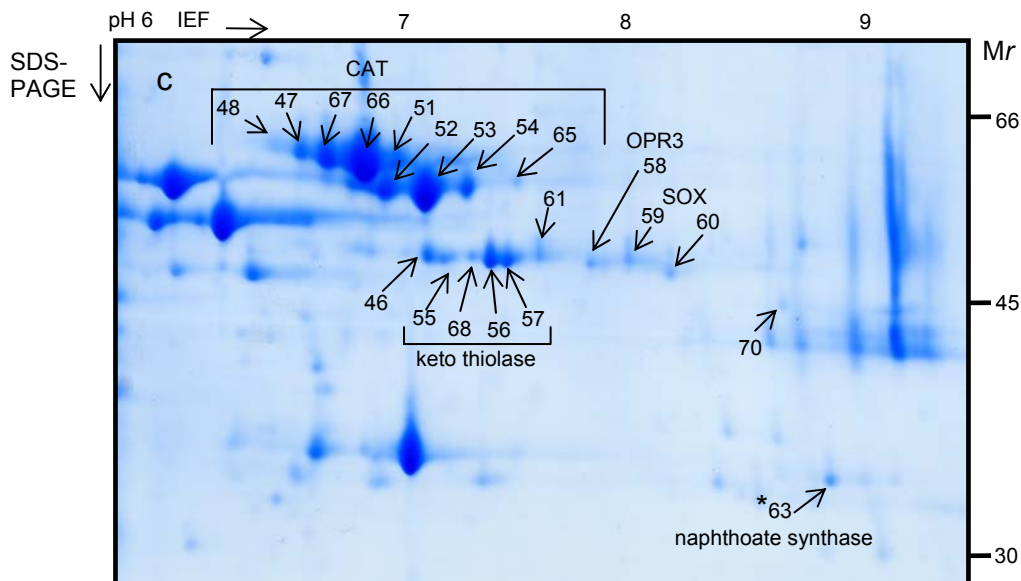
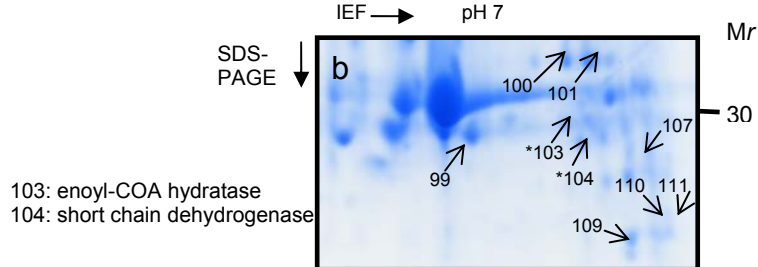
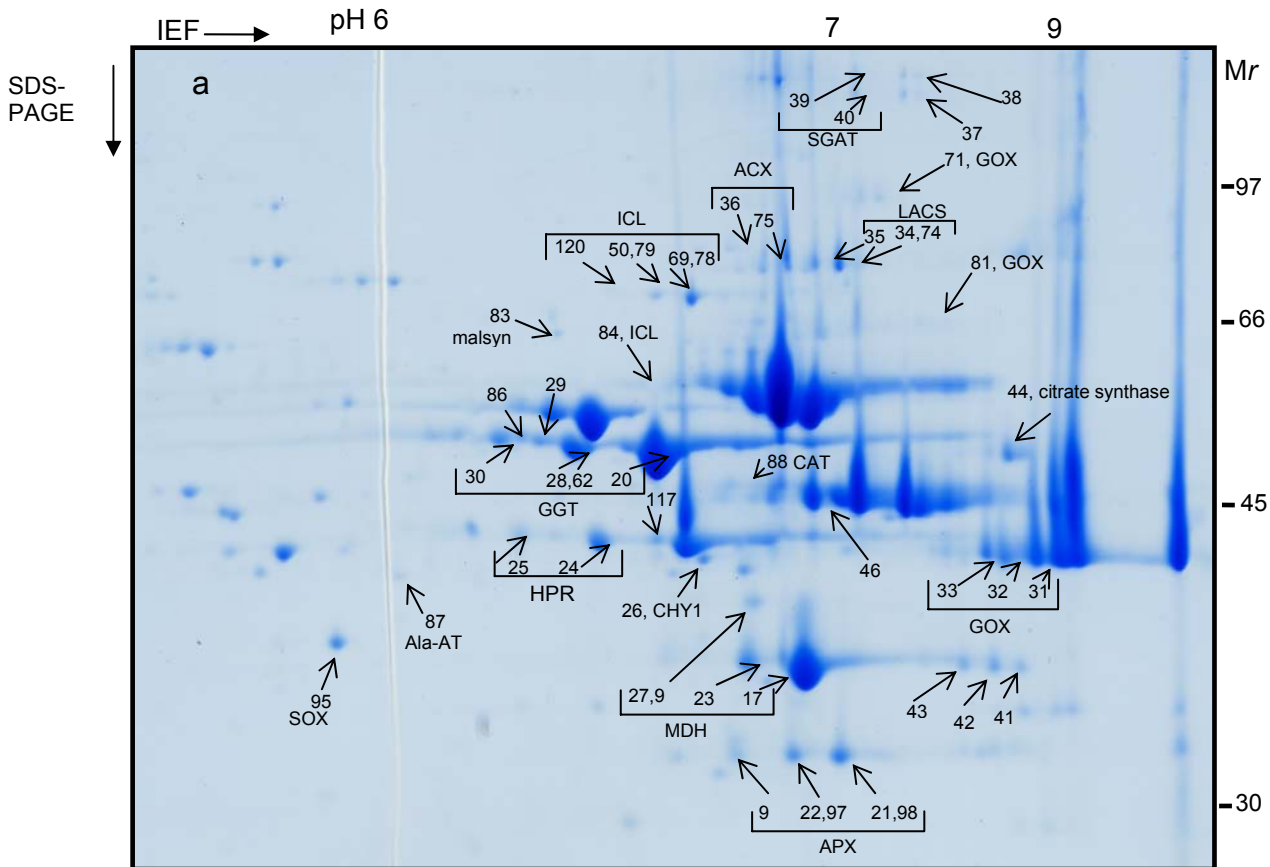
The analysis of leaf peroxisomal proteins by two-dimensional gel electrophoresis offered valuable insights to the enzymatic composition of the organelle. For convenience, the protein content of leaf peroxisomes has been grouped under two main categories, namely known proteins and novel proteins.

### 3.3.1. Known proteins of leaf peroxisomes

In line with their relative abundance and their central role in photorespiration, the most dominant proteins on the 2-D gels of leaf peroxisomes were catalase (CAT) and glycolate oxidase (GOX) each represented by multiple spots (Fig. 3.11). It was possible to identify all the known photorespiratory enzymes on the two-dimensional gels. These included homologs of hydroxypyruvate reductase (HPR, Mano *et al.*, 1997), serine-glyoxylate aminotransferase (SGAT), glutamate-glyoxylate aminotransferase (GGT, Liepman and Olsen, 2003; Igarashi *et al.*, 2003), aspartate aminotransferase (AAT, Schultz and Coruzzi, 1995), alanine-glyoxylate aminotransferase (AGT, Liepman and Olsen, 2001), malate dehydrogenase (MDH, Berkemeyer *et al.*, 1998; Fukao *et al.*, 2002; Fukao *et al.*, 2003;; Hayashi *et al.*, 1998) and alanine aminotransferase (Ala AT). Most of these enzymes were identified in multiple spots. Except for a distinct CAT spot (spot no. 88) and a second spot identified as sulfite oxidase (spot no. 95), both of which were identified as lower molecular mass polypeptide spots on the 2-D gel, the multiple spots representing the different proteins had identical apparent molecular mass and differed only in their isoelectric points. The two spots representing the photorespiratory enzyme SGAT, on the other hand, were located at a much higher molecular weight on the gel than their predicted values.

Surprisingly, enzymes involved in the  $\beta$ -oxidation of fatty acids and in the glyoxylate cycle were also identified as dominant protein spots on the spinach leaf peroxisomal proteome map. These were homologs of the long chain acyl CoA synthetase (LACS, Fulda *et al.*, 2002), acyl CoA oxidase (AOX, Hooks *et al.*, 1999; Froman *et al.*, 2000; Eastmond *et al.*, 2000), ketoacyl thiolase (Hayashi *et al.*, 1998), malate synthase, isocitrate lyase (ICL), and citrate synthase (CS).

Other proteins identified included homologs of 12-oxophytodienoate reductase 3 (OPR3) involved in the jasmonic acid biosynthetic pathway (Schaller *et al.*, 2000), the molybdenum cofactor enzyme sulfite oxidase (SOX, Eilers *et al.*, 2001; Nakamura *et al.*, 2002), uricase and 3-hydroxy isobutyryl coenzyme hydrolase (CHY1, involved in valine catabolism, Zolman *et al.*, 2001).



See facing page for legend

**Fig. 3.11: Leaf peroxisomal proteins from *Spinacia oleracea* L. identified by two-dimensional electrophoresis and mass spectrometry**

Spinach leaf peroxisomal proteins were resolved by 2-DE using broad range (pH 3-10 NL) (a) and (b) or (c) narrow range (pH 6-11) IPG strips and visualized by colloidal Coomassie. (b) shows the location of spots including two novel proteins. Protein identification was done by either LC-MS/MS or ESI-MS/MS (LSMBO, Strasbourg, France). The identified spots are labeled in the figure. The novel proteins identified are indicated with an asterisk. A number of proteins were identified in multiple spots indicating some kind of a post translational modification. Abb.: ACX: acyl CoA oxidase, Ala-AT: alanine aminotransferase, APX: ascorbate peroxidase, CAT: catalase, CHY1: 3-hydroxyisobutyryl CoA hydrolase, GGT: glutamate-glyoxylate aminotransferase, GOX: glycolate oxidase, ICL: isocitrate lyase; LACS: long chain acyl CoA synthetase, MDH: malate dehydrogenase, OPR3: 12-oxophytodienoate reductase, SGAT: serine glyoxylate aminotransferase, SOX: sulfite oxidase.

*Arabidopsis thaliana* as the first higher plant to have its genome fully sequenced (The *Arabidopsis* Genome Initiative, 2000) is the ideal model plant for proteomic studies. Despite the lower purity obtained as compared to spinach, a number of putative peroxisomal protein spots were selected from the two-dimensional (2-D) gel of peroxisomal proteins from *Arabidopsis* (this was due to the striking similarity between the 2-D maps of spinach and *Arabidopsis*) and analyzed. Results of mass spectrometric analysis of the limited number of spots analyzed from *Arabidopsis* have been integrated below. The samples were analyzed by matrix-assisted laser desorption ionization-mass spectrometry (MALDI-MS) at the laboratory of Dr. H. Kratzin, Max-Planck-Institut für Experimentelle Medizin, Goettingen, Germany.

Among the samples analyzed, some of the well-known photorespiratory enzymes were identified. These included three isoforms of glycolate oxidase, (acc. nos. At3g14415, At3g14420, At4g18360), multiple spots for catalase 3 (At1g20620), two isoforms of malate dehydrogenase, (At5g09660 and At2g22780), glutamate-glyoxylate aminotransferase (GGT1, At1g23310) and hydroxypyruvate reductase (At1g68010). One of three isoforms of the enzyme ketothiolase (At2g33150) was also identified from *Arabidopsis* (Fig. 3.12).

Together, these proteins represent many of the proteins known so far from the plant peroxisomal matrix. Some proteins such as the multifunctional protein (MFP) known to be present in the peroxisomal matrix had not been identified in this study for unknown reasons. However, the leaf peroxisomal proteome presented here is by no means complete and there are several more proteins that are yet to be identified from the gels, so it will be premature to conclude that these proteins are absent on the 2-D gels. On the other hand, some basic proteins as well as hydrophobic proteins may be difficult to detect by 2-DE and the MFP being highly basic (isoelectric point of *Arabidopsis* MFP2: 9.24) may be one such 'difficult' protein.



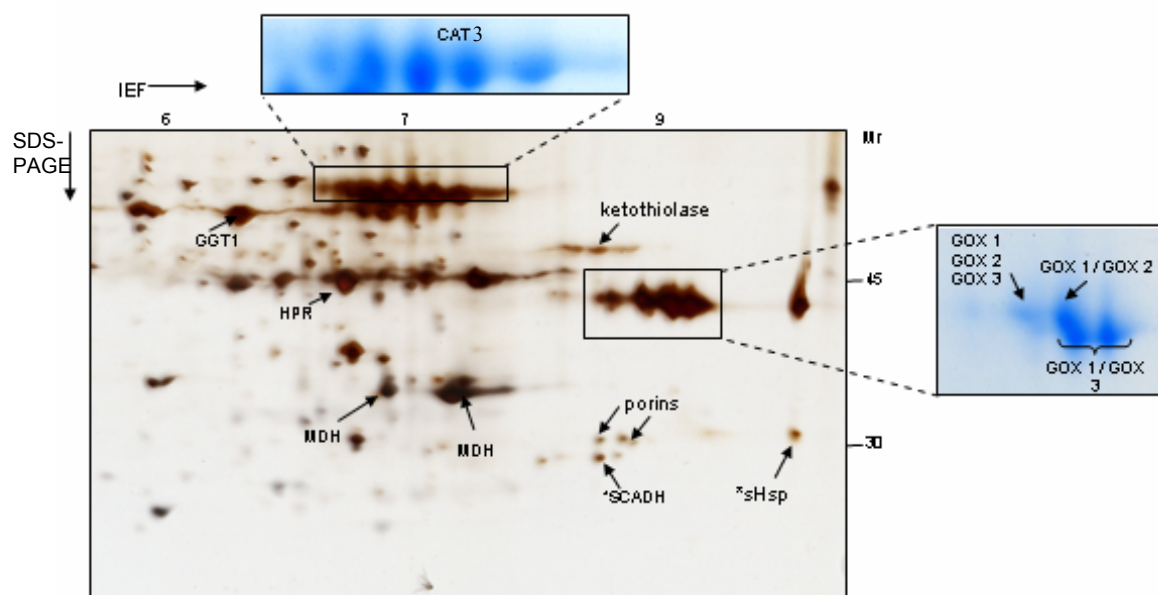


**Fig. 3.12: Leaf peroxisomal proteins from *Arabidopsis thaliana* identified by two-dimensional electrophoresis and MALDI-MS**

*Arabidopsis* leaf peroxisomal proteins purified using two consecutive sucrose density gradients were resolved by 2-DE using a broad range (pH 3-10) IPG strip, visualized by MS-compatible silver staining (section 2.9.1.2) and analyzed by MALDI-MS. The identified spots are labeled in the figure. The novel proteins (SCADH and sHsp) identified are indicated with an asterisk. The multiple spots of CAT 3 were better visualized by colloidal Coomassie staining (respective projection). GOX spots may be mixtures due to inadequate resolution (see projected region). SCADH: short chain alcohol dehydrogenase; sHsp: small heat-shock protein

### 3.3.2. Novel proteins of leaf peroxisomes

In addition to the proteins mentioned above, three and two novel proteins were identified on the leaf peroxisomal two-dimensional maps of spinach and *Arabidopsis*, respectively, one of which was identified in both plant species. All four proteins contained a recognizable peroxisomal targeting signals (PTS), providing strong support that these proteins are targeted to plant peroxisomes.

#### 3.3.2.1. Putative naphthoate synthase (At1g60550)

One protein spot from spinach leaf peroxisomes (Fig. 3.11 c, spot no. 63) with an apparent molecular mass of about 32 kDa and an isoelectric point (pI) of about 9 was identified by LC-MS/MS (Dr. V. Wurtz, Strasbourg, France) as a homolog of an unknown

*Arabidopsis* protein of the family of monofunctional enoyl-CoA hydratases/isomerases, annotated as “putative naphthoate synthase” (At1g60550, 337 amino acids, pI: 7.06, M: 41.8 kDa). Targeting of this protein to peroxisomes is supported by several lines of in silico analyses as well as experimental evidence. First, the enzyme carries a putative peroxisomal targeting signal (PTS2) nonapeptide of the sequence RLX<sub>5</sub>HL, which has been defined as a major PTS (Reumann, *in press*) and is located at position 13 to 20 in close proximity to the N-terminal end of the protein. The lower apparent molecular mass is in line with the fact that the targeting signal of PTS2-targeted plant proteins, such as malate dehydrogenase, thiolase, and citrate synthase, are processed and the presequence cleaved upon protein import into peroxisomes (Gietl *et al.*, 1994; Kato *et al.*, 1995, 1996; Berkemeyer *et al.*, 1998; Hayashi *et al.*, 1998). Second, predicted localization of the protein in peroxisomes was supported by the detection of a homolog from *Oryza sativa* of the same size (NP\_917386, 331 amino acids, RLX<sub>5</sub>HL, 73% identity over the entire length) that carries a putative PTS2 as well even though the domain surrounding the putative PTS2 is only weakly conserved (Fig. 3.13). Finally, the putative PTS2 was shown to be conserved in homologous expressed sequence tags (ESTs) from various plant species. For this analysis, homologous ESTs were identified by BLAST analysis (tblastn) based on sequence similarity and the nonapeptide analyzed after reverse translation of the region that aligned with the N-terminal end of the *Arabidopsis* protein (At1g60550) and followed a neighboring putative start methionine and after alignment of the sequences (Fig. 3.13). Homologous ESTs were detected both in monocots as well as in dicots. All homologous ESTs from higher plants (e.g. *Oryza*, *Triticum*, *Lycopersicon*, *Glycine*) contained a putative PTS2 that aligned with the putative PTS2 from the *Arabidopsis* protein within a moderately conserved N-terminal domain, of which five and three ESTs carried the major PTS2 RLX<sub>5</sub>HL and Rlx<sub>5</sub>HL, and three ESTs carried the minor PTS2 RVX<sub>5</sub>HL. Only one EST from *Populus tremuloides* contained a yet unknown but related PTS2 nonapeptide.

```

At1g60550      : ----MADSNEGSASRRLSVVTNHLPIGFSPAR----ADSVELCSAS--SMDDRHKVHGEVPTHEVW  : 60
Os_g_NP_917386 : -----MDAAGRRLRVTAHLLPSSLPLPLASAPTLPASPAAS---PASDSYRRVHGDVPSPEPWA  : 57
Bn_CD813717    : ----MADSKEGTASRRLSVFTNHLLPVETILTR---VHVELSTAS--SMNDNYHKVHGEVPTHQVW  : 60
Mc_CA833777    : -----EAVRRRLSNVTSHLNPNSSNPNSDPNPLQGSIGLSN---SMNDSYRRVHGDLPVHPVW  : 56
Bv_BQ587056    : MNMSRIEEREEVVNRRSNVTANHLNPLLKSHQS---YPSISLSTT---SMNDNYHKVHGEVSLDPEVW  : 63
St_BG887061    : ----MSEKDNTMRRVASVANHLLP--IPLAQNVSIGSSNCSSS---SMNDNYHKVHGEVENHEPVW  : 61
Le_BM410312    : ----MIEDNTMRRVASVANHLLP--IPLAQNVSIGSFNCSSS---SMNDNYHKVHGEVENHEPVW  : 61
Pt_BU826458    : -MAQTLSEKEYSVRRKMASVANHLMVPSPPTASSKCDSELVLPNAA--SMNDNYHRVHCNVSNKEVW  : 67
Vv_CB970316    : -MAQIANKDLNANARRRLASVAHHLLPLHSTTPN---CSSLGFHTT---SAPDSYRRVHGEVPTHVW  : 62
Hv_BE196313    : -----MDAARRLRVTAHLLPSSLPL--VSAPLLAPFPAAASSSPAGDSYRRVHGDVSLPEPWA  : 58
Ta_CA699738    : -----MDAARRLRVTAHLLPSSLPL--ASAPLLAPSPAAGSSXPAGDSYRRVHGDVSSGASGX  : 58
Lj_AV422084    : -MADNND--LHTAIRRLASVAHHLLPISPPSA--ALAPLALCHTSS---SSSTYRRVHGDVPSHDVW  : 60
Gm_AW620784    : -MAENNNNHLETATRRLASVTNHLLPSSYHN--APGELAP-CLTSG---GNNSYRRVHGEVPSHD  : 59

```

**Fig. 3.13: Alignment of homologous N-terminal ESTs from various plant species with an unknown *Arabidopsis* protein, annotated as putative naphthoate synthase, identified in spinach leaf peroxisomes.**

The N-terminal domain of about 100 residues of the *Arabidopsis* protein At1g60550, annotated as putative naphthoate synthase and identified as a homolog of a protein from spinach leaf peroxisomes (Fig. 3.11 c), was blasted against the non-redundant database at NCBI (<http://www.ncbi.nlm.nih.gov/>) and the level of sequence similarity with other *Arabidopsis* proteins determined (<40% identity, <55% similarity, E value >7\*10<sup>-7</sup>). Next, the N-terminal domain of At1g60550 was blasted against the nucleotide database of ESTs at NCBI and homologous ESTs from various plant species covering the putative PTS2 were identified based on sequence similarity (about 40% identity, > 60% similarity, E value <10<sup>-15</sup>). The nucleotide sequence was reverse translated ([www.expasy.org](http://www.expasy.org)) and the protein sequence including the putative start methionine in front of the putative PTS2 and about 50 residues in total was retrieved. The sequences irrespective of the nature of the putative PTS2 were aligned using ClustalX and shaded using Genedoc. The sequence of the putative PTS2 is underlined. The Genbank accession numbers or the ESTs are provided. (Abbreviations: At: *Arabidopsis thaliana*; Bn: *Brassica napus*; Bv: *Beta vulgaris*; g: full-length gene; Gm: *Glycine max*; Hv: *Hordeum vulgare*; Le: *Lycopersicon esculentum*; Lj: *Lotus japonicus*; Mc: *Mesembryanthemum crystallinum*; Os: *Oryza sativa*; Pt: *Populus tremuloides*; St: *Solanum tuberosum*; Ta: *Triticum aestivum*; Vv: *Vitis vinifera*).

In summary, it was concluded that this putative naphthoate synthase is expressed in mesophyll cells and targeted to leaf peroxisomes with high probability. Considering the well visible intensity of the spinach protein on a Coomassie-stained two-dimensional gel (Fig. 3.11 c) and the relatively low number of proteins in leaf peroxisomes from non-stressed plants that are neither involved in photorespiration nor fatty acid  $\beta$ -oxidation, it was concluded that this enoyl-CoA hydratases/isomerases has an important role in leaf peroxisomal metabolism. Because more detailed phylogenetic and homology analyses suggested that this enzyme plays an interesting role in biosynthesis or degradation of aromatic compounds (see 4.4), the gene was cloned by reverse transcription polymerase chain reaction (RT-PCR, see 3.3.4.2) to verify the subcellular localization by targeting

analysis of fusion proteins of spectral variants of green fluorescent protein with this protein in onion epidermal cells and to study the catalytic function by heterologous overexpression in *E. coli*.

### 3.3.2.2. Short chain dehydrogenase/reductase family protein

A second protein spot from spinach leaf peroxisomes with an apparent molecular mass of about 38 kDa and an isoelectric point of about 9 (Fig. 3.11 b, spot no. 104) was identified by LC-MS/MS (Dr. V. Wurtz, Strasbourg, France) as a homolog of an unknown *Arabidopsis* protein of the family of short chain dehydrogenases/reductases (At4g05530, 254 aa, pI: 8.68, M: 26.7 kDa). In addition, the *Arabidopsis* protein was identified directly on 2-D gels from *Arabidopsis* by MALDI (short-chain alcohol dehydrogenase, SCADH, Fig. 3.12, Dr. H. Kratzin, Max-Planck-Institut für Experimentelle Medizin, Goettingen, Germany). These results provided two-fold evidence for its localization in peroxisomes because the organelles from both plant species were contaminated by mitochondria and proplastid-like organelles to a differing extent (Table 3.1). The protein carries the putative peroxisome targeting signal (PTS1) SRL>, which has been defined as a major PTS (Reumann, in press). Predicted targeting to peroxisomes is further supported by the finding that the PTS1 is conserved in several homologous ESTs from various plant species (e. g. *Brassica*, *Citrus*, *Vitis*, *Solanum* etc., Fig. 3.14), even though it needs to be stressed that almost all homologs carry the same C-terminal tripeptide and that the entire C-terminal domain is highly conserved, reducing the significance of PTS1 conservation.

The primary structure of SCADH shows one of two sequence motifs that are common to members of the family of short chain dehydrogenases/reductases. The N-terminal coenzyme (NAD) binding motif of the sequence Gx<sub>3</sub>GxG is conserved in the *Arabidopsis* protein, whereas the second short motif of the sequence Yx<sub>3</sub>L, which is also located in the active site of these enzymes (Jornvall *et al.*, 1995), is lacking in the putative peroxisomal SCADH. Kamada *et al.* (2003) proposed recently that the SCADH identified on our 2-D gels represents the plant ortholog of NADP-dependent dienoyl-CoA reductase from yeast and mammals, which is involved in degradation of unsaturated fatty acids (Gurvitz *et al.*, 2001; De Nys *et al.*, 2001). A more detailed analysis including multiple sequence alignment, however, demonstrated that SCADH is distantly related to two other

short chain dehydrogenases (At3g59710, 302 amino acids, SKL>; At3g12790 or At3g12800, 298 amino acids, SKL>) which also possess a putative major PTS and that the latter is the corresponding ortholog of NADP-dependent dienoyl-CoA reductase (Reumann et al., submitted). Recent MS/MS results provided evidence that also this protein (At3g12790 or At3g12800) is detected on spinach 2-D gels from leaf peroxisomes as well but need to be confirmed.

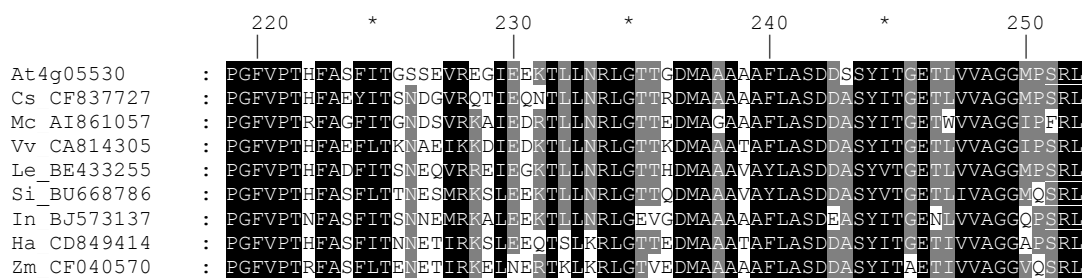


**Fig. 3.14: Alignment of homologous C-terminal ESTs from various plant species with an unknown *Arabidopsis* protein, annotated as a short chain alcohol dehydrogenase, identified in spinach leaf peroxisomes.**

The C-terminal domain of about 100 residues of the *Arabidopsis* protein At4g05530, annotated as a short chain alcohol dehydrogenase and identified on 2-D gels of spinach leaf peroxisomes (Fig. 3.11), was blasted against the non-redundant database at NCBI (<http://www.ncbi.nlm.nih.gov/>) and the level of sequence similarity with other *Arabidopsis* proteins determined (<50% identity, <75% similarity, E value >10<sup>-14</sup>). Next, the C-terminal domain of At1g60550 was blasted against the nucleotide database of ESTs at NCBI and homologous ESTs from various plant species covering the putative PTS2 were identified based on sequence similarity (about >60% identity, > 75% similarity, E value <10<sup>-30</sup>). The nucleotide sequence was reverse translated ([www.expasy.org](http://www.expasy.org)) and the C-terminal 50 residues including the C-terminal tripeptide of the ORF retrieved. The sequences irrespective of the nature of the putative PTS1 were aligned using ClustalX and shaded using Genedoc. Redundant homologous ESTs from other plant species that also carried the peptide SRL> are not shown (e.g., *Solanum tuberosum*, *Nicotiana tabacum*, *Glycine max*, *Gossypium arboreum*, *Pinus pinaster*, *Saccharum officinalis*, *Populus balsamifera*). The numbers at the top refer to the *Arabidopsis* protein. Abbreviations: At: *Arabidopsis thaliana*; Cs: *Citrus sinensis*; Ha: *Helianthus annuus*; In: *Ipomoea nil*; Le: *L. esculentum*; Mc: *Mesembryanthemum crystallinum*; Si: *Sesamum indicum*; Vv: *Vitis vinifera*; Zm: *Zea mays*)

On the other hand, this experimentally detected SCADH shares about 40% identity over almost the entire length with mammalian homologs that also carry a PTS and represent homologs of mitochondrial NADP-dependent retinol dehydrogenase involved in vitamin A biosynthesis. Because plants do not require the synthesis of retinol, it has been

proposed that the plant homolog of mammalian NADP-dependent retinol dehydrogenase is involved in an inverse catabolic reaction of carotenoids and/or phytol deriving from chlorophyll during senescence (Giuliano *et al.*, 2003; Reumann, pers. com.). The corresponding gene of this SCADH is currently being cloned in the course of a diploma research project by Ms. Franziska Lueder in the laboratory of Dr. S. Reumann, Albrecht von Haller Institut für Pflanzenwissenschaften, Goettingen, Germany. *Arabidopsis* T-DNA insertion knock-out mutants are available and expected to yield valuable insights into the function of this enzyme.

### 3.3.2.3. Small heat shock protein (At1g06460)

Members of multiple superfamilies of heat-shock proteins (HSP) are expressed in response to increased temperature and other forms of abiotic stresses (Sun *et al.*, 2002; Young *et al.*, 2003). Many HSPs are molecular chaperones that recognize and bind protein non-native states thereby suppressing aggregation and facilitating refolding and/or subsequent degradation. Small heat shock proteins (sHSP) are an ubiquitous superfamily of HSPs characterized by the relatively small mass of the polypeptide chain (16-42 kDa) and the presence of a conserved C-terminal domain, the  $\alpha$ -crystallin domain, and they assemble into oligomeric structures with varying degree of order and substantial divergence in size (9 to >24 subunits, Kim *et al.*, 1998; Scharf *et al.*, 2001; Sun *et al.*, 2002; Haslbeck, 2002). Plants house an exceptionally large family of 13 closely and six more distantly related members plus 25 proteins with domains homologous to the  $\alpha$ -crystallin domain (Scharf *et al.*, 2001). Homologs of sHSPs have been localized to several cell compartments, including the cytosol, plastids, mitochondria, and the ER (Banzet *et al.*, 1998; Löw *et al.*, 2000; Scharf *et al.*, 2001; Sun *et al.*, 2001), but experimental evidence for the presence of a small heat-shock protein in peroxisomes has not been provided yet for any organism.

One *Arabidopsis* protein (sHsp15.7, At5g37670, SKL>) carries the major PTS1 SKL> and is targeted to plant peroxisomes (Ma and Reumann, unpublished). This protein was not detected on 2-D gels probably because its expression is induced by heat and oxidative stress (Ma and Reumann, unpublished). A second protein of the family of small heat-shock proteins, however, was identified on the 2-D gels from *Arabidopsis* (Fig. 3.12). This protein

(285 amino acids, pI: 9.82, M: 31.2 kDa) contains the putative PTS1 PKL> which has been defined as a minor PTS (Reumann, in press) and is found in some but not all homologous ESTs (data not shown). Interestingly, a putative PTS2 specified by RLx<sub>5</sub>HF (minor PTS) is also present at the N-terminus of the protein sequence. The protein is more distantly related to the other sHSPs but clearly belongs to the superfamily (4.4). The closest homologs are found in prokaryotes, e.g., a molecular chaperone of the sHsp family from *Magnetococcus*, with which it shares 34% identity over about 100 residues. A putative role for the protein during cold stress has been suggested (Reumann, pers. com.). The gene of this *Arabidopsis* sHsp has been cloned in the course of this study (see 3.3.4.2).

#### **3.3.2.4. Monofunctional enoyl-CoA hydratase (At4g16210)**

This protein (265 amino acids, pI: 8.24, M: 26.3 kDa) identified on the 2-D gels from spinach (Fig. 11 b, spot no. 103) contains a putative PTS1 SKL> which has been defined as a major PTS (Reumann, in press) and was identified based on homology to an enoyl-CoA hydratase from *Cicer* (acc. no.: AJ27305) with which the *Arabidopsis* protein shares about 80% sequence identity over the entire length. For analysis of the putative function of this protein, see 4.4.

Other interesting proteins identified included a protein annotated as a ferrityochelin binding protein-like- protein (acc. no. At5g66510) with a putative major peroxisome targeting signal (PTS2) represented by an N-terminal nonapeptide RLx<sub>5</sub>HF and identified from *Arabidopsis* two-dimensional gels. A putative prohibitin (acc. no. AY087293) and a porin (At5g67500) were also identified from the two-dimensional gels of *Arabidopsis* leaf peroxisomes.

### 3.3.3. Stress inducible proteins of leaf peroxisomes from *Spinacia oleracea* L.

In contrast to the static genome, the proteome is highly dynamic. Two-dimensional electrophoresis (2-DE) is a useful technique to track alterations in protein content occurring within a cell or a subcellular compartment in time or following external stimuli. The approach could enable the detection of several proteins whose synthesis may be switched on only under specific conditions and therefore cannot be detected on proteome maps generated from normal tissues. Thus, it may be a useful approach to increase proteome coverage. For this reason soluble proteins were additionally extracted out of peroxisomes isolated from plants subjected to various stresses and the protein pattern documented by 2-DE. Comprehensive protein profiles generated from paired samples (e.g. control and stressed plants) were compared in order to identify proteins that are unique to one sample or the other. Such a differential profiling of protein expression was used as a tool to examine the response of the peroxisomal proteins towards different abiotic stress treatments and to identify novel proteins from leaf peroxisomes.

Hydroponically grown spinach plants were subjected to different independent abiotic stress treatments. Oxidative stress was induced by treatment with the catalase inhibitor 3-amino-1,2,4-triazole that specifically binds to the active site of catalase and inhibits the enzyme irreversibly. High light stress was induced by subjecting the plants to an increased illumination of about  $700 \mu\text{mol photons m}^{-2}\text{sec}^{-1}$  in a 9/15 h light-dark cycle.

Following oxidative stress or high light stress, stress symptoms began to appear on leaves characterized by the appearance of pale grey-colored lesions that turned brown (Fig. 3.15, plants to the left) indicating damage to the tissues within. The plants were harvested before extensive damage to leaf tissue could occur to enable the isolation of peroxisomes and to prevent characterization of apoptotic proteins. Peroxisomes were isolated from the stress treated and control plants following the new analytical method that was developed in this study in which the 'post-plastidic supernatant' was directly applied on Percoll density gradients prepared with raffinose.



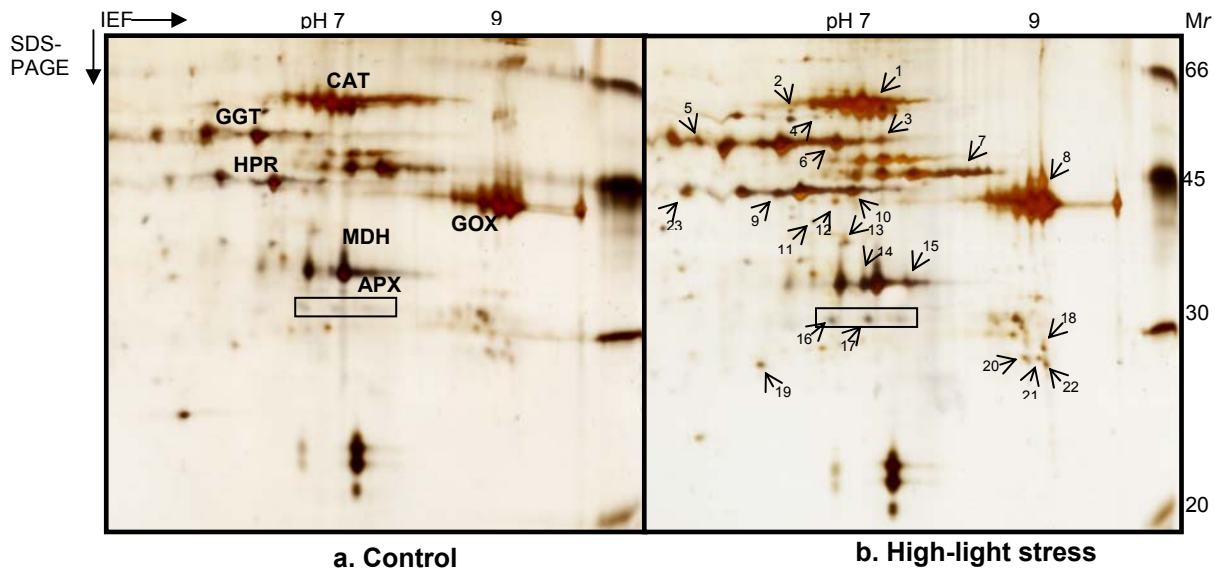


Fig. 3.15: Oxidative stress treatment of *Spinacia oleracea* L.

Hydroponically grown spinach plants (8 weeks old) were cultivated in medium supplemented with the catalase inhibitor 3-amino-1, 2, 4-triazole (10 mM). The plants were grown under normal light intensities ( $350 \mu\text{molm}^{-2}\text{sec}^{-1}$ ) for a 9/15 h light-dark period until the onset of oxidative stress symptoms. Treated plants (left) showed characteristic greyish to brownish colored lesions indicating damage to the tissues. Plants were harvested 3 d after the application of the inhibitor at the end of the light period for peroxisome isolation. Untreated plants (right) served as the controls.

The alterations in expression pattern of some proteins during light stress and oxidative stress is shown (Fig. 3.16 and 3.17, respectively). There are indications that some proteins are induced in the 'stressed' peroxisomes (indicated with arrows). This could indicate novel proteins expressed only during stress that were previously undetectable or may correspond to novel stress induced modifications of some proteins e.g. protein oxidation, nitration, phosphorylation etc. Besides these 'newly appearing' proteins that were present only on the stressed proteome, there were others present on both types of gels albeit at different intensities. These represent the class of proteins whose synthesis could be altered during stress. Based on their migration co-ordinates, the identity of some of these proteins may be inferred. For example, the level of glutamate-glyoxylate aminotransferase increased significantly during both oxidative and light stress. Similarly, for other proteins, such as ascorbate peroxidase, and hydroxypyruvate reductase, the expression levels were increased, in comparison with the control, irrespective of the type of stress. Such a pattern may suggest that common regulatory pathways may be involved in the activation of the response pathways in similar modes during both oxidative stress and light stress. The proteins that are greatly up-regulated in

response to oxidative/light stress will be identified by mass spectrometric approaches in the near future.



**Fig. 3.16: Induction of proteins in leaf peroxisomes from *Spinacia oleracea* L. by high light stress**

Hydroponically grown spinach plants (8 weeks old) were illuminated with high light intensity ( $700 \mu\text{mol photons m}^{-2}\text{sec}^{-1}$ ) for a 9/15 h light-dark period for 24 h. Plants grown under normal light intensities ( $350 \mu\text{mol photons m}^{-2}\text{sec}^{-1}$ ) served as controls. Peroxisomes were prepared from the treated (b) and control (a) plants harvested at the end of the light period using the newly developed analytical method in which the 'post-plastidic' supernatant was directly loaded on Percoll density gradients prepared with raffinose. Proteins were quantified using the Bradford method prior to precipitation using chloroform-methanol. Equal protein quantities of  $50 \mu\text{g}$  were resolved by 2-DE and stained with silver (Blum *et al.*, 1984). The induced proteins are denoted with arrowheads. Some known proteins are labeled. Results shown are from two independent experiments ( $n=2$ ).

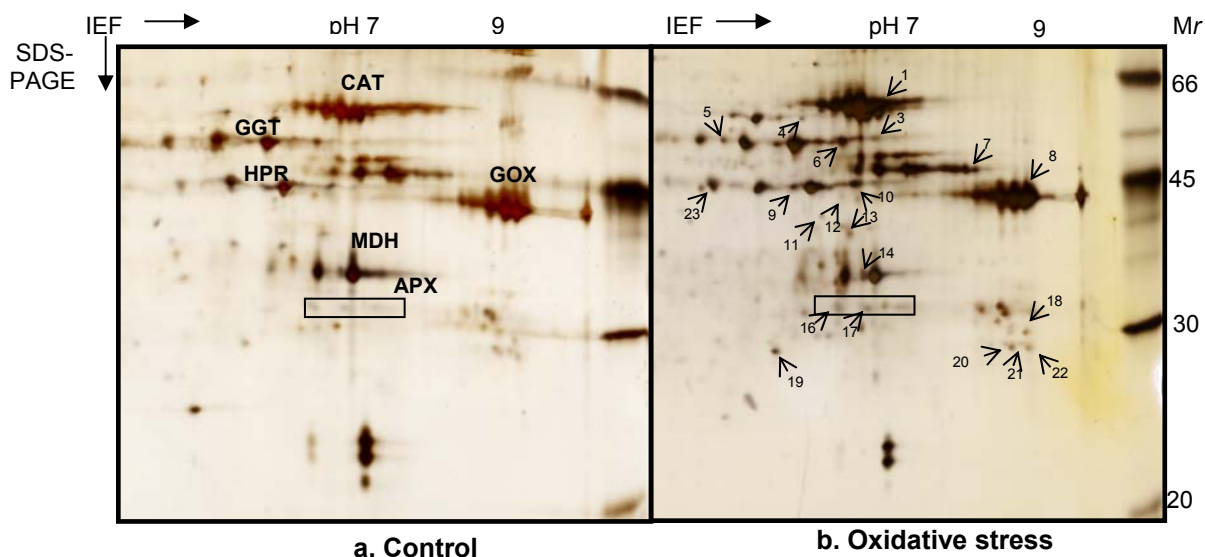


**Fig. 3.17: Induction of proteins in leaf peroxisomes from *Spinacia oleracea* L. by oxidative stress treatment**

Hydroponically grown spinach plants (8 weeks old) were treated for 3 days with 10 mM catalase inhibitor 3-amino-1,2,4-triazole in a 9/15 h light-dark period until the appearance of pale brown lesions. Plants were grown under normal light intensities ( $350 \mu\text{mol photons m}^{-2}\text{sec}^{-1}$ ). Untreated plants served as controls. Peroxisomes were prepared from the treated (b) and control (a) plants harvested at the end of the light period using the newly developed analytical method in which the 'post-plastidic' supernatant was directly loaded on Percoll density gradients prepared with raffinose. Proteins were quantified using the Bradford method prior to precipitation using chloroform-methanol. Equal protein quantities of 50  $\mu\text{g}$  were resolved by 2-DE and stained with silver (Blum *et al.*, 1984). The induced proteins are denoted with arrowheads or are encircled. Some known proteins are labeled. Results shown are from two independent experiments ( $n=2$ ).

### 3.3.4 Evidence for peroxisomal localization of novel proteins

In order to validate the localization of the novel proteins identified from spinach leaf peroxisomes, a method based on differential profiling of proteins between a peroxisome enriched sample and a sample enriched for proplastid-like organelles was used.

#### 3.3.4.1. Differential profiling

The major contaminant of the peroxisome fractions was the proplastid-like organelle. Therefore, fractions enriched for peroxisomes and proplastid-like organelles were taken from the same density gradient and the pattern of their constituent proteins

was resolved by two-dimensional electrophoresis. These fractions differed by a factor of more than 25 in their purity based on the ratio of HPR to NADP-GAPDH. The relative intensities of proteins known to be present in these organelles were different in these fractions that allowed distinguishing proteins that may be unique to one of them. The approach appeared specific and sensitive enough as indicated by a barely visible silver stained spot such as that of a homolog of enoyl CoA hydratase (spot no. 103, Fig. 3.11 b and arrowhead 1, Fig. 3.18) to be a peroxisomal protein. Thus the constraint with purity was overcome by a fairly simple method to deduce peroxisomal proteins.

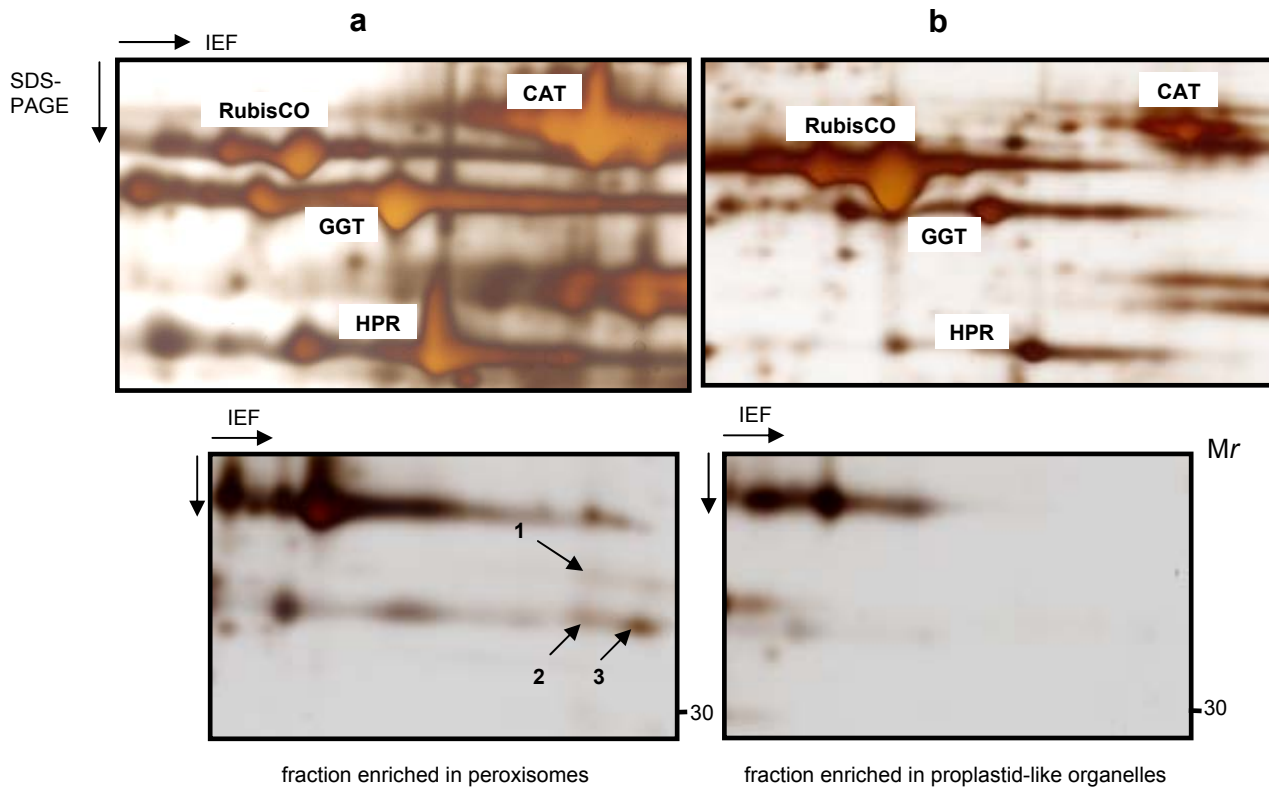


**Fig. 3.18: Subtractive two-dimensional electrophoresis to deduce peroxisomal proteins by differential profiling**

Two fractions designated as peroxisomes (a) and proplastid-like organelles (b) were chosen to generate differential 2-D protein profiles with equal amounts of protein. The fractions differed in their HPR/NADP-GAPDH ratio by a factor of 25. A protein spot that was more dominant on one gel as compared to the other was considered to be located in the organelle which was enriched in that sample. The relative abundance of some of the peroxisomal proteins (CAT, GGT, and HPR) and the plastid protein RubisCO are shown. Novel proteins identified are indicated by arrowheads. 1: enoyl CoA hydratase, 2: short chain dehydrogenase/reductase family protein, 3: naphthoate synthase like protein.

In summary for the novel proteins, except for the small heat shock protein, evidence could be provided in the form of differential profiling that support their peroxisomal localization. Such a differential profiling was not carried out with samples from *Arabidopsis* due to insufficient amounts of protein derived from most single gradients. Instead, spots were selected based on analogy of their migration coordinates with peroxisomal proteins on spinach gels. This strategy was successful and resulted in the identification of some well-known peroxisome proteins as well as some novel ones among the selected spots.

#### **3.3.4.2. Cloning of genes encoding novel peroxisomal proteins**

Four novel proteins were detected on 2-D gels of leaf peroxisomes from spinach and *Arabidopsis*. Several lines of evidence strongly supported their localization in plant peroxisomes and indicated an important yet unknown function in metabolism of mesophyll cells. Because a functional hypothesis was concluded by *in silico* homology analyses for naphthoate synthase and because one small heat-shock protein had already been demonstrated to be targeted to plant peroxisomes (Ma and Reumann, unpublished), a subsequent goal of this thesis was cloning of the *Arabidopsis* genes of the naphthoate synthase homolog (At1g60550) and of the second small heat-shock protein (At1g06460). Gene cloning is a prerequisite to verify the predicted subcellular localization of the proteins in peroxisomes by analyzing subcellular targeting of fusion proteins with spectral variants of green fluorescent protein in onion epidermal cells by fluorescence microscopy (Fulda *et al.*, 2002; Ma, Mayer and Reumann, unpublished) as well as for functional studies of heterologously expressed recombinant proteins.

Oligonucleotide primers were designed based on the sequence of the *Arabidopsis* gene that is publicly available at the National Center for Biotechnological Information (NCBI) for cloning of the full-length open reading frame and supplemented with appropriate restriction sites of DNA endonucleases to facilitate subcloning. Initial attempts to amplify both full-size cDNAs gene using first strand cDNAs synthesized from total RNA of leaves failed for unknown reasons. An alternative strategy was subsequently chosen, which was based on *in silico* and proteome data. First, an analysis of various *Arabidopsis* collections of expressed sequence tags (ESTs) suggested that both genes are induced by stress

treatment, such as cold and dehydration (data not shown). Second, the proteome studies indicated that the protein spot of the small heat-shock protein increased with prolonged storage of the *Arabidopsis* plants in the cold prior to the isolation of leaf peroxisomes (data not shown). Thus, total RNA was subsequently isolated from *Arabidopsis* plants subjected to cold treatment for one hour. Indeed, full-length PCR fragments of expected size could be amplified from the first-strand cDNA derived from RNA isolated from cold-treated *Arabidopsis* leaves for both genes. The amplified fragments were ligated into pGEMT-easy vector. The nucleotide sequences verified cloning of the intended genes and did not reveal any exchanges at the amino acid level as compared to the protein sequence predicted from the *Arabidopsis* genome (AGI 2000), allowing straightforward subcloning of the genes into the *E. coli* expression vector pDEST17 for functional analyses.

For verification of subcellular targeting, subcloning of both full-length genes as well as of deletion constructs lacking the predicted PTS into the vector pCAT-YFP was started. For naphthoate synthase with a predicted N-terminal PTS2, the gene is being cloning via NcoI in front of yellow fluorescent protein (YFP) to allow exposition of the PTS2 in the fusion protein, recognition by the cytosolic receptor Pex7 and targeting to peroxisomes. By contrast, the small heat-shock protein, which carries both, a predicted PTS1 (PKL>) and a PTS2 (RLx<sub>5</sub>HF), was first cloned via NotI/XbaI in the back of YFP to guarantee exposure of the C-terminal PTS1 for targeting to peroxisomes. Because subcloning of the genes into the pCAT-YFP is not trivial due to a lack of blue-white screening, the results could not be accomplished in the last weeks of experimental work of this thesis and were handed over to colleagues in the laboratory due to time constraints.

### **3.4. Post-translational modifications of peroxisomal proteins from spinach**

Post-translational modifications (PTMs) are covalent processing events that change the properties of a protein by proteolytic cleavage or by addition of a modifying group to one or more amino acids. These kinds of modifications of a protein can determine its activity state, subcellular localization, turnover, and interactions with other proteins.

### 3.4.1. Detection of post translational modifications of spinach leaf peroxisomal proteins by two-dimensional electrophoresis

One of the robust tools available till date to study post-translational modifications (PTMs) is two-dimensional electrophoresis (2-DE) combined with mass spectrometry (MS). Identification is based on the characteristic change in electrophoretic behaviour of the modified protein (detected by 2-DE) and the subsequent analysis by MS. Some among the more than 300 different post-translational modifications (PTMs) include phosphorylation, acetylation, methylation, acylation, fatty acid modification, glycosylation, sulfation, ubiquitination and nitration of tyrosine residues (Krishna and Wold, 1993; Mann and Jensen, 2003). An indication for PTMs of peroxisomal proteins from the present study was the identification of the same protein in multiple spots. For example, in *Arabidopsis thaliana* three genes encode subunits that form the six isoforms of catalase. However, the detection of the same polypeptide subunit in about 6 spots on the *Arabidopsis* 2-D gel (Fig. 3.12) of similar relative molecular mass but with different isoelectric points (Fig. 3.19) indicates a PTM of the polypeptide.

Multiple protein spots containing the same protein were also observed for several enzymes on 2-D gels from spinach leaf peroxisomes, including hydroxypyruvate reductase, isocitrate lyase, ascorbate peroxidase (Fig. 3.19), acyl Co-A oxidase, thiolase and sulfite oxidase (data not shown). In most of the cases, the pattern of protein distribution was such that the molecular mass did not differ but the isoelectric point was shifted, a pattern observed for protein phosphorylation. Additionally, the acidic forms were relatively less abundant than the basic forms. The results of investigations carried out in the present study on protein phosphorylation in leaf peroxisomes is presented in the following section. These results strongly suggested that the activity of enzymes involved in photorespiration (e.g. hydroxypyruvate reductase) and fatty acid  $\beta$ -oxidation (e.g. isocitrate lyase, thiolase) is regulated by PTMs including, perhaps, reversible phosphorylation.

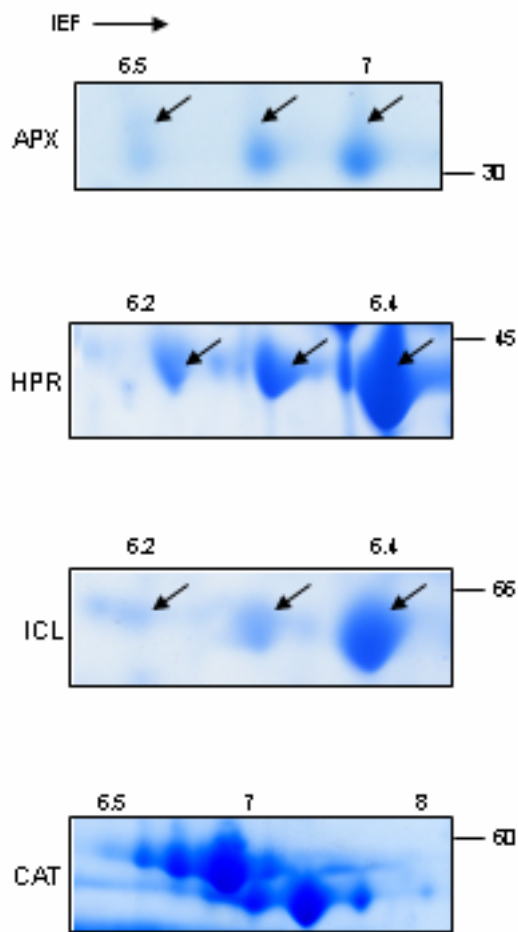


**Fig. 3.19: Indications for post-translational modifications of known leaf peroxisomal matrix proteins from *Spinacia oleracea* L.**

Many leaf peroxisomal proteins were identified in multiple spots on 2-D gels. 2-D patterns for ascorbate peroxidase (APX), hydroxypyruvate reductase (HPR), isocitrate lyase (ICL) and catalase (CAT) are presented. Numbers to the right indicate approximate molecular masses and those at the top of each panel are approximate pH units estimated based on the 3-10 non-linear pH gradient in the IPG strip. The proteins showed similar apparent molecular mass but differed in their isoelectric point. For CAT, two sets of protein spots that differed in their molecular masses were also seen.

### 3.4.2. Studies on protein phosphorylation in leaf peroxisomes

It has been estimated that over a third of the total number of eukaryotic proteins may be modified post-translationally by phosphorylation (Hubbard and Cohen, 1993) although only a small proportion (about 10%) of the proteins may exist as the phosphorylated form at any instant. We pursued to explore the leaf peroxisomal proteome for the probable presence of phosphorylated proteins based on several lines of indirect



evidence that suggest that this PTM may be prevalent among peroxisomal proteins. These include reports for indications for posttranscriptional regulation of peroxisomal proteins such as, malate synthase and isocitrate lyase (Ettinger and Harada, 1990), the recent demonstration of *in vitro* phosphorylation of thiolase (Fukao *et al.*, 2003), identification of kinases in the peroxisome (Fukao *et al.*, 2002) (see also 4.5.1). Because of a lack of knowledge for the probable induction of phosphorylation, if any, under any specific condition, analysis of probable phosphorylation was carried out with normal plant tissues.

#### **3.4.2.1. Phosphate metal affinity enrichment of phosphorylated proteins from leaf peroxisomes of *Spinacia oleracea* L.**

Phosphorylated proteins from the spinach leaf peroxisomal matrix were enriched using a commercially available phosphoprotein enrichment column based on the principle of phosphate metal affinity chromatography (PMAC, Fig. 3.20). The principle of phosphate metal affinity chromatography is the selective binding of phosphate to a resin (normally a chelating resin involving metal ion such as  $\text{Fe}^{3+}$ ,  $\text{Ga}^{3+}$ , Ni or Zn) followed by their elution using phosphate buffer.

The phosphate metal affinity chromatography enrichment of phosphorylated proteins is presented in Fig. 3.20. A total protein lysate from spinach leaf peroxisomes was used as the starting material. The loading, binding, washing of unbound proteins and elution of phosphorylated proteins with phosphate buffer were performed as described in methods according to the manufacturer's instructions but with minor adaptations (2.14). Complete solubilization of proteins could be achieved with the protocol, yet, it was not possible to solubilize the proteins if they were precipitated (in order to concentrate them). Therefore, dilute solutions of protein (containing between 0.1 and 0.5 mg/mL) were loaded on the column. Purification was carried out under native conditions in the absence of urea. About 98% of the loaded proteins were present in the flow through that predominantly contained non-phosphorylated proteins and the remaining 2%, corresponding to the phosphorylated proteins, were recovered in the eluted fractions, mainly in the 2<sup>nd</sup> and the 3<sup>rd</sup> fractions (lanes 4 and 5, respectively). Several protein bands were enriched in the eluted fraction (Fig. 3.20, arrowheads). The binding appeared to be specific since the protein patterns were different in the eluted fraction and in the flow through. The common

protein bands could correspond to the most abundant proteins (that may or may not be phosphorylated) or to enriched phosphorylated proteins with molecular masses similar to those of the most abundant proteins and therefore remained 'masked' in the loaded fraction.

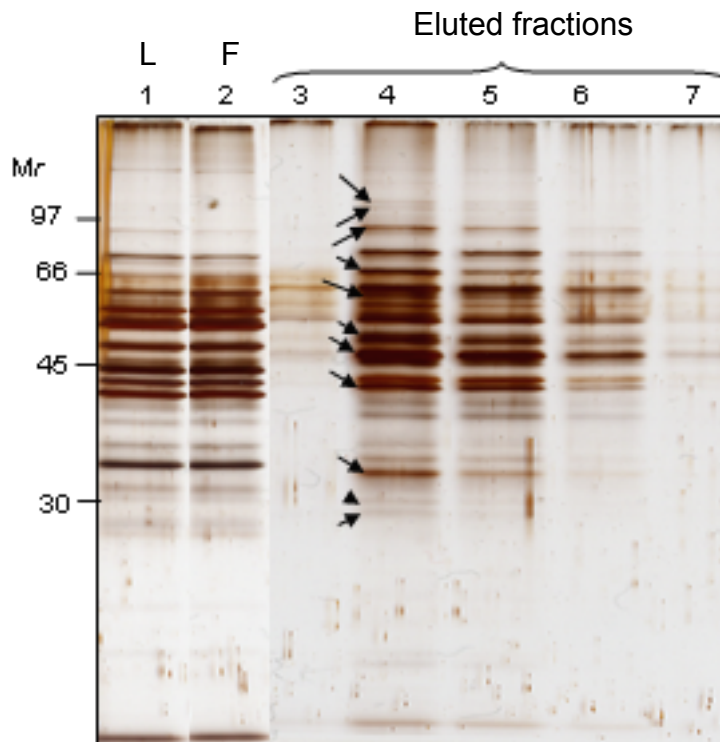


Fig. 3.20: Enrichment of phosphoproteins from *Spinacia oleracea* L. leaf peroxisomes

A clarified lysate from 3 mg solubilized protein sample from spinach leaf peroxisomes (isolated according to a preparative method using two successive density gradients) was enriched for phosphoproteins by PMAC. Binding was performed at 4 °C. The flow through (non-phosphorylated proteins) was collected for analysis. The bound proteins were eluted with phosphate buffer, precipitated with chloroform-methanol, solubilized and resolved by SDS-PAGE. In lane 1 (L: loaded fraction) and in lane 2 (F: flow through), 2 µg protein were loaded. In lanes 3-7 (eluted fraction) equal volumes were loaded. The relative phosphoprotein content in the sample was estimated at about 2% based on silver staining. Arrows indicate proteins enriched in the eluted fraction as compared to the flow through. A representative gel from two independent experiments is shown (n=2).

### **3.4.2.2. Resolution of phosphorylated proteins from leaf peroxisomes of *Spinacia oleracea* L. by two-dimensional gel electrophoresis**

The protein composition in the flow through consisting of presumably non-phosphorylated proteins and in the eluted fractions (which is enriched for phosphoproteins) was compared after two-dimensional (2-D) gel electrophoresis. An image of a silver stained 2-D gel showing the protein pattern obtained in the eluted fraction following column purification is shown in Fig. 3.21. More than 20 protein spots were enriched or were present only in the eluted fractions indicating that they were phosphorylated. Most of the enriched proteins showed a distinct pattern, with a progressive shift in their isoelectric points (by about 0.1 pH units) but no apparent change in the molecular mass. Such a pattern is characteristic of post-translational modification by phosphorylation. At least five “trails” of spots (Fig. 3.21, boxes 1-5) were enriched in the eluted protein fraction. In addition, some ‘single’ proteins were also enriched. In some trails, the most acidic spot was enriched in the eluted fraction (Fig. 3.21, boxes 6 and 7). These are discussed below.

The proteins of trail 1 have a size of approximately 66 kDa and a pI range roughly between 6.5 and 7. This trail comprises at least four protein spots of different relative abundances. At least three out of the four spots most likely derive from isocitrate lyase (ICL) by analogy to three previously identified protein spots (Fig. 3.11 a, spots 50, 69, 120) from spinach peroxisomal 2-D gels. This trail from spinach leaf peroxisomes was almost completely absent on the 2-D gel of the flow through, indicating a high percentage of phosphorylated ICL.

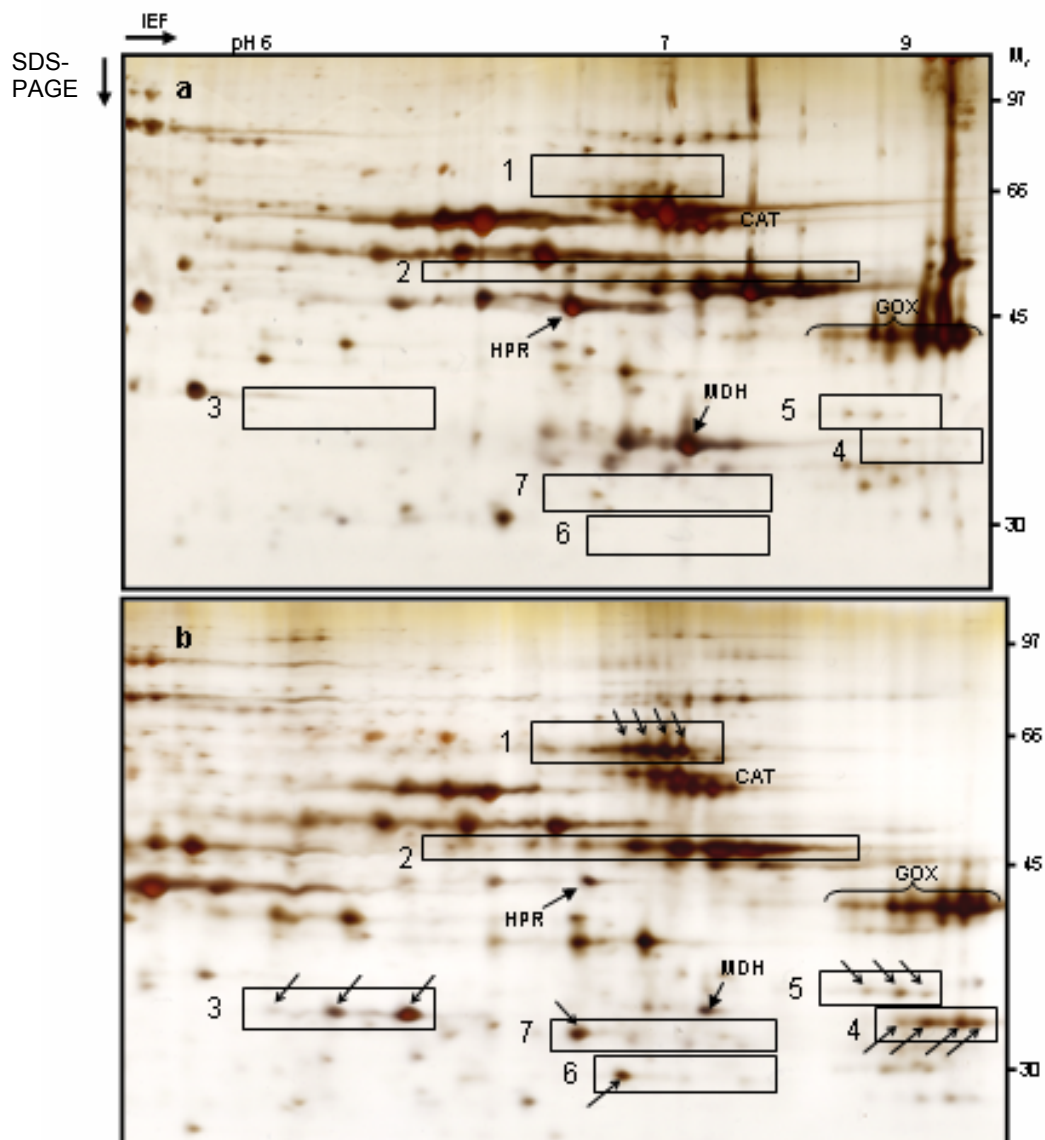


**Fig. 3.21: Phosphoproteins from *Spinacia oleracea* L. leaf peroxisomes resolved by two-dimensional electrophoresis**

A clarified lysate from a 3 mg sample of solubilized spinach leaf peroxisome proteins was enriched for phosphoproteins by phosphate metal affinity chromatography. Binding was performed at 4 °C. The flow through (non-phosphorylated proteins) was collected for analysis. The bound phosphorylated proteins were eluted with phosphate buffer, precipitated with chloroform-methanol, solubilized and resolved by 2-DE. Spots enclosed by boxes (1-7) represent proteins that were enriched in the eluted fractions as compared to the flow through. The enriched proteins show a pattern characteristic for phosphorylation. In boxes 6 and 7 only the most acidic spots were enriched.

The proteins of trail 2 (Fig. 3.21) have a size of about 48 kDa, a pI range between 6.5 and 7.5 and comprise at least eight protein spots. The migration coordinates of some of these correspond to thiolase and/or sulfite oxidase. The third protein trail (Fig. 3.21) is interesting, in particular, because it was seen only in the eluted fraction and was completely absent in the flow through. The proteins have a molecular mass of 35 kDa and the isoelectric point of the more basic spot is around 6. By analogy to the recently published *Arabidopsis* peroxisome proteome (Fukao *et al.*, 2002) these spots may represent the protein kinase At4g31220 which carries a PTS1, namely the tripeptide PKL>. Trail four is comprised of four proteins (Fig. 3.21); trail five is represented by at least three proteins (Fig. 3.21). While the former could be porins, the identity of the latter is not known. In trails six and seven, the acidic form of the protein was enriched, in line with the shift of the isoelectric point of a protein to an acidic range due to the attachment of  $\text{PO}_4^{3-}$ .

In future, the putatively phosphorylated proteins will be identified from the corresponding gels and their phosphorylation confirmed by one of the several analytical tools available for the purpose.

## 4. Discussion

The objective of this study was to analyze the leaf peroxisomal proteins using a proteomics approach to identify novel proteins, as well as isoforms of known leaf peroxisomal proteins, and to characterize their post-translational modifications, the rationale being the elucidation of the organelle's novel functions based on its protein complement. The ideal model plant for proteome studies should (i) offer the possibility to isolate large quantities of leaf peroxisomes in a reasonably pure state, (ii) enable realization of the full potential of the highly sensitive analytical tools (e.g. mass spectrometry), and (iii) enable downstream applications such as subcellular localization of the interesting proteins and/or their further characterization by generating mutants etc. Unfortunately, no single plant system satisfied all these requirements. Therefore we chose to systematically identify leaf peroxisomal proteins from *Spinacia oleracea*, a plant for which the organelle preparation protocol is well-established. Although the organism is barely represented in the database (< 1,500 protein entries in the NCBI, March, 2004), thanks to advanced *in silico* analysis techniques and growing databases (especially those for ESTs), identification based on homology, for instance, to sequences from other plants, is possible. However, because of the distinct advantages offered by the fully sequenced genome of the model plant *Arabidopsis thaliana* (AGI, 2000), efforts towards the characterization of its peroxisomal proteome were pursued earnestly.

### 4.1. Isolation of leaf peroxisomes from *Spinacia oleracea* L. and *Arabidopsis thaliana* (L.) Heynh. for proteome analyses

Isolation of highly pure organelles from different kinds of organs is a biochemical challenge. Since the highly coordinated metabolic networks within the cell necessitate a close *in vivo* association of its compartments with another, their *in vitro* separation is often difficult. The isolation of leaf peroxisomes is particularly challenging for several reasons. In comparison to the double-membraned chloroplasts and mitochondria that are more abundant within the cell, the single-membraned leaf peroxisomes are relatively fragile organelles and are present at much lower abundance (0.3-0.4% of cell volume in mesophyll cells of spinach, Winter *et al.*, 1994). The pattern of distribution of the relative

amounts of intact and broken peroxisomes and mitochondria indicates the significantly higher fragility of the former (Fig. 3.2) despite a relatively gentle homogenization (using a mortar and pestle). Particularly, because of their synergistic interaction during photorespiration, leaf peroxisomes are closely associated with mitochondria and chloroplasts (Gerhardt, 1978), and this physiological association is difficult to disrupt. Additionally, peroxisomes and mitochondria are prone to an *in vitro* aggregation during the isolation procedure that essentially involves an enrichment of the organelles by sedimentation via differential centrifugation.

#### **4.1.1. On the improvement of purification of leaf peroxisomes from *Spinacia oleracea* L. for proteome analyses**

The extent of purity of organelle preparations that is required depends on the analytical application. In 'classical' studies such as immunological characterizations, highly specific analytical tools (e. g. antibodies) can compensate for a lack of high purity. Large-scale proteome studies, on the other hand, are aimed at generating protein profiles of whole entities such as that of an entire subcellular compartment and for such applications, purity is of utmost concern unless innovative methods are devised to differentiate genuine novel proteins from contaminants.

*Spinacia oleracea* L. was chosen in the present study to generate a proteome map of leaf peroxisomes because of the long-standing experience of several former colleagues of our department (Heupel *et al.*, 1991; Heupel and Heldt, 1994; Reumann *et al.*, 1998). For initial subcellular fractionation of leaf peroxisomes, a modified protocol was used which is based on the method of Yu and Huang (1986). In this method, the low viscosity of Percoll solutions enables quick organelle separations under iso-osmotic conditions. The high yield of leaf peroxisomes from the above method directed efforts towards exploring the possibility of further improving their purity by a second density gradient. Several methods were tested before resorting to a sucrose density gradient purification. The utility of two consecutive Percoll density gradients to separate mitochondria (Millar *et al.*, 2001) has been reported. However, when a second Percoll density gradient was applied to enhance purity of leaf peroxisomes, it appeared that extended exposure of peroxisomes to

colloidal silica (Percoll) had a negative influence on their integrity since the yield was significantly low (data not shown), an effect also noticed earlier (Heupel *et al.*, 1991).

An optimized purification scheme for the isopycnic separation of peroxisomes employing a sucrose density gradient (2.2.1.1) reduced the chlorophyll content of the peroxisome fraction to almost undetectable levels (Table 3.1), while the yield was not affected significantly. However, the peroxisome fractions appeared to be significantly contaminated with enzymes of the Calvin cycle such as aldolase, transketolase, NADP-glyceraldehyde-3-phosphate dehydrogenase and phosphoglycerate kinase. These were detected by two-dimensional electrophoresis (appendix 1) and, as judged by their relative dominance (data not shown), appeared to be present at significant levels in the peroxisomal preparations. The absence of chlorophyll and the equilibrium density of these organelles similar to peroxisomes pointed towards proplastids as contaminating organelles. On the other hand, proplastids are, by definition, non-differentiated plastids and not reported to contain enzymes of the Calvin cycle. Therefore the term proplastid-like organelle is used to denote the contaminant. The pronounced presence of these proplastid-like organelles in spinach and their absence in *Arabidopsis* is intriguing but could not be analyzed any further within the scope of this study. A systematic approach was followed to eliminate the proplastid-like organelles. In order to devise ways to minimize the contaminant, the following possible reasons for the cross-contamination of these organelles were considered

1. artificial *in vitro* aggregation by sedimentation
2. similar equilibrium density in sucrose density gradients
3. pronounced *in vivo* association

The pattern of distribution of hydroxypyruvate reductase and NADP-dependent glyceraldehydes-3-phosphate dehydrogenase (NADP-GAPDH) in an initial linear sucrose density gradient of high resolution showed an apparent comigration of the two organelles. An attempt was made to overcome a possible sedimentation-related *in vitro* aggregation. The fraction of resuspended organelles was subjected to an intensified homogenization of the organelle suspension prior to their density gradient centrifugation. A partial separation could be achieved as a result of this treatment and distinct peaks for peroxisomes and



proplastid-like organelles could be obtained close to each other (Fig. 3.1). The fractions corresponding to these peaks differed in their purification factor with respect to the contaminant by a factor of 25 to 50 (data not shown). However, the intensity of the homogenization did not enhance resolution of the peroxisomes and proplastids proportionally. Rather a reduction in purity was encountered, probably as a consequence of reduced yield of intact peroxisomes. Therefore a Potter-Elvehjem homogenizer (5 mL capacity) that gave consistent results was used to homogenize the peroxisomes before their further purification. As an alternative, the effect of certain components with proven capacity to reduce artificial aggregation of organelles was investigated. These included salts such as  $MgCl_2$  and KCl that are known to serve the purpose of minimizing aggregation and have been used to substitute for EDTA for e.g. in plasma membrane preparations. However, these salts when added to the density gradient solutions did not reduce aggregation significantly. The effects of EDTA and  $MgCl_2$  may have to be investigated independently at different concentrations. Due to time constraints, a simple experimental design for determining the optimum concentrations was not possible and therefore not pursued further in this study.

For proteome studies, the fractions corresponding to the peroxisomes and the proplastid-like organelles were harvested separately and comparative two-dimensional patterns were generated (Fig. 3.17). The peroxisome fraction was characterized by dominant spots of catalase, glycolate oxidase (GOX) and many alkaline proteins that were later identified to be peroxisomal. The spot that corresponded to RubisCO was much less abundant but still visible in this fraction. By contrast, in the proplastid fraction RubisCO was one of the most abundant spots as was NADP-GAPDH. Thus, the peroxisomal proteins could be differentiated from those originating from the proplastid-like organelles based on their relative abundance on the corresponding gels (Fig. 3.15). This strategy, based on differential profiling proved to be an effective method to identify contaminants. In the subsequent mass spectrometric analyses carried out on more than 100 spots, no contaminant, other than one minor RubisCO spot, was detected which obviously originated from a non-peroxisomal compartment.

During the experimental studies of this thesis, a method was published for the isolation of leaf peroxisomes and glyoxysomes from *Arabidopsis* (Fukao *et al.*, 2002; 2003). It differed from other protocols in using a less common osmoticum, raffinose, for purification of peroxisomes via Percoll density gradients. Although the authors did not comment on the reason, it may be speculated that raffinose was used instead of sucrose to increase the equilibrium density of the peroxisomes in order to achieve a better separation of the organelles. It has been shown earlier that the equilibrium density of peroxisomes increases with the size of the sugar used as the osmoticum. Peroxisomes equilibrated at a relatively low density in mannitol, which increased in sucrose and was much higher in raffinose (Reumann, 1993). By contrast, the equilibrium density of the other organelles remained largely unchanged (data not shown), leading to an enhanced purity of leaf peroxisomes in raffinose. This is an effect inherent to the differential permeability of the organelles to various osmotically active ingredients, especially sugars, which was substantiated in the present study (data not shown). Purification of peroxisomes over the proplastid-like organelles was superior in raffinose-based Percoll density gradients to those based on sucrose/mannitol (data not shown). A novel strategy applied in this study to minimize the contamination of leaf peroxisomes is discussed elsewhere (4.1.2).

Some further interesting observations were made during the course of this study, which suggested a significant impact of the pre-treatment of plants on the purity of leaf peroxisomes. Preparations of peroxisomes from spinach leaves from a commercial source that had been, probably, subjected to a long-term cold-storage, consistently resulted in a better separation between peroxisomes and the proplastid-like organelles (in more than three independent experiments). This was reflected in the purity of peroxisomes obtained which was several fold higher than that of those from the growth chamber-cultivated plants that were not subjected to this treatment. The higher purity of leaf peroxisomes was probably a consequence of an *in vivo* separation of organelles due to decreased peroxisomal metabolism at low temperatures. To test this, leaf peroxisome preparations were compared between leaves that were freshly harvested and those that had been stored at 4 °C for three days. No difference in purity was observed. It was possible that this

result was due to diametrically opposed effects although cultivar specific variations may not be ruled out entirely.

Leaf peroxisome isolation was normally carried out from plants harvested at the beginning of the light period to allow for sufficient reduction in the starch content in the chloroplasts. Since significant quantities of starch accumulate in the chloroplasts during the day, their presence results in extensive damage to the chloroplasts and perhaps also to peroxisomes during tissue homogenization. However, when peroxisomes were prepared from tissues harvested at the end of the light period, levels of RubisCO in the peroxisome fraction were significantly reduced as evidenced by two-dimensional electrophoresis. Thus, the quality of the peroxisomes prepared is governed not only by the efficiency of the method but also depends on several other less well-defined factors that need to be closely monitored in order to obtain reproducible results. That these effects are not exerted exclusively on peroxisomes but also on the other subcellular compartments, such as, mitochondria and chloroplasts is also an issue to be considered.

#### **4.1.2. Establishment of an analytical method for the isolation of leaf peroxisomes from *Spinacia oleracea* L. for proteome analysis**

In order to compare protein profiles of leaf peroxisomes from different physiological states, it was necessary to prepare them without much temporal separation. Reproducibility and the possibility to handle two samples simultaneously (especially with respect to the light period and the duration of the stress applied), rather than yield were of utmost concern for such an analytical method. In line with reasons stated earlier for the possible aggregation of organelles, the following modifications were made:

(i) **Reduction of artificial aggregation:** Since repeated sedimentation and resuspension may contribute to an artificial aggregation of organelles, such steps were eliminated. Instead, the leaf tissue was ground in a small quantity of the homogenizing buffer and the post-plastidic supernatant (after sedimenting most of the plastids) was directly applied on a gradient for a one-step purification of peroxisomes. Besides, the advantage was a reduced duration for the entire isolation procedure and the elimination of any variation incurred due to extensive handling. The gradient had to be shortened considerably to accommodate

relatively large volumes of the sample to be applied. Also the number of gradients that had to be used was considerably higher.

**(ii) Use of a different osmoticum to achieve superior separation of peroxisomes from the other organelles:** In order to keep the proplastid contamination minimal, the 55% (v/v) Percoll, (see 2.2.1.2) solution was prepared in raffinose instead of sucrose. It was considered necessary and even advantageous to prepare the upper layers of the density gradient in raffinose. A linear gradient of Percoll (18 to 27% v/v) prepared in sucrose was used, to prevent the possible formation of a migration barrier by the relatively more abundant plastids. The use of the 'dual' osmoticum while allowing a gradual transition of the osmoticum from mannitol to the trisaccharide raffinose also helped to cut down on the expense of the latter. Interestingly, the survival of protoplasts was reported to be greater in a sucrose/raffinose mixture as compared to pure sucrose, trehalose, raffinose and mannitol (Xiao *et al.*, 2001). Although the exact mechanism for this phenomenon has not yet been clarified, it is possible that the sugars played a role in preservation of the structure and function of membranes (Koster *et al.*, 2000).

**(iii) Leaf peroxisomes were always prepared from leaf tissues harvested at the end of the light period** as there were indications for lower RubisCO contamination as compared to those harvested at the end of the dark period (data not shown).

Purification of peroxisomes could be achieved with relative ease using this method with minimum standard deviation between experiments and was also effective in yielding peroxisomes from leaf tissues of plants that had been subjected to stress, thereby opening up the possibility of comparative proteome analyses (stress treated vs. control).

#### **4.1.3. On the development of a method to enrich leaf peroxisomes from *Arabidopsis thaliana***

*Arabidopsis thaliana* is the first higher plant to have its fully sequenced genome publicly accessible. Characterization of the proteome from *A. thaliana* therefore offers several advantages such as cloning of the genes that encode novel proteins, generation and analysis of mutants for the functional characterization of the genes etc. In the context

of the stress proteome, the situation is even more advantageous since the isoforms specifically involved in a stress response may be identified unambiguously. For example, a 'digital' northern analysis suggested significant differences in isoform-specific gene-expression between normal and stressed tissues of *A. thaliana* (data not shown). About 70% of the ESTs (30 out of 42) of a particular isoform of alanine-glyoxylate aminotransferase (AGT1) gene (acc. no. At2g13360) was represented in libraries constructed from stressed tissues while the distribution of other AGT isoforms (At3g08860, At4g39660 and At4g38400) did not show such a bias in either type of tissues (data not shown) suggesting a possible stress-related function for AGT1 and house keeping roles for the other AGTs. Thus, because of its sequenced genome, a large number of proteomic investigations has been carried out using this organism. Mitochondria (Kruft *et al.*, 2001; Millar and Heazlewood, 2003; Heazlewood *et al.*, 2003), the plasma membrane (Santoni *et al.*, 1998), Golgi membranes (Prime *et al.*, 2000) and different sub-compartments of chloroplasts (Peltier *et al.*, 2002; Schubert *et al.*, 2002; Froehlich *et al.*, 2003) have been analyzed from *Arabidopsis* tissues, and heterotrophic cell-suspension cultures served as organelle sources for some of them. When the present work was initiated, no protocol was available for the isolation of pure peroxisomes from leaf tissues of *A. thaliana* that allowed for proteomic investigations to be carried out; only recently has such a protocol been published (Fukao *et al.*, 2002). This procedure, however, was not as effective in our hands (data not shown). Therefore a great deal of effort was invested during the course of this study into developing an effective method to enrich leaf peroxisomes from *Arabidopsis*.

Six buffers were shortlisted after an extensive survey of literature for their efficiency in plant peroxisome preparation. The selected buffers allowed for sufficient variations with respect to the osmotica that were employed (different concentrations of sucrose for pea, castor bean and cucumber, mannitol for spinach and sorbitol for yeast) or the pH (pH 7.5 for most of them except for the 'yeast' and the *Arabidopsis* buffer that had a slightly acidic pH of 6). The efficacy of these buffers was tested based on their ability to sustain the stability of leaf peroxisomes over a time course.

Stability was optimal in a hypertonic medium (1 M sucrose), yet, inferior to that sometimes achieved using 0.5 M sucrose buffered with Tris. The inconsistency of results was thought to be related to the greater sensitivity of Tris to fluctuations in temperature.

Therefore the pea- grinding buffer (with tricine) was used to isolate leaf peroxisomes from *Arabidopsis*. Interestingly, the 'yeast'-buffer with sorbitol as the osmoticum and a pH at 6 also gave good results with respect to maintenance of stability. The positive influence of KCl and MgCl<sub>2</sub> on the stability of leaf peroxisomes may be due to the stabilizing effect of these additives on the peroxisomal membranes. On the other hand, the negative effect of PMSF may be due to its preparation in isopropanol. Glycerol is thought to have resulted in a negative effect due to its profound effect on osmolarity of the buffer. The optimized buffer was also found to be suitable for the isolation of peroxisomes from a number of plant sources including tomato and rape (data not shown).

Further, differential centrifugation, to enrich peroxisomes, while keeping plastid contamination to a minimum, was also optimized.

The sedimentation of peroxisomes by differential centrifugation presented two independent problems. These were:

1. the artificial aggregation of organelles (as already mentioned for the spinach leaf peroxisome isolation procedure) and
2. the necessity to mechanically resuspend the sediment enriched for peroxisomes prior to its homogenization.

In order to overcome these problems simultaneously, attempts were made to enrich peroxisomes over a cushion of sucrose during differential centrifugation. However, a different kind of problem was encountered. This was related to the lack of stability of the organelles when diluting the peroxisomes-containing fraction which was of a high sucrose concentration.

The method that was suitable to isolate highly pure leaf peroxisomes from spinach by the 'post-plastidic' supernatant loading analytical method was not efficient for *Arabidopsis*. When such a fraction was applied on a shortened sucrose density gradient, the yield of peroxisomes was low, probably, because of very high concentrations of active proteases. Yields could not be increased even when the grinding buffer was supplemented with protease inhibitors.

Therefore, it was decided to sediment the peroxisomes from the post-plastidic supernatant and then carefully resuspend it prior to gentle homogenization. A relatively short centrifugation time was highly preferred to isolate leaf peroxisomes. Therefore,

several density gradient media such as Percoll (colloidal silica), Ficoll (high molecular weight sucrose-polymers formed by copolymerization of sucrose with epichlorohydrin) and Nycodenz (5-(N-2,3-dihydroxypropylacetamido)2,4,6-triiodo-N, N'-bis (2,3-dihydroxypropyl) isophthalamide) were tested. Hayashi *et al.* (1975) purified peroxisomes from rat liver using Ficoll as the density gradient medium. Nycodenz has been previously shown to be useful for the preparation of peroxisomes from mammalian tissues (Ghosh and Hajra, 1986; Yoshihara *et al.*, 2001; Kovacs *et al.*, 2001) and from yeast (Erdmann and Bloebel, 1996). While Percoll based density gradients gave good result when used with raffinose, reproducibility was still a major concern. The other media gave poor results. However Ficoll- and Nycodenz-based methods were not pursued intensively due to time constraints.

A sucrose-based density gradient was optimized and used for routine isolation. The peroxisome-enriched fraction obtained from the sucrose density gradient was subjected further to a different kind of density gradient separation. This was because of the difficulty with washing the peroxisomes obtained from the first purification in order to concentrate them. For the second centrifugation, the concentrated 52% (w/w) sucrose fraction containing the peroxisomes was diluted gradually to 48% (w/w) and the contaminants were floated away. When such a method comprising two successive density gradient centrifugations was applied, the extent of purity was quite high and allowed for proteomic analysis.

## ***4.2. Two-dimensional electrophoresis for resolving soluble proteins from leaf peroxisomes***

### **4.2.1. On the optimization of the method for two-dimensional electrophoresis**

Sample solubilization is a critical pre-electrophoretic step, which directly influences the quality of results significantly. Therefore it is important that the solubilization buffer is

optimized so that the final protein profile reflects a nearly true profile of the sample. A chaotrope aids in solubilization by disrupting the secondary structure of proteins and is thus an essential ingredient in 2-D solubilization buffers. For spinach leaf peroxisomal proteins, it was shown that a concentration of 8 M urea gave good yet sub-optimal protein recoveries (Rittstieg, 2001). In the present study, the visualization of several previously undetected proteins was enabled due to the inclusion of thiourea during solubilization (Fig. 3.4 and 3.5). This can be attributed to the enhanced chaotropic power of 2-D buffers in the presence of thiourea that has been implicated in the recovery of hydrophobic and isoelectrically neutral proteins (reviewed by Molloy, 2000; Rabilloud, 1998). The negative effect on resolution as reported in a particular instance (Musante *et al.*, 1998) was not encountered for the soluble component of the leaf peroxisomal proteins analysed in this study, and the apparent 'smearing' of protein spots (Fig. 3.5) is thought to be a consequence of higher protein recovery.

In addition, it was found that the post-solubilization recovery of high molecular mass proteins was greater in the presence of thiourea (Fig. 3.4). The loss of low molecular mass proteins was more acute, as such proteins were represented (although not adequately) only when considerably high protein concentrations were used initially. In fact, the inability to resolve the low and high molecular mass proteins simultaneously is one of the drawbacks of the 2-D methodology and several improvements to overcome this problem are available from a survey of relevant literature (Tastet *et al.*, 2003). The loss of low molecular weight proteins due to this technical constraint may be a reason for the under-representation of such proteins in this study.

Chaotropes disrupt the secondary structure of proteins at the cost of exposing their hydrophobic domains, which may lead to increased protein aggregation due to hydrophobic interactions. In order to disrupt these interactions, detergents are included in the two-dimensional solubilization buffer. At least one representative of the three distinct classes of detergents (see 3.2.2) was tested for their efficiency in protein solubilization for two-dimensional electrophoresis (2-DE). Of these, the sulfobetaine-type zwitterionic detergent CHAPS (3-[(3-cholamidopropyl)-dimethylammonio]-propanesulfonate) gave optimum recovery and resolution. A streaky effect obtained with ASB-14 (amidosulfobetaine-14, another sulfobetaine-type detergent) observed in the present



study, has also been reported earlier for rat brain homogenates (Carboni *et al.*, 2002). The use of detergent cocktails enhanced recovery of proteins (e.g. CHAPS or ASB-14 plus N-octyl glucoside) but the concentrations may have to be further optimized depending on the critical micelle concentration of the detergents. A non-detergent sulfobetaine (NDSB 256) was also tested as an additive to the 2-D buffer because of its beneficial effects in preventing aggregation during protein renaturation and improved isoelectric focusing under non-denaturing conditions (Bezancon *et al.*, 2003), however, without success (data not shown). The differential extent of solubilization of the detergents has been exploited to selectively enrich for low abundant proteins. For leaf peroxisomes, it may be useful to remove the abundant soluble proteins using a less efficient detergent (such as Nonidet P-40) for the enrichment of the less abundant proteins which may be resolubilized by a more efficient detergent.

The recovery or resolution of soluble alkaline proteins from leaf peroxisomes seemed relatively easier to achieve. A very good recovery and reasonably good resolution were obtained for such proteins using the buffer that was routinely used to solubilize proteins for two-dimensional electrophoresis. When different additives such as alcohols, were supplemented to this buffer, an inferior resolution and/or recovery were encountered. The high concentrations of alcohols used may have contributed to this effect by an increase in viscosity of the protein solution. It is concluded that improved detection of proteins in this range may be possible after the removal of the overwhelmingly abundant proteins. This could be the reason why usefulness of zoom-in gels was only marginal in this investigation.

#### **4.2.2. On the proteome coverage achieved by two-dimensional electrophoresis for leaf peroxisomes**

The number of proteins that could be reproducibly detected on the two-dimensional gels of leaf peroxisomes from *S. oleracea* was about 200. However, if the non-peroxisomal proteins are subtracted away, the actual number of 'truly' peroxisomal spots is estimated between 100 and 150. If it is assumed that every individual protein spot on the gel represents an independent gene product, this number represents about 50% of the total

number of approximately < 300 proteins predicted by *in silico* analyses to have the potential to be targeted to the peroxisomal matrix (Fukao *et al.*, 2003; Reumann *et al.*, submitted). Furthermore, it is known that the old paradigm 'one gene=one product' is not the case with eukaryotic genomes where a large majority of proteins are subjected to some kind of post-translational modification (such as phosphorylation or glycosylation) that often result in a shift in their isoelectric point and/or molecular weight. Therefore, the number of spots on the two-dimensional gels that are actually products of independent genes is in general much smaller, creating an apparent gap between genomic prediction and proteomic representation. However, there are additional issues to be considered. Several genes may encode proteins specifically expressed in organs such as seeds and roots and therefore may not be expected to be represented on the leaf peroxisomal proteome. Whether an *in silico* expression analysis can provide reliable information on such specificity is questionable, especially for low abundant proteins. Additionally, algorithms to predict subcellular localization of proteins may predict some false-positives. Finally, the issue of some pseudogenes that do not code for any protein product should also be considered. Therefore, it may be concluded that reasonably good representation of the proteome was achieved in this study.

Some proteins that were not identified in this study included the peroxisomal multifunctional protein (MFP), CuZn superoxide dismutase (CuZn-SOD, Bueno *et al.*, 1995), Mn-SOD (Pastori *et al.*, 1996; Palma *et al.*, 1997), NADP dehydrogenases (three isoforms of glucose-6-phosphate dehydrogenase and isocitrate dehydrogenase and 6-phosphogluconate dehydrogenase, Corpas *et al.*, 1998). Interestingly, isocitrate dehydrogenase was reported to be present in trace amounts in spinach leaf peroxisomes (Tolbert *et al.*, 1971). Although the presence of these enzymes in low quantities may be a possible reason for their non-identification, yet the more plausible reason could be that protein identification by mass spectrometry has not been carried out for all the 'peroxisomal' proteins on the two-dimensional gel. In future, as protein identification is extended to a larger number of spots, it is likely that such proteins may be detected. Another reason could be related to the inherent properties of, at least, some of these proteins. For example, the multifunctional functional protein has a basic isoelectric point (>9.2) which could have hindered its detection by two-dimensional electrophoresis. It may

be worthwhile to analyze the gels for the presence of known peroxisomal proteins by immunodetection.

### **4.3. A comparison of the peroxisomal proteome of *Spinacia oleracea* with the recently published *Arabidopsis thaliana* peroxisomal proteome**

The proteome of peroxisomes from mesophyll cells of spinach leaves has been partially defined in this study. The glyoxysomal (Fukao *et al.*, 2003) and the leaf peroxisomal proteome from greening cotyledons (Fukao *et al.*, 2002) have been defined for *Arabidopsis* recently by two-dimensional electrophoresis combined with mass spectrometry. A comparison of these proteomes is presented below.

#### **Known enzymes**

In the present study, several proteins including enzymes involved in, the photorespiratory pathway,  $\beta$ -oxidation, glyoxylate pathway and, the metabolism of reactive oxygen species were identified based on sequence homology after mass spectrometric analyses of two-dimensionally resolved proteins (Fig. 3.11 and Appendix 1). In addition, homologs of some proteins that have only been recently described from peroxisomes, such as, sulfite oxidase (involved in sulphur metabolism, Eilers *et al.*, 2001; Nakamura *et al.*, 2002), 3-hydroxyisobutyryl-CoA hydrolase (CHY1, involved in valine catabolism, Zolman *et al.*, 2001), OPR3 (involved in biosynthesis of jasmonic acid, Strassner *et al.*, 2002) were also found in this proteome. Most of the photorespiratory enzymes including glycolate oxidase, photorespiratory aminotransferases, catalase, malate dehydrogenase and hydroxypyruvate reductase were identified in the leaf peroxisomal proteome (the present study) as well as in the proteome of peroxisomes from greening cotyledons (Fukao *et al.*, 2002). The presence of such enzymes in the latter is in line with reports on leaf peroxisomal enzymes present in the transition stage of glyoxysomes to leaf peroxisomes (as is the case with the greening cotyledons). The migration coordinates for most of these

proteins were identical in all the investigations. The identification of peroxisomal proteins, such as, glutamate-glyoxylate aminotransferase, hydroxypyruvate reductase and malate dehydrogenase was also possible using *Arabidopsis* leaf peroxisomes in this study (Fig. 3.12 and Appendix 2).

Enzymes of the glyoxylate cycle and for  $\beta$ -oxidation detected from the glyoxysomal proteome of *Arabidopsis* (Fukao *et al.*, 2003) were also detected from the leaf peroxisomal proteome from spinach in the present study. These were absent in the proteome of peroxisomes from greening cotyledons of *A. thaliana* (Fukao *et al.*, 2003) while at least one  $\beta$ -oxidation enzyme, namely, thiolase was also present in the *Arabidopsis* leaf peroxisomal proteome generated in the present study (Fig. 3.12). Whether this difference of the proteome is inherent to the plant species or due to technical limitation is not clear. The presence of glyoxysomal enzymes in leaf peroxisomes is not uncommon and an analogous situation has been reported for enzymes such as isocitrate lyase and malate synthase in cucumber (Koeller and Kindl, 1978) and in developing leaves of tomato (Janssen, 1995). The activity of isocitrate lyase was detected in leaves of several species including wheat, maize (Godavari *et al.*, 1973), pea (Hunt and Fletcher, 1977) and tobacco (Zelitch, 1988). The activity of multifunctional protein was reported in leaves by Guehnmann-Schaefer and Kindl (1994). Indeed, Gerhardt (1986) proposed that the presence of the  $\beta$ -oxidation pathway is *the* distinctive general biochemical characteristic of peroxisomes from plants based on the detection of such enzyme activities in leaf peroxisomes. It was thought that in non-fatty tissues, this system played a role in the turnover of lipids in plant membranes (Gerhardt, 1986) and in the net breakdown during the senescence (Gerhardt, 1992).

#### **Transmembrane- and membrane-associated proteins**

None of the analyses (neither this study nor Fukao *et al.*, 2002 and 2003) was specifically aimed at identifying membrane proteins. Despite this, membrane-associated proteins such as, ascorbate peroxidase and malate synthase could be detected from the two-dimensional maps, the latter identified immunologically by Fukao *et al.* (2003).

### **Novel proteins with unknown function**

The set of novel proteins identified from each of these independent investigations (present study and Fukao *et al.*, 2002 and 2003) was different. In the present study, four novel proteins were identified all of which possess specific targeting sequences that fit the recent description of either a major or minor PTS that increase their targeting probability to peroxisomes (Reumann, in press). By contrast, 20 novel proteins were identified from the proteome of peroxisomes from greening cotyledons of *A. thaliana* five of which possess putative PTS with a single amino acid substitution (IRL>, SKD>, SNI>, SKP> and IIL>). None of the substituted tripeptides, however, fits the description of major or minor PTS2 described by Reumann (in press). Twelve proteins did not possess any recognizable PTS (Fukao *et al.*, 2002). Therefore, the actual peroxisomal localization of these novel proteins is questionable and needs solid experimental support.

### **Proteins with regulatory roles**

A protein, annotated as a member of the small heat-shock protein family, having a probable regulatory function was identified in the present study from the proteome of *Arabidopsis* leaf peroxisomes. An *in silico* expression analysis showed that the protein was represented by numerous ESTs (data not shown) indicating a high level of expression that may have enabled its detection by two-dimensional electrophoresis.

Several proteins with putative regulatory function were identified in the peroxisomes of greening cotyledons (Fukao *et al.*, 2002). These included kinases, a phosphatase, a ubiquitin-activating enzyme none of which were identified in the present study either because of the fact that the identification of only a subset set of proteins from leaf peroxisomes has been accomplished (within the time restrictions of the present study) or because of a probable developmental stage-specific expression of regulatory proteins. Interestingly, resolution of phosphoprotein enriched proteins from leaf peroxisomal proteins of spinach revealed the presence of two previously undetected spots, the location of one of which corresponded to that of a kinase identified in the greening cotyledon proteome. Besides, the pattern of the two spots correlated well with that for phosphoproteins. Phosphorylation of several leaf peroxisomal proteins including thiolase was evident in the present study after phosphoprotein enrichment and 2-DE and is supported by the

demonstration of its *in vitro* phosphorylation by Fukao *et al.* (2003). On the other hand, indirect evidence for the occurrence of post-translational modifications for proteins such as, hydroxypyruvate reductase and isocitrate lyase, due to their identification from multiple spots, was exclusive to the present study.

#### **4.4. Novel proteins identified in the present proteomic investigation of leaf peroxisomes**

One protein spot from spinach leaf peroxisomes was identified as a homolog of prokaryotic naphthoate synthase (At1g60550), which belongs to a larger protein family in *Arabidopsis* of monofunctional enoyl-CoA hydratases/isomerases. The lower apparent molecular mass of the spinach protein as compared to the calculated size of the *Arabidopsis* homolog may be related to the fact that the N-terminal targeting sequence of PTS2-targeted proteins is cleaved upon import into peroxisomes. Three lines of evidence provided strong support for the idea that this unknown protein is indeed localized in plant peroxisomes. First, the protein carried a putative PTS2 nonapeptide of the sequence RLx<sub>5</sub>HL, which has been defined as a major PTS and is considered a strong indicator for targeting to peroxisomes (Reumann, in press). Second, the putative PTS2 was conserved in a full-length homolog from *Oryza* and in all homologous ESTs from various plant species, even though the N-terminal domain was only moderately conserved (Fig. 3.13). The targeting domain was further characterized by the presence of properties that have been determined to be conserved in PTS2-targeted proteins from higher plants (Reumann, in press), such as an additional basic residue in front of the PTS2 (pos. -1) and a P shortly behind the PTS2. Third, the peroxisomal localization was also supported by subtractive gel analysis by a differential profiling of proteins in the peroxisome and plastid enriched fractions of the sucrose density gradient. Postulated targeting to peroxisomes is currently underway and will be verified experimentally as fusion proteins of spectral variants of green fluorescent protein with the unknown protein in onion epidermal cells.

An important prerequisite for subsequent functional analysis of unknown proteins is a more or less precise idea about their physiological function to study the postulated function in a straightforward experimental approach. This can be determined by bioinformatics analysis, such as analysis of public databases for homologs characterized in other organisms and phylogenetic analyses. In such an approach, it was detected that this *Arabidopsis* protein together with the second enoyl-CoA hydratase/isomerase family protein (At4g16210) detected on spinach 2-D gels belongs to a larger family of monofunctional enoyl-CoA hydratases (Fig. 4.1). Interestingly, approximately six members of these enzymes carry a putative PTS and are likely to play a role in peroxisomal metabolism next to the enoyl-CoA hydratase activity of MFP, the basic enzyme of fatty acid  $\beta$ -oxidation (Preisigmüller *et al.*, 1994).

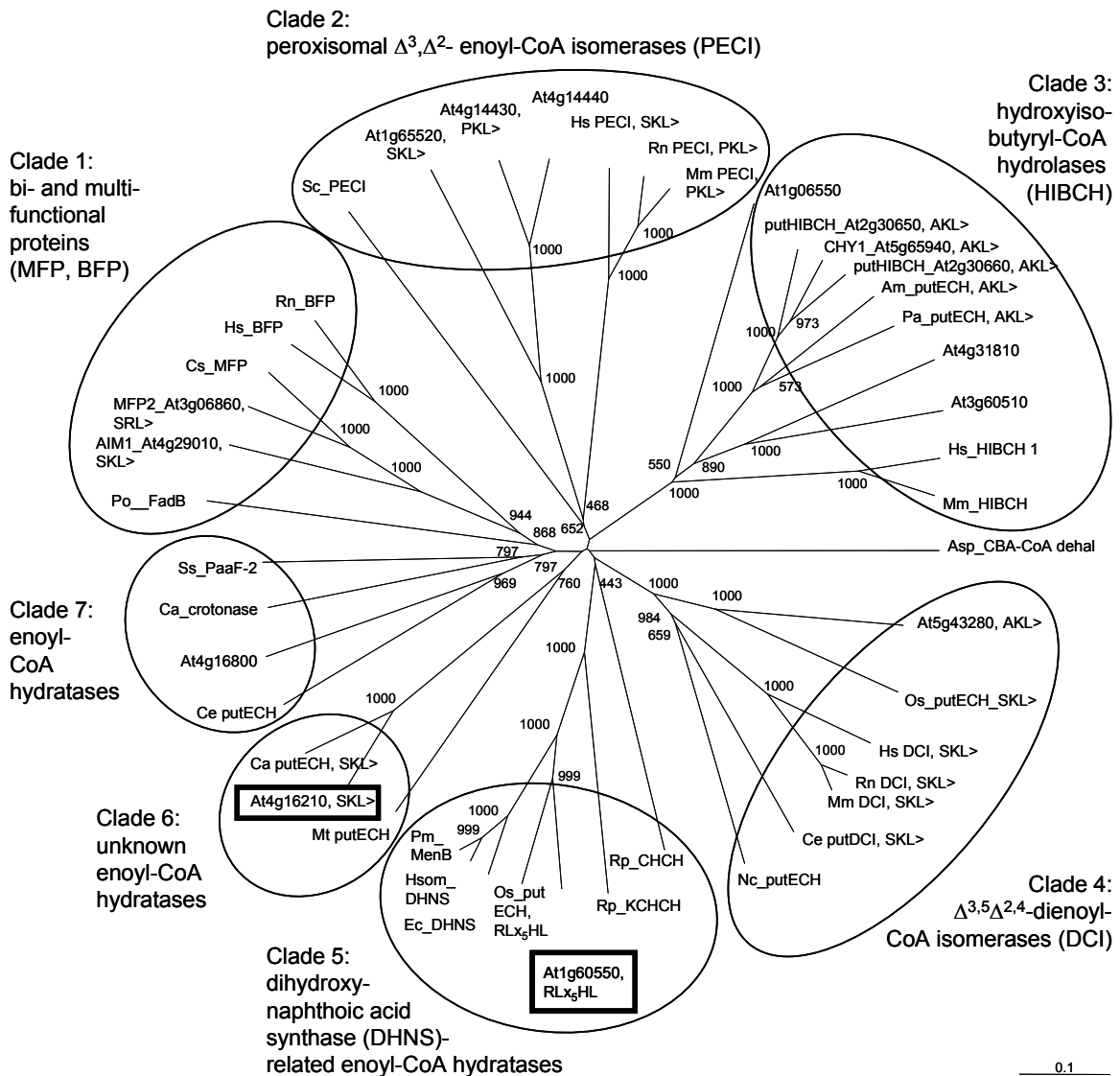


Fig. 4.1: Phylogenetic analysis of putative *Arabidopsis* enoyl-CoA hydratases from peroxisomes

Eukaryotic and prokaryotic homologs of unknown *Arabidopsis* enoyl-CoA hydratases with a putative PTS, two of which were identified on 2-D gels from spinach leaf peroxisomes in this study (see boxed proteins, clade 5: naphthoate synthase, At1g60550; clade 6: enoyl-CoA hydratase: At4g16210) were retrieved from the protein database at NCBI using blastp, aligned and a phylogenetic tree calculated using ClustalX (1000 bootstraps), and an unrooted phylogenetic tree was graphically constructed by Treeview (taken from Reumann et al., submitted). For eukaryotic proteins, recognizable PTS are indicated. Due to space limitations, bootstrap values are omitted in the centre of the tree (clade 1 with clade 7: 955; clade 1/7 with clade 6: 339; clade 2 with clade 3: 400; clade 2/3 with clade 1/6/7: 129; clade 4 with clade 5: 452).



To gain more insights into the possible function of the putative naphthoate synthase in plant peroxisomes, the public databases were analyzed for homologs of the *Arabidopsis* protein (At1g60550). It was found that the protein is not closely related to proteins from mammals, insects, or fungi, suggesting a plant-specific function. Instead, the enzyme shares about 70% identity with prokaryotic dihydroxynaphthoic acid synthases (e.g., MenB *Pasteurella multocida*, acc. number NP\_246033, 65% identity over 280 residues). These enzymes are involved in biosynthesis of menaquinone and catalyze the bicyclic ring formation of O-succinyl-benzoyl-CoA to 1,4-dihydroxy-2-naphthoate while releasing CoASH (Sharma *et al.*, 1992). In *Synechocystis* sp. PCC 6803, naphthoate synthase is part of the biosynthetic pathway of phyloquinone (Johnson *et al.*, 2000). The homolog from *Rhodospseudomonas palustris* is involved in anaerobic benzene ring biodegradation (Egland *et al.*, 1997). It is therefore reasonable to predict that the plant homolog of naphthoate synthase is involved in metabolism of an aromatic compound and, in analogy to menaquinone, possibly involved in metabolism of phyloquinone or a derivative thereof. Based on the detection of several *Arabidopsis* enzymes with a putative PTS, such as coumarate-CoA ligases (Shockey *et al.*, 2003), enoyl-CoA hydratases, 3-hydroxybutyrate CoA dehydrogenases and small thioesterases (Reumann *et al.*, submitted), which represent homologs of prokaryotic enzymes of a novel aerobic hybrid degradation pathway of aromatic compounds, an important function of these enzymes in the biosynthesis of the plant hormones jasmonic and salicylic acid as well as auxin has been proposed (Reumann *et al.*, submitted). The gene of naphthoate synthase was cloned in the course of this thesis. Functional analysis of the enzymatic activity of the protein after heterologous expression in *E. coli* or *S. cerevisiae* are underway and will yield more insights into the physiological function of the enzyme in metabolism of leaf peroxisomes.

A second protein spot, which was present on 2-D gels of both spinach and *Arabidopsis* leaf peroxisomes (At4g05530), a short chain dehydrogenases/reductases family protein, was targeted to peroxisomes with high probability and identified as a homolog of mitochondrial NADP-dependent retinol dehydrogenase involved in vitamin A biosynthesis. Interestingly, a second mammalian homolog also carries a PTS. This homolog has not been analyzed experimentally yet but probably catalyzes a similar reaction in peroxisomes. Because plants do not require the synthesis of retinol for eye

pigments, it has been proposed that the plant homolog of mammalian NADP-dependent retinol dehydrogenase is involved in an inverse catabolic reaction of carotenoids and/or the chlorophyll-derivative phytol during senescence (Reumann, pers. com.). The corresponding gene of this short chain alcohol dehydrogenase is currently being cloned in the course of a diploma research project by Ms. Franziska Lueder in the group. *Arabidopsis* T-DNA insertion knock-out mutants are available and expected to yield valuable insights into the function of this enzyme.

Our knowledge on peroxisomal matrix proteins of regulatory function is rather limited due to difficulties in identifying low-abundant and inducible proteins by biochemical approaches. Small HSPs are an ubiquitous superfamily of HSPs characterized by the relatively small mass of the polypeptide chain (16-42 kDa) and the presence of a conserved C-terminal domain, the  $\alpha$ -crystallin domain (Kim *et al.*, 1998; Scharf *et al.*, 2001). Plants house an exceptionally large family of 13 closely and six more distantly related members plus 25 proteins with domains homologous to the  $\alpha$ -crystallin domain (Scharf *et al.*, 2001). Experimental evidence for the presence of small heat-shock proteins in peroxisomes has not been provided yet for any organism but two members of this family carry a putative PTS1 (At5g37670, 137 aa, SKL>; [At1g06460](#), PKL> and [RLx<sub>5</sub>HF](#)). For Hsp15.7 (At5g37670) targeting to peroxisomes has been demonstrated as fusion proteins with yellow fluorescent protein in onion epidermal cells (Ma and Reumann, unpublished). The second sHSP is intriguing because of the presence of a putative PTS1 (PKL>) as well as a putative PTS2 ([RLx<sub>5</sub>HF](#)), which has so far only been reported for plant LACS7 (Fulda *et al.*, 2002), the biogenesis protein Pex8p from *Hansenula polymorpha* (Waterham *et al.*, 1994) and dienoyl-CoA isomerase Dci1p of *Saccharomyces cerevisiae* (Karpichev and Small, 2000). In an *in silico* expression analysis ("Digital Northern", Mekhedov *et al.*, 2000), at least 18 homologous ESTs have been detected, suggesting that the protein may be highly expressed in *Arabidopsis* from which the protein was indeed identified in the current investigation. Evidence for the existence of regulatory proteins, such as heat-shock proteins, kinases and phosphatases, in peroxisomes is just emerging. Regarding heat-shock proteins expressed in response to increased temperature and other forms of abiotic stresses, a chloroplastidic isoform of an Hsp70 homolog from *Citrullus vulgaris* is also targeted to peroxisomes by alternative use of two successive translation start codons

(Wimmer *et al.*, 1997), and a DnaJ homolog from *Cucumis sativus* L. is located in the glyoxysomal membrane and thought to be involved in the import of matrix proteins (Diefenbach and Kindl, 2000). This second heat-shock protein was cloned in the course of this study and investigations to verify predicted subcellular targeting to peroxisomes are underway.

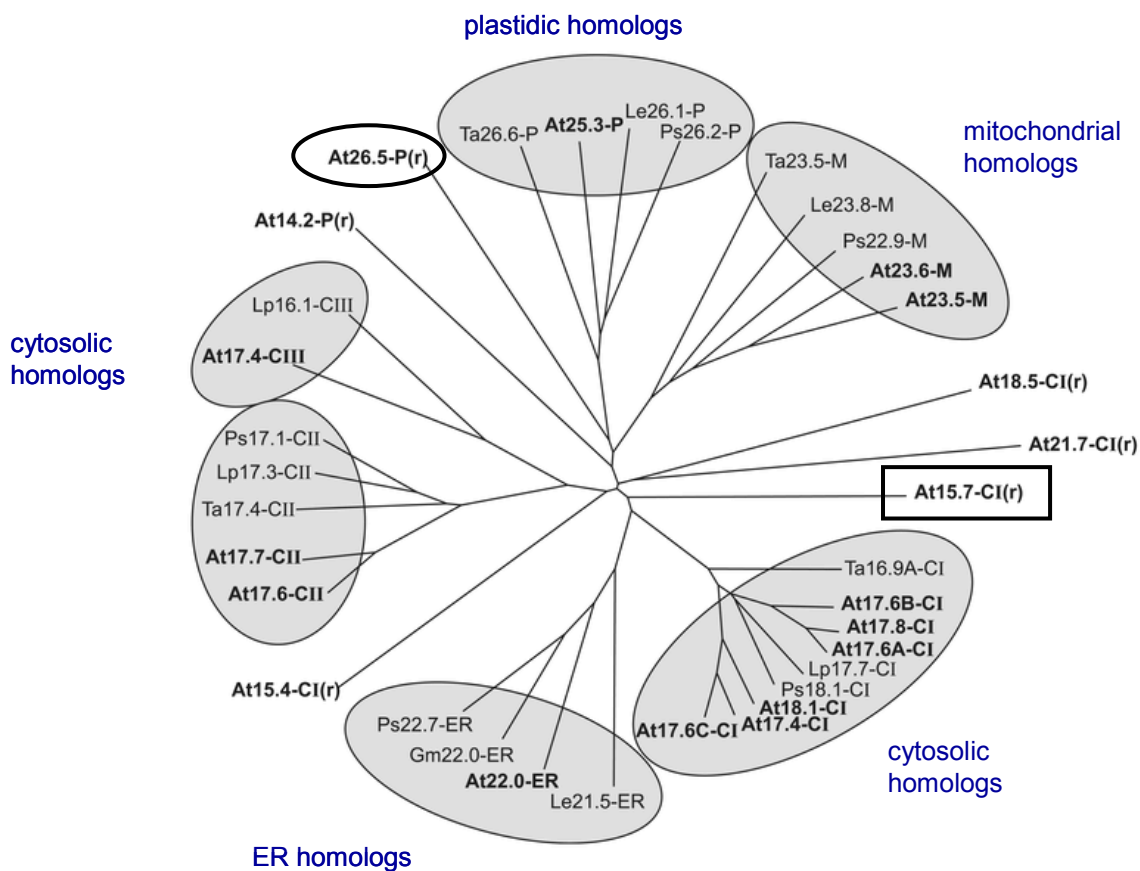


Fig. 4.2: Phylogenetic analysis of small heat-shock proteins from *Arabidopsis*.

*Arabidopsis* possesses a large family of small heat-shock proteins, many of which have been demonstrated or suggested to be targeted to the cytosol, chloroplasts, the ER, and mitochondria. Two homologs carry a putative PTS1, one of which is targeted to peroxisomes in onion epidermal cells (see boxed protein, Ma and Reumann, unpublished). The second homolog with a putative PTS (PKL> and RLX<sub>5</sub>HL) has been detected on 2-D gels from spinach leaf peroxisomes in the course of this study (encircled protein). The phylogenetic tree has been published in Scharf *et al.* (2001).

#### **4.5. On the occurrence of post-translational modifications of proteins in leaf peroxisomes of *Spinacia oleracea* L.**

Many proteins are altered after translation, apart from the typically tight control of the gene expression process because it may be far easier to create a spectrum of slightly different proteins by taking one basic protein scaffold and fine-tuning or even entirely switching its properties, than to build each protein from scratch just to find that it may not be needed at a given time (Davis, 2004). Post-translational modifications (PTMs) create a dynamic combinatorial library of properties that can rapidly respond to systemic stimuli such as oxygen levels. Post-translational modifications range from the widespread (such as glycosylation, phosphorylation, ubiquitination, and methylation) to the obscure (such as glutathionylation, hydroxylation, sulfation, transglutamination, and epimerization).

Our understanding of post-translational regulation of peroxisomal proteins is rather limited, and fragmentary signalling cascades have yet not been unraveled in any case, even though some lines of evidence suggest that some peroxisomal enzymes, such as, catalase (CAT), are modified post-translationally (Kleff *et al.*, 1997). Carbonylation of glyoxysomal proteins from the endosperm of *Ricinus* such as isocitrate lyase, malate synthase, and malate dehydrogenase, as well as catalase, was detected by dinitrophenylhydrazine (DNP) derivatization and detection with DNP antibody in immunoblots. However, there was no correlation of enzymatic activity for each of these proteins with the intensity of carbonylation of the respective protein (Donaldson *et al.*, 2003). The possible modification of isocitrate lyase (ICL) by sulfhydryl oxidation has also been suggested (Donaldson *et al.*, 2003). Malate synthase of castor bean also appeared to be phosphorylated by a peroxisomal protein kinase which appeared to be stimulated by calcium, but again the function of such phosphorylation is unknown (Yang *et al.*, 1998). It was suggested that phosphorylation targeted these proteins for degradation (Lopez Boado *et al.*, 1988). Malate synthase was specifically degraded in peroxisomes of greening pumpkin cotyledons but the mechanism is unknown (Mori and Nishimura, 1989).

An interesting feature for many peroxisomal proteins identified in this study was the indication for their post-translational modification (PTM), inferred based on their presence in multiple spots (Fig. 3.11 and 3.19). For example, hydroxypyruvate reductase is encoded

by a single copy gene in *Arabidopsis* (Mano *et al.*, 1997) and also in other plant species, such as cucumber (Greenler *et al.*, 1989) and pumpkin (Hayashi *et al.*, 1996). It was identified from at least three well resolved spots on the two-dimensional map of spinach leaf peroxisomal proteins (Fig. 3.11 and 3.19), suggestive of a post-translational modification. All three spots had an identical molecular mass, but differed in their isoelectric point. This pattern is indicative of phosphorylation, but none of the spots was enriched by phosphate metal affinity chromatography (PMAC, 3.4.2).

#### 4.5.1. On the analysis of protein phosphorylation in leaf peroxisomes

Several recent reports support the occurrence of protein phosphorylation as an important regulatory mechanism that may be involved in the modulation of several peroxisomal enzymes. For instance, a glyoxysomal protein kinase (GPK1) has recently been identified in a proteome study of the organelle from *Arabidopsis* and was shown to phosphorylate an unidentified protein of molecular mass 40 kDa (Fukao *et al.*, 2003). A modification of thiolase and NADP-dependent isocitrate dehydrogenase by phosphorylation was also suggested in the same report although the GPK1 was not involved in this phosphorylation. Also, a calcium-dependent protein kinase was recently demonstrated to be anchored in the peroxisomal membrane (Damman *et al.*, 2003). An activation of catalase by its interaction with a calmodulin in the presence of  $Ca^{2+}$  was recently shown to occur in peroxisomes (Yang and Poovaiah, 2002). A light-responsive nucleoside diphosphate kinase is reported to interact specifically *in vitro* with all three CAT isoforms and form a native complex with CAT *in vivo* (Fukamatsu *et al.*, 2003).

To identify target proteins of kinases and autophosphorylated kinases and to obtain information on a potential regulation of peroxisomal enzymes by phosphorylation, phosphoproteins from spinach leaf peroxisomes were enriched by phosphoprotein metal affinity chromatography, in the present study. The pattern of proteins in the eluted fraction as resolved by one-dimensional SDS-PAGE (Fig. 3.15) suggested that about 2% of the proteins were phosphorylated. This may be an under-estimation of the *in vivo* situation because phosphate groups are labile, and in these experiments, phosphatase inhibitors were not included because of their interference with subsequent purification.

For further resolution, two-dimensional electrophoresis (2-DE) was employed and the probable identities for some of the proteins were deduced based on their migration coordinates on the gels. That the enriched proteins were phosphorylated was supported by their identification from multiple spots whose pattern correlated with phosphorylation (a shift in isoelectric point to an acidic range but no apparent shift in molecular mass). The proteins tentatively identified, by their 2-DE parameters, include isocitrate lyase, thiolase, ascorbate peroxidase and sulfite oxidase. Several lines of evidence support the possibility that these proteins are regulated by phosphorylation. It is reported that isocitrate lyase is phosphorylated by a peroxisomal protein kinase in castor bean and cucumber, but the function is as yet unknown (Finnessy *et al.*, 1994). An *in vitro* phosphorylation of the glyoxysomal thiolase has been demonstrated in the recent proteomic investigation on the organelle from *A. thaliana* (Fukao *et al.*, 2003). The regulation of ascorbate peroxidase by phosphorylation has been speculated to play a role in the regulation of its activity especially during high H<sub>2</sub>O<sub>2</sub> levels (Fukao *et al.*, 2002). Although direct evidence is lacking, by analogy to the modulation of activity of nitrate reductase, a molybdenum enzyme similar to sulfite oxidase, by phosphorylation (LaBrie and Crawford, 1994) a similar mechanism has been postulated for the phosphorylation of the latter (Nakamura *et al.*, 2002). Interestingly, multiple spots for these proteins were identified even prior to a specific enrichment for phosphoproteins suggesting that the levels of phosphorylated forms of these proteins may be quite high.

Support for our indications for phosphorylation of isocitrate lyase (ICL) is also provided by reports on homologs from lower eukaryotes and prokaryotes. The phosphorylation of ICL has been reported for the enzyme from *Acinetobacter calcoaceticus* (Hoyt and Reeves, 1992). The ICL1 from *S. cerevisiae* was shown to contain two putative cAMP dependent protein kinase phosphorylation sites (Fernandez *et al.*, 1992). Further ICL from *S. cerevisiae* was reported to be phosphorylated in response to glucose treatment, but with reduced activity (Lopez-Boado *et al.*, 1988). Evidence for the phosphorylation of ICL from *E. coli* at a histidine residue has been shown by Robertson *et al.* (1988) who reported a loss of catalytic activity of the enzyme after treatment with potato acid phosphatase, indicating that the phosphorylated form is the catalytically active form of ICL. Studies that demonstrate the phosphorylation and modulation of ICL from *E. coli* have

been reviewed by Robertson and Reeves (1989). A multiple alignment of several ICL homologs with that of *E. coli* reveals conserved histidine residues including the one reported to be phosphorylated (data not shown). Interestingly, the pattern of ICL protein spots on the spinach 2-D gels is such that the acidic form is much less abundant than the basic. Since ICL has no major role in the metabolism of leaf peroxisomes but is probably involved in lipid turnover and recycling (Gerhardt, 1992) and in analogy to the regulation in *E. coli*, it is possible that the enzyme is mostly present in the dephosphorylated inactive form. Phosphorylation of histidine residues in eukaryotic proteins is relatively less common than that of serine, threonine or tyrosine phosphorylation but has been reported (reviewed by Loomis *et al.*, 1997). Additionally, since at least three spots of similar molecular mass, but different isoelectric point were identified as isocitrate lyase, it may be possible that the enzyme is subjected to multiple phosphorylations.

In the future, the identities of the putatively phosphorylated proteins have to be revealed from the corresponding gels. Further, the phosphorylation may be analyzed using specific and sensitive tools. A simple approach may be to use stains that enable the detection of phosphorylated proteins (Schulenberg *et al.*, 2003). Another interesting approach may be to cleave away the phosphate group using enzymes such as alkaline phosphatase and resolve the resulting protein pattern by two-dimensional electrophoresis. Such a technique may indicate phosphorylation for protein spots whose isoelectric point shifts to a basic range due to the treatment. A rather straightforward approach would be to analyze such proteomes by immunodetection using antibodies raised against phosphorylated amino acids. Additionally, phosphopeptide mapping may also be possible using mass spectrometric tools.

#### **4.6. On stress-inducible proteins of leaf peroxisomes from *S. oleracea***

In plant cells, as in most eukaryotic organisms, peroxisomes are probably the major sites of intracellular H<sub>2</sub>O<sub>2</sub> production, as a result of their essentially oxidative type of metabolism. Like mitochondria and chloroplasts, peroxisomes also produce superoxide radicals (O<sub>2</sub><sup>\*-</sup>). There are, at least, two sites of superoxide generation: one in the organelle matrix, the generating system being xanthine oxidase, and another site in the peroxisomal

membranes which is dependent on NAD(P)H (see also Fig. 1.3, del Rio *et al.*, 1992) and represented by three integral membrane polypeptides with molecular masses of 18 kDa (probably a cytochrome b), 29 kDa (probably a NADPH:cytochrome P-450 reductase), and 32 kDa (probably a monodehydroascorbate reductase, Lopez-Huertas *et al.*, 1996, 1997).

Peroxisomes possess several antioxidant proteins that keep a probable 'burst' of reactive oxygen species (ROS) at bay and protect cells from its toxic effects. Catalase is present ubiquitously in all types of peroxisomes and is one of the most abundant enzymes in leaf peroxisomes (Tolbert, 1980). The enzyme is the vanguard of defence against H<sub>2</sub>O<sub>2</sub>, and effectively dismutates this toxic molecule to water and molecular oxygen. Plants that were antisense with respect to catalase were more sensitive to paraquat, high-light and hydrogen peroxide (Willekens *et al.*, 1997). Expression of catalase genes is stimulated under different conditions of stress and seems to be subjected to extensive post-translational regulation. Regulatory aspects of this enzyme continue to be revealed.

Besides catalase, three superoxide dismutases (SOD) have been found in plant peroxisomes. SODs belong to a family of metalloenzymes that catalyse the disproportionation of reactive oxygen radicals into hydrogen peroxide and molecular oxygen. A CuZn-superoxide dismutase and two Mn-SODs (Bueno *et al.*, 1995; Pastori *et al.*, 1996; Palma *et al.*, 1997) have been reported from peroxisomes. Another enzyme that has an oxygen scavenging role in peroxisomes is ascorbate peroxidase (APX). The active site of the enzyme most likely faces the cytosol (Ishikawa *et al.*, 1998; Jimenez *et al.*, 1997; Yamaguchi *et al.*, 1995) even though one report concluded the opposite topology (Bunkelmann and Trelease, 1996). Thus, it is thought that APX scavenges intraperoxisomal H<sub>2</sub>O<sub>2</sub> as well as the excess H<sub>2</sub>O<sub>2</sub> that leaks out of the peroxisomes.

Since these scavenging mechanisms are themselves susceptible to attack by ROS, it seems likely that alternative or additional resistance and repair systems exist in the peroxisome where reactive oxygen species are permanently produced and their detoxification at the site of production is crucial for survival of the cell.

Indeed, an operational ascorbate-glutathione cycle (Foyer-Halliwell-Asada cycle) exists in the peroxisomal membranes (del Rio *et al.*, 1998) which serves to dispose hydrogen peroxide, especially, when catalase is inactive (Halliwell and Gutteridge, 2000). All four enzymes of the cycle, namely, ascorbate peroxidase, monodehydroascorbate



reductase, dehydroascorbate reductase, and glutathione reductase (Corpas *et al.*, 1998) have been detected in leaf peroxisomes by biochemical means. In addition, antioxidant molecules such as, ascorbate and glutathione (Jimenez *et al.*, 1997) have been found in peroxisomes.

Under stress conditions, an imbalance in the accumulation and removal of reactive oxygen species such as hydrogen peroxide ( $H_2O_2$ ), occurs. A co-ordinated global cellular shift in gene expression is most likely involved in the metabolic and molecular adjustment to such unfavourable conditions. Alteration in activity of peroxisomal enzymes has been reported stress situations induced by chilling, wounding, leaf senescence (Pastori and del Rio., 1997), xenobiotics (del Rio *et al.*, 1992, 1996), heavy metals (Palma *et al.*, 1991; Puertas *et al.*, 1999) and salinity (Mittova *et al.* 2003). Peroxisomal proteins respond differently in different kinds of stresses. For example, the activity of glycolate oxidase increased during salt stress where as those of hydroxypyruvate reductase and urate oxidase decreased simultaneously (Corpas *et al.*, 1993). Induction of new isoforms has also been reported during stress conditions such as that for Cu-Zn superoxide dismutase during senescence (Pastori and del Rio, 1997). The photorespiratory enzymes such as hydroxypyruvate reductase and peroxisomal aminotransferases have also reported to play defence-mediating roles during pathogen attack (Okinaka *et al.*, 2002; Taler *et al.*, 2004)

To summarize, two mutually opposed roles are indicated for peroxisomes, namely, the production of harmful reactive oxygen species and the coordinated defences against these stresses involving the scavenging of ROS. Further research is required in order to understand the role of peroxisomes in cellular metabolism. Such information may be useful to design effective strategies to improve the stress-tolerance in plants.

Thus, to investigate which proteins are induced in its leaf peroxisomes when *S. oleracea* is exposed to conditions of high light or oxidative stress, two-dimensional electrophoresis was employed to track protein expression changes. The catalase inhibitor 3-amino 1,2,4-triazole (3-AT) was used to induce oxidative stress since it is known that it inhibits peroxisomal catalase activity and leads to accumulation of  $H_2O_2$  in these organelles. A high light stress ( $700 \mu\text{molm}^{-2}\text{s}^{-1}$ ) was also applied independent of the oxidative stress treatment. It was found that a small subset of proteins was induced upon stress treatment (Fig. 3.16 and 3.17). The majority of these proteins were induced both

after a high light and an oxidative stress. Among the most strongly induced proteins, the identities of ascorbate peroxidase (APX), glutamate glyoxylate aminotransferase and hydroxypyruvate reductase were deduced based on analogy to their migration coordinates on a different gel.

Indications for a modification of APX by phosphorylation were evident from its identification in a trail of at least three spots on normal gels as well as those from stressed leaves. This pattern, by contrast to other 'phosphorylated' trails had a higher abundance of the acidic forms than the basic forms implicating perhaps a specific involvement of the phosphorylated form in stress response. Interestingly, the amount of proteins in this trail is reversed in normal and stressed conditions that may probably suggest a modulation of enzyme activity by a post-translational mechanism that may be related to stress. The *Arabidopsis* gene APX3 was able to provide protection specifically against oxidative stress originated from peroxisomes when heterologously expressed in tobacco (Wang *et al.*, 1999). Both high light intensities and 3-AT increased the level of APX protein. This may not be a contradictory result to that reported for the transcript levels of the spinach APX gene that remained unchanged under different stress conditions including that imposed by high light intensity, drought, salinity, and applications of paraquat and abscisic acid (Yoshimura *et al.*, 2000). A post-translational modification may be implicated in such situations to explain this apparent lack of correlation between transcript abundance.

Much information may be derived from comparative proteome analyses once the identities of the differentially induced proteins are known.

## 5. Summary

The results of the proteome analysis of leaf peroxisomes are summarized as follows

1. A reported method for the isolation of leaf peroxisomes from *Spinacia oleracea* L. was improved by inclusion of a second density gradient and applied to proteome analyses. The contamination of leaf peroxisomes by other cell compartments was reduced for chloroplasts and mitochondria to an undetectable minimum as determined by the measurement of compartment-specific marker enzyme activities and chlorophyll.
2. In addition, an ingenious method was designed to enable comparative proteome analyses of highly pure spinach leaf peroxisomes from stress-treated plants in a minimal time of two hours, allowing the isolation of leaf peroxisomes from two different plant sets in parallel and their direct comparison. This analytical method takes advantage of peroxisome isolation from a 'post-plastidic' supernatant without previous sedimentation in a Raffinose-based Percoll density gradient and yielded leaf peroxisomes with contamination by mitochondria and chloroplasts both at the sensitivity limit.
3. To take advantage of the information of the first genome sequence of a higher plant, namely that of *Arabidopsis thaliana* L., for proteome analyses of leaf peroxisomes, a novel efficient procedure for the enrichment of leaf peroxisomes from *Arabidopsis* was developed as well.
4. The method of two-dimensional electrophoresis was established in the department and optimized for soluble matrix proteins of leaf peroxisomes with respect to the choice and concentration of chaotropes, detergents as well as alcohols to yield maximum resolution, protein recovery and proteome coverage.

5. From spinach, a total of 120 spots that were resolved by two-dimensional electrophoresis was analyzed by mass spectrometry, and from *Arabidopsis*, a smaller number of spots was analyzed and resulted in the identification of proteins that are involved in different aspects of peroxisomal metabolism.
6. Known proteins of plant peroxisomes that were related to distinct protein spots as identified by mass spectrometry included enzymes involved in the photorespiratory cycle (glycolate oxidase, catalase, serine-glyoxylate and glutamate-glyoxylate aminotransferases, hydroxypyruvate reductase, malate dehydrogenase, aspartate aminotransferase), fatty acid  $\beta$ -oxidation and the glyoxylate cycle (long chain acyl CoA synthetase, acyl CoA oxidase, ketoacyl thiolase, malate synthase, isocitrate lyase, citrate synthase) as well as uricase, ascorbate peroxidase, 12-oxophytodienoate reductase isoform 3, sulfite oxidase, and 3-hydroxyisobutyryl CoA hydrolase.
7. The proteome of leaf peroxisomes from *Arabidopsis* allowed first insights into the expression of specific isoforms. Of three catalase isoforms, only catalase 3 was identified, and of five novel genes encoding for glycolate oxidase, three isoforms were detected in leaf peroxisomes. Of two isoforms of glutamate-glyoxylate aminotransferase, only isoform 1 was detected in leaf peroxisomes and accordingly plays a major role in glycolate recycling during photosynthesis.
8. Four novel proteins were identified in leaf peroxisomes, namely a short chain alcohol dehydrogenase (At4g05530) and a naphthoate synthase-like protein of the family of enoyl-CoA hydratases (At1g60550), a second enoyl-CoA hydratase (At4g16210) and a small heat shock protein ([At1g06460](#)). All four novel proteins possess peroxisome targeting signals of type 1 or type 2, most of which were found to be conserved in homologous expressed sequence tags (ESTs) from various plant species, providing strong support for localization of these unknown proteins in peroxisomes. Experimental evidence for peroxisome localization was provided by differential profiling-based subtractive analysis of 2-D gels from spinach. As

deduced from homology analysis of known prokaryotic and eukaryotic proteins, the short chain alcohol dehydrogenase (At4g05530) and the naphthoate synthase-like protein of the family of enoyl-CoA hydratases (At1g60550) are predicted to metabolize aromatic or cyclic fatty acids and to have an important yet unknown function in leaf peroxisomal metabolism.

9. The *Arabidopsis* genes encoding for the naphthoate synthase-like protein (At1g60550) and the small heat shock protein ([At1g06460](#)) were cloned by reverse transcription polymerase chain reaction (RT-PCR) from cold-treated leaves and allow straightforward verification of subcellular targeting of fusion proteins with spectral variants of green fluorescent protein by fluorescence microscopy and functional analysis of heterologously expressed recombinant protein.
10. To identify stress-inducible proteins from plant peroxisomes, methods for the isolation of leaf peroxisomes from plants subjected to high-light and oxidative stress were established and inducible proteins identified by comparative 2-D analysis that remain to be identified by mass spectrometry. These methods are expected to allow valuable insights into the yet largely unknown function of plant peroxisomes in oxidative stress tolerance and signal transduction via hydrogen peroxide in the near future.
11. In addition, the proteome analysis of leaf peroxisomes indicated that peroxisomal enzymes are subjected to intensive post-translational modifications. Several enzymes, including catalase, ascorbate peroxidase, hydroxypyruvate reductase and isocitrate lyase, were detected in several spots that were arranged in a horizontal line of similar spot distance to each other, indicating that the polypeptides do not differ significantly in molecular mass but in their isoelectric point. Such a pattern of one polypeptide is indicative of post-translational modification in form of reversible phosphorylation.

12. By 2-D analysis of matrix proteins from spinach leaf peroxisomes further support was provided that several proteins, including known proteins such as ascorbate peroxidase as well as several unknown proteins, which remain to be identified by mass spectrometry, are regulated post-translationally by reversible phosphorylation.

## 6. List of figures and Tables

### 6.1. List of figures

- Fig. 1.1: Reactions and transport of intermediates of the photorespiratory C<sub>2</sub> cycle
- Fig. 1.2: Reactions of fatty acid β-oxidation and glyoxylate cycle
- Fig. 1.3: Model proposed to explain the production of O<sub>2</sub><sup>-</sup> radicals by peroxisomes from pea leaves
- Fig. 1.4: Targeting of proteins to peroxisomes
- Fig. 3.1: Separation of leaf peroxisomes and proplastid-like organelles from *Spinacia oleracea* L. by a second density gradient
- Fig. 3.2: Analytical method to purify leaf peroxisomes from *Spinacia oleracea* L. by a single Percoll density gradient using raffinose
- Fig. 3.3: Distribution of marker enzyme activities in a linear sucrose density gradient used to enrich leaf peroxisomes from *Arabidopsis thaliana* (L.) Heynh.
- Fig. 3.4: Effect of thiourea on protein recovery demonstrated by one-dimensional sodium dodecylsulfate polyacrylamide gel electrophoresis
- Fig. 3.5: Effect of thiourea on protein recovery and resolution in two-dimensional electrophoresis
- Fig. 3.6: Effect of different detergents on protein recovery and resolution in two-dimensional electrophoresis
- Fig. 3.7: Effect of alcohols on resolution of alkaline proteins in two-dimensional electrophoresis
- Fig. 3.8: Two-dimensional map of leaf peroxisomal proteins from *Spinacia oleracea* L. using a broad range immobilized pH gradient (IPG) strip
- Fig. 3.9: Two-dimensional electrophoresis of leaf peroxisomal proteins from *Spinacia oleracea* L. using narrow pH range immobilized pH gradient (IPG) strips in the first dimension
- Fig. 3.10: Sub-fractionation of leaf peroxisomes from *Spinacia oleracea* L. by Triton X-100 treatment for the selective enrichment of low-abundant proteins
- Fig. 3.11: Leaf peroxisomal proteins from *Spinacia oleracea* L. identified by two-dimensional electrophoresis and mass spectrometry
- Fig. 3.12: Leaf peroxisomal proteins from *Arabidopsis thaliana* identified by two-dimensional electrophoresis and matrix-assisted laser desorption ionization mass spectrometry
- Fig. 3.13: Alignment of homologous N-terminal ESTs from various plant species with an unknown *Arabidopsis* protein, annotated as putative naphthoate synthase, identified in spinach leaf peroxisomes.

- Fig. 3.14: Alignment of homologous C-terminal ESTs from various plant species with an unknown *Arabidopsis* protein, annotated as a short chain alcohol dehydrogenase, identified in spinach leaf peroxisomes.
- Fig. 3.15: Oxidative stress treatment of *Spinacia oleracea* L.
- Fig. 3.17: Induction of proteins in leaf peroxisomes from *Spinacia oleracea* L. by oxidative stress treatment
- Fig. 3.18: Subtractive two-dimensional electrophoresis to deduce peroxisomal proteins by differential profiling
- Fig. 3.19: Indications for post-translational modifications of known leaf peroxisomal matrix proteins from *Spinacia oleracea* L.
- Fig. 3.20: Enrichment of phosphoproteins from leaf peroxisomes of *Spinacia oleracea* L.
- Fig. 3.21: Phosphoproteins from *Spinacia oleracea* L. leaf peroxisomes resolved by two-dimensional electrophoresis
- Fig. 4.1: Phylogenetic analysis of putative *Arabidopsis* enoyl-CoA hydratases from leaf peroxisomes
- Fig. 4.2: Phylogenetic analysis of small heat-shock proteins from *Arabidopsis*.

## 6.2. List of tables

- Table 3.1: Comparison of methods for the purification of leaf peroxisomes isolated from *Spinacia oleracea* L. and *Arabidopsis thaliana* (L.) Heynh.
- Table 3.2: Summary of solubilization of proteins from leaf peroxisomes of *S. oleracea* in the presence or absence of thiourea as revealed by one-dimensional sodium dodecylsulfate polyacrylamide gel electrophoresis
- Table 3.3: Summary of protein solubilization in the presence of different chaotropes and detergents



## 7. List of abbreviations

1-D	one-dimensional
2-DE	two-dimensional gel electrophoresis
3-AT	3-amino-1,2,4-triazole
3-PGA	3-phosphoglyceric acid
AGT	alanine-glyoxylate aminotransferase
Amp	ampicillin
Amp <sup>R</sup>	ampicillin resistance
AOX	acyl coA oxidase
APS	ammonium peroxy disulfate
APX	ascorbate peroxidase
ASB-14	amidosulfobetaine-14
ATP	adenosine 5' triphosphate
bp	base pair
BSA	bovine serum albumin
CAT	catalase
cDNA	complementary DNA
CHAPS	[(3-cholamidopropyl)-dimethylammonio]-propanesulfonate
Chl	chlorophyll
CHY1	3-hydroxy isobutyryl coA hydrolase
ddH <sub>2</sub> O	double distilled water
DMSO	dimethyl sulfoxide
DNA	deoxyribonucleic acid
dNTPs	deoxyribonucleotides
DTT	dithiothreitol
EDTA	ethylenediamine tetraacetic acid
ESI	electrospray ionization mass spectrometry
EtOH	ethanol
FW	fresh weight
GAPDH	glyceraldehyde 3-phosphate dehydrogenase
GFP	green fluorescent protein
GGT	glutamate-glyoxylate aminotransferase
GOX	glycolate oxidase
HEPES	hydroxyethyl-piperazinethane sulfonic acid
HPR	hydroxypyruvate reductase
ICL	isocitrate lyase
IEF	isoelectric focusing
IPG	immobiline pH gradient
IPTG	isopropyl-β-D-thiogalactopyranoside
kb	kilobase pair
kDa	kilodalton
K <sub>m</sub>	kanamycin
K <sub>m</sub> <sup>R</sup>	kanamycin resistance
LACS	long-chain acyl CoA-synthetase
LB-medium	Luria-Bertani medium
LC	liquid chromatography
MALDI	matrix-assisted laser desorption ionization
MCS	multiple cloning site
MDH	malate dehydrogenase
MFP	multifunctional protein
MOPS	morpholinopropane sulfonic acid
MS medium	Murashige-Skoog medium
MS	mass spectrometry
MS/MS	tandem mass spectrometry
NAD	nicotinamide adenine dinucleotide (oxidized)
NADH	nicotinamide adenine dinucleotide (reduced)
NADP	nicotinamide adenine dinucleotide phosphate (oxidized)

NADPH	nicotinamide adenine dinucleotide phosphate (reduced)
NOG	N-octylglucoside
NP-40	Nonidet P-40
OD	optical density
OPR3	12-oxophytodienoate reductase
ORF	open reading frame
PAGE	polyacrylamide gel electrophoresis
PBS	phosphate buffered saline
PCR	polymerase chain reaction
Pi	inorganic phosphate
pI	isoelectric point
PMAC	phosphate metal affinity chromatography
PMSF	phenyl methyl sulfonyl fluoride
PTM	post-translational modification
PTS	peroxisomal targeting signal
PVP	polyvinylpyrrolidone
RNA	ribonucleic acid
ROS	reactive oxygen species
rpm	revolutions per minute
RT	reverse transcription
RubisCO	ribulose biphosphate carboxylase/oxygenase
SD	standard deviation
SDS	sodium dodecylsulfate
SGAT	serine-glyoxylate aminotransferase
SOX	sulfite oxidase
T <sub>ann</sub>	annealing temperature
<i>Taq</i>	<i>Thermus aquaticus</i>
TEMED	N,N,N',N'-tetramethylene diamine
T <sub>m</sub>	melting temperature
TOF	time-of-flight
Tricine	N-Tris-(hydroxymethyl)-methyl glycine
Tris	tris-(hydroxymethyl)-aminomethane
TX-100	Triton X-100
U	unit; $\mu\text{mol}$ substrate per minute
UV	ultraviolet
v/v	volume to volume
w/v	weight to weight
w/w	weight to weight
X-Gal	5-bromo-4-chloro-3-indolyl- $\beta$ -D-galactopyranoside

## 8. Appendices

### Appendix 1: List of proteins from *Spinacia oleracea* L. analyzed by mass spectrometry

(Analysis was performed by Dr. Virginie Wurtz at the laboratory of Dr. Alain Van Dorsselaer, Strasbourg, France)

Spot No.	Protein ID	Organism	Accession	Mol mass /pI	Sequence coverage
1	RubisCO activase	<i>Spinacia oleracea</i>	P10871	51.5/6.62	55%
2	Fructose-bisphosphate aldolase	<i>Spinacia oleracea</i>	P16096	42.4/6.85	26%
3	Glycerate dehydrogenase	<i>Cucumis savitum</i>	P13443	41.7/5.95	18%
4	RubisCO activase	<i>Spinacia oleracea</i>	P10871	51.5/6.62	65%
5	Transketolase	<i>Solanum tuberosum</i>	Q43848	79.9/5.94	8%
6	Acyl-CoA oxidase	<i>Glycine max</i>	gij15553478	74.2/7.27	4%
7	ATP-dependent clp protease ATP-binding subunit clp	<i>Lycopersicon esculentum</i>	P31542	102/5.86	34%
8	Phosphoglycerate kinase	<i>Spinacia oleracea</i>	P29409	45.5/5.83	17%
9	Carbonic anhydrase	<i>Spinacia oleracea</i>	P16016	34.5/7.0	32%
10	Glyceraldehyde 3 P dehydrogenase A	<i>Spinacia oleracea</i>	P19866	43/7.62	50%
11	Glyceraldehyde 3 P dehydrogenase A	<i>Spinacia oleracea</i>	P19866	43/7.62	37%
12	putative alanine aminotransferase	<i>Oryza savita</i>	gij23617059	53.3/8.01	15%
13	Elongation factor Tu - Chloroplast precursor	<i>Glycine max</i>	Q43467	52/6.21	21%
14	RubisCO activase	<i>Spinacia oleracea</i>	P10871	45.4/5.4	55%
15	Phosphoribulokinase	<i>Spinacia oleracea</i>	P09559	44.9/5.82	38%
16	Alanine glyoxylate aminotransferase	<i>Arabidopsis thaliana</i>	gij15225026	44.2/7.69	4%
17	Malate dehydrogenase	<i>Citrillus lanatus</i>	P19446	35.5/7.06	25%
18	RubisCO	<i>Spinacia oleracea</i>	P00875	52.7/6.13	46%
19	Glycerate dehydrogenase	<i>Cucumis savitus</i>	P13443	41.7/5.95	21%
20	Putative alanine aminotransferase	<i>Arabidopsis thaliana</i>	gij23297208	53.3/6	25%
21	Cytosolic ascorbate peroxidase	<i>Mesembryanthemum crystallinum</i>	Q9XFC0	31.5/8.25	7%
22	Cytosolic ascorbate peroxidase	<i>Mesembryanthemum crystallinum</i>	Q9XFC0	31.5/8.25	7%
23	Malate dehydrogenase	<i>Citrillus lanatus</i>	P19446	35.5/7.06	23%
24	Hydroxypyruvate reductase	<i>Cucurbita</i>	Q42708	42.3/5.87	25%
25	Hydroxypyruvate reductase	<i>Cucurbita</i>	Q42708	42.3/5.87	20%
26	?				AGGDV, IKGLAFQLLR
27	Malate dehydrogenase	<i>Medicago sativa</i>	O48903		
28	-				
29	-				
30	Putative alanine aminotransferase	<i>Arabidopsis thaliana</i>	Q9C5K2	53.3/6.91	18%
31	(S)-2-hydroxy-acid oxidase, peroxisomal	<i>Spinacia oleracea</i>	P05414	40.2/9.16	62%
32	(S)-2-hydroxy-acid oxidase, peroxisomal	<i>Spinacia oleracea</i>	P05414	40.2/9.16	39%
33	(S)-2-hydroxy-acid oxidase, peroxisomal	<i>Spinacia oleracea</i>	P05414	40.2/9.16	59%
34	Long chain acyl-CoA synthetase	<i>Arabidopsis thaliana</i>	Q8LKS6	76.6/8.11	3%
35	Long chain acyl-CoA synthetase	<i>Arabidopsis thaliana</i>	Q8LKS6	76.6/8.11	2%
36	?				KTLVVDASR, LTEEEASQLR
37	-				
38	-				
39	Putative serine-glyoxylate aminotransferase	<i>Fritillaria agrestis</i>	O49124	44/7.63	TNNLTAVR

40	Putative serine-glyoxylate aminotransferase	<i>Fritillaria agrestis</i>	O49124	44/7.63	LFVPGPVNIPEPVI R
41	?				KEEVLN, ATEL, VYLRFLLVV
42	Uricase (or) Malate dehydrogenase	<i>Arabidopsis thaliana</i> <i>Arabidopsis thaliana</i>	O04420 Q9ZP05	34.9/8.6 37.3/8.1	3% 3%
43	Malate dehydrogenase (or) Uricase	<i>Medicago sativa</i> <i>Arabidopsis thaliana</i>	O48903 O04420	38.1/8.5 34.9/8.6	16% 3%
44	Citrate synthase-like protein	<i>Arabidopsis thaliana</i>	Q9LXS6	56.5/8.73	11%
45	-				
46	Alanine:glyoxylate aminotransferase (or)  Putative hydroxypyruvate reductase	<i>Arabidopsis thaliana</i> <i>Arabidopsis thaliana</i>	O81248 Q9C9W5	44.1/7.69 42.2/6.68	6% 6%
47	Catalase	<i>Suaeda maritima</i>	Q941J0	33.3/6.4	27%
48	Catalase	<i>Helianthus annuus</i>	Q9M502	56.9/6.62	14%
49	Putative NADH-dependent hydroxypyruvate reductase	<i>Glycine max</i>	AA073866	42.2/6.97	33%
50	Isocitrate lyase	<i>Lycopersicon esculentum</i>	P49297	64.7/6.56	9%
51	Catalase isozyme 1	<i>Nicotiana glumbaginifolia</i>	P49315	55.82/6.75	15%
52	Catalase 2	<i>Arabidopsis thaliana</i>	P25819	56.9/6.63	26%
53	Catalase 2	<i>Arabidopsis thaliana</i>	P25819	56.9/6.63	23%
54	Catalase 2	<i>Arabidopsis thaliana</i>	P25819	56.9/6.63	23%
55	3-ketoacyl-CoA thiolase	<i>Arabidopsis thaliana</i>	Q9S7M3	48.5/8.62	17%
56	3-ketoacyl-CoA thiolase	<i>Arabidopsis thaliana</i>	Q9S7M3	48.5/8.62	17%
57	3-ketoacyl-CoA thiolase	<i>Arabidopsis thaliana</i>	Q9S7M3	48.5/8.62	17%
58	12-oxophytodienoate reductase 3	<i>Lycopersicon esculentum</i>	Q9FEW9	43.5/8.51	4%
59	Moco containing protein (or) Putative serine-glyoxylate aminotransferase	<i>Oryza sativa</i> <i>Fritillaria agrestis</i>	Q8LP96 O49124	43.8/8.13 44.1/7.63	7% 6%
60	Moco containing protein	<i>Oryza sativa</i>	Q8LP96	43.8/8.13	11%
61	Putative serine-glyoxylate aminotransferase  3-ketoacyl-CoA thiolase precursor	<i>Fritillaria agrestis</i> <i>Cucurbita</i>	O49124 P93112	44.1/7.63 48.6/8.21	6% 4%
62	Putative alanine aminotransferase	<i>Arabidopsis thaliana</i>	Q9C5K2	53.3/6.91	27%
63	Putative enoyl-CoA hydratase/isomerase (or)  Putative naphthoate synthase	<i>Arabidopsis thaliana</i> <i>Oryza sativa</i>	Q8GYN9 Q8LR33	37.1/6.77 35.9/8.88	7% 7%
64	Ascorbate peroxidase	<i>Arabidopsis thaliana</i>	Q42564	31.6/6.47	12%
65	Catalase	<i>Suaeda maritima</i>	Q94EV9	56.7/6.76	15%
66	Catalase 4	<i>Helianthus annuus</i>	Q9M502	56.9/6.62	13%
67	Catalase	<i>Suaeda maritima</i>	Q94EV9	56.7/6.76	22%
68	3-ketoacyl-CoA thiolase	<i>Arabidopsis thaliana</i>	Q9S7M3	48.5/8.62	11%
69	Isocitrate lyase	<i>Ipomoea batatas</i>	Q9FQD2	64.4/7.25	9%
70	(S)-2-hydroxy-acid oxidase, peroxisomal (or) Aspartate aminotransferase	<i>Spinacia oleracea</i> <i>Arabidopsis thaliana</i>	P05414 P46645	40.3/9.16 44.2/6.8	18% 13%
71	(S)-2-hydroxy-acid oxidase, peroxisomal	<i>Spinacia oleracea</i>	P05414	40.3/9.16	5%
72	-				
73	-				
74	Long chain acyl-CoA synthetase 6	<i>Arabidopsis thaliana</i>	Q8LKS6	76.6/8.11	3%
75	Acyl-CoA oxidase (ACX1)	<i>Glycine max</i>	Q945U4	74.2/7.27	6%
76	BSA				
77	BSA				
78	Isocitrate lyase	<i>Arabidopsis thaliana</i>	P28297	64.2/6.72	9%
79	Isocitrate lyase	<i>Arabidopsis thaliana</i>	P28297	64.2/6.72	9%
80	-				

81	(S)-2-hydroxy-acid oxidase, peroxisomal	<i>Spinacia oleracea</i>	P05414	40.3/9.16	18%
82	Keratin, type II cytoskeletal 1				
83	Malate synthase, glyoxysomal	<i>Cucumis sativus</i>	P08216	64.9/8.45	11%
84	Isocitrate lyase	<i>Arabidopsis thaliana</i>	P28297	64.2/6.72	9%
85	-				
86	Glycerate dehydrogenase	<i>Cucumis sativus</i>	P13443	41.7/5.95	29%
87	Putative alanine aminotransferase	<i>Arabidopsis thaliana</i>	Q9C5K2	53.3/6.91	11%
88	Catalase (Fragment)	<i>Suaeda maritima</i>	Q941J0	33.3/6.4	32%
89	-				
90	Malate dehydrogenase, glyoxysomal precursor	<i>Citrullus lanatus</i>	P19446	37613/8.67	23%
91	Malate dehydrogenase, glyoxysomal precursor (or) Putative serine-glyoxylate aminotransferase	<i>Citrullus lanatus</i> <i>Fritillaria agrestis</i>	P19446 O49124	37.6/8.67 44.1/7.63	23% 6%
92	Glyceraldehyde 3-phosphate dehydrogenase A	<i>Spinacia oleracea</i>	P19866	43/7.62	8%
93	-				
94	-				
95	Moco containing protein	<i>Oryza sativa</i>	Q8LP96	43.8/8.13	9%
96	RubisCO (or) Ascorbate peroxidase	<i>Atriplex rosea</i> <i>Capsicum annum</i>	P20455 Q8W4V7	52.6/6.22 31.7/7.74	15% 8%
97	Malate dehydrogenase, (or) Cytosolic ascorbate peroxidase	<i>Citrullus lanatus</i> <i>Mesembryanthemum crystallinum</i>	P19446 Q9XFC0	37.6/8.67 31.5/8.25	23% 10%
98	Ascorbate peroxidase	<i>Arabidopsis thaliana</i>	Q42564	31.6/6.47	17%
99	Ascorbate peroxidase (or) Citrate synthase (or) Malate dehydrogenase	<i>Arabidopsis thaliana</i> <i>Cucurbita maxima</i> <i>Arabidopsis thaliana</i>	Q42564 P49299 Q9ZP05	31.6/6.47 56.7/8.84 37.3/8.14	12% 4% 3%
100	Malate dehydrogenase, glyoxysomal precursor (or) Uricase	<i>Citrullus lanatus</i> <i>Arabidopsis thaliana</i>	P19446 O04420	37.6/8.67 34.9/8.6	7% 3%
101	(S)-2-hydroxy-acid oxidase, peroxisomal	<i>Spinacia oleracea</i>	P05414	40.3/9.16	7%
102	-				
103	Putative enoyl CoA hydratase	<i>Cicer arietinum</i>	Q9SMK7	29.0/9.02	7%
104	Short-chain alcohol dehydrogenase	<i>Arabidopsis thaliana</i>	Q9S9W2	26.7/8.46	12%
105	-				
106	-				
107	(S)-2-hydroxy-acid oxidase, peroxisomal	<i>Spinacia oleracea</i>	P05414	40.3/9.16	20%
108	-				
109	(S)-2-hydroxy-acid oxidase, peroxisomal	<i>Spinacia oleracea</i>	P05414	40.3/9.16	25%
110	(S)-2-hydroxy-acid oxidase, peroxisomal	<i>Spinacia oleracea</i>	P05414	40.3/9.16	25%
111	(S)-2-hydroxy-acid oxidase, peroxisomal	<i>Spinacia oleracea</i>	P05414	40.3/9.16	21%
112	RubisCO	<i>Amaranthus tricolor</i>	P48682	52.6/6.14	9%
113	-				
114	BSA				
115	-				
116	-				
117	Putative NADH-dependent hydroxypyruvate reductase (or) Aspartate aminotransferase	<i>Glycine max</i> <i>Arabidopsis thaliana</i>	AAO73866 (Q84L66) P46644	42.2/6.97 48.9/9.34	36% 8%
118	(S)-2-hydroxy-acid oxidase, peroxisomal	<i>Spinacia oleracea</i>	P05414	40.3/9.16	37%

	(or) Glycerate dehydrogenase	<i>Cucumis sativus</i>	P13443	41.7/5.95	15%
119	(S)-2-hydroxy-acid oxidase, peroxisomal (or) Putative serine-glyoxylate aminotransferase	<i>Spinacia oleracea</i>  <i>Fritillaria agrestis</i>	P05414  O49124	40.3/9.16  44.1/7.63	25%  6%
120	Isocitrate lyase	<i>Lycopersicon esculentum</i>	P49297	64.7/6.56	8%

### Appendix 2: List of proteins from *Arabidopsis thaliana* (L). Heynh. analyzed by mass spectrometry

(Analysis was performed at the laboratory of Dr. H. Kratzin, Max-Planck-Institut für Experimentelle Medizin, Goettingen, Germany)

Spot No.	Mass spectrometric identification	Accession
At1.1	catalase 3	AAL08303
At1.5	catalase 2	T05779
At1.8, 9, 10, 11	catalase 3	At1g20620
At1.2, 29	glycolate oxidase 1 glycolate oxidase 3	BAB01334 At4g18360
At1.12	glycolate oxidase 2 glycolate oxidase 3	At3g14420 At4g18360
At1.29,35	glycolate oxidase	At3g14415
At1.16	malate dehydrogenase 1	At5g09660
At1.17	malate dehydrogenase 2/ ferripyochelin binding protein -like-protein	At5g66510 At5g66510
At1.3	alanine transaminase	B86367
At1.24	prohibitin prohibitin	AAM64845 At5g40770
At1.18	voltage dependent anion selective channel protein- hsr2	
At1.19	putative porin	At5g67500
At1.14	hydroxypyruvate reductase	At1g68010
AtS2	catalase 3	At1g20620
AtS3	3-ketoacyl thiolase	At2g33150
AtS6	short chain dehydrogenase	At4g05530
AtS7	small heat shock protein	At1g06460
At S10	glycolate oxidase	At3g14415

## 9. REFERENCES

- Andr n PE, Emmett MR, Caprioli RM** (1994) Micro-electrospray: zeptomole/attomole per microlitre sensitivity for peptides. *J Am Soc Mass Spectrom* 5, 867–869
- Arabidopsis Genome Initiative** (2000) Analysis of the genome sequence of the flowering plant *Arabidopsis thaliana*. *Nature* 408, 796-815
- Arnon DI** (1949) Copper enzymes in isolated chloroplasts. Polyphenol oxidase in *Beta vulgaris*. *Plant Physiol* 24, 1-15
- Banzet N, Richaud C, Deveaux Y, Kazmaier M, Gagnon J, Triantaphylides C** (1998) Accumulation of small heat shock proteins, including mitochondrial HSP22, induced by oxidative stress and adaptive response in tomato cells. *Plant J* 13, 519-527
- Barroso JB, Corpas FJ, Carreras A, Sandalio LM, Valderrama R, Palma JM, Lupianez JA, del Rio LA** (1999) Localization of nitric-oxide synthase in plant peroxisomes. *J Biol Chem* 274, 36729-36733
- Beevers H** (1979) Microbodies in higher plants. *Annu Rev Plant Physiol* 30, 159-193
- Expert-Bezancon N, Rabilloud T, Vuillard L, Goldberg ME.** (2003) Physical-chemical features of non-detergent sulfobetaines active as protein-folding helpers. *Biophys Chem.* 100, 469-79.
- Berkemeyer M, Scheibe R, Ocheretina O** (1998) A novel, non-redox-regulated NAD-dependent malate dehydrogenase from chloroplasts of *Arabidopsis thaliana* L. *J Biol Chem* 273, 27927-27933
- Blee KA, Wheatley ER, Bonham VA, Mitchell GP, Robertson D, Slabas AR, Burrell MM, Wojtaszek P, Bolwell GP** (2001) Proteomic analysis reveals a novel set of cell wall proteins in a transformed tobacco cell culture that synthesises secondary walls as determined by biochemical and morphological parameters. *Planta* 212, 404-415
- Blum H, Beier H, Gross HJ** (1987) Improved silver staining of plant proteins, RNA and DNA in polyacrylamide gels. *Electrophoresis* 8, 93-99
- Bradford, M** (1976) A rapid and sensitive method for the quantitation of microgram quantities of protein utilizing the principles of protein-dye binding. *Anal. Biochem.* 72, 248-254.
- Bueno P, Varela J, Gimeenez-Gallego G, del Rio LA** (1995) Peroxisomal copper, zinc superoxide dismutase. Characterization of the isoenzyme from watermelon cotyledons. *Plant Physiol* 108, 1151-1160.
- Bunkelmann JR, Trelease RN** (1996) Ascorbate peroxidase. A prominent membrane protein in oilseed glyoxysomes. *Plant Physiol* 110, 589-598
- Campo S, Carrascal M, Coca M, Abian J, San Segundo B** (2004) The defense response of germinating maize embryos against fungal infection: a proteomics approach. *Proteomics* 4, 383-396.
- Carboni L, Piubelli C, Righetti PG, Jansson B, Domenici E** (2002) Proteomic analysis of rat brain tissue: comparison of protocols for two-dimensional gel electrophoresis analysis based on different solubilizing agents. *Electrophoresis* 23, 4132-4141.
- Chevallet M, Santoni V, Poinas A, Rouquie D, Fuchs A, Kieffer S, Rossignol M, Lunardi J, Garin J, Rabilloud T** (1998) New zwitterionic detergents improve the analysis of membrane proteins by two-dimensional electrophoresis. *Electrophoresis* 19, 1901-1909
- Consoli L, Damerval C** (2001) Quantification of individual zein isoforms resolved by two-dimensional electrophoresis: Genetic variability in 45 maize inbred lines. *Electrophoresis* 22, 2983-2989
- Cooper TG** (1971) The activation of fatty acids in castor bean endosperm. *J Biol Chem* 246, 3451-3455

- Corpas FJ, Barroso JB, Sandalio LM, Distefano S, Palma JM, Lupianez JA, Del Rio LA** (1998) A dehydrogenase-mediated recycling system of NADPH in plant peroxisomes. *Biochem J* 330, 777-784
- Corpas FJ, Gomez M, Hernandez JA, Del Rio LA** (1993) Metabolism of activated oxygen in peroxisomes from *Pisum sativum* L. cultivars with different sensitivity to sodium chloride. *J. Plant Physiol.* 141, 160-165
- Corpillo D, Gardini G, Vaira AM, Basso M, Aime S, Accotto GP, Fasano M** (2004) Proteomics as a tool to improve investigation of substantial equivalence in genetically modified organisms: the case of a virus-resistant tomato. *Proteomics* 4, 193-200
- Dammann C, Ichida A, Hong B, Romanowsky SM, Hrabak EM, Harmon AC, Pickard BG, Harper JF** (2003) Subcellular targeting of nine calcium-dependent protein kinase isoforms from *Arabidopsis*. *Plant Physiol* 132, 1840-1848
- de Hoop MJ, Ab G** (1992) Import of proteins into peroxisomes and other microbodies. *Biochem J* 286, 657-669
- De Nys K, Meyhi E, Mannaerts GP, Fransen M, Van Veldhoven PP** (2001) Characterisation of human peroxisomal 2,4-dienoyl-CoA reductase. *Biochim Biophys Acta* 1533, 66-72
- del Rio LA, Corpas FJ, Sandalio LM, Palma JM, Gomez M, Barroso JB** (2002) Reactive oxygen species, antioxidant systems and nitric oxide in peroxisomes. *J Exp Bot* 53, 1255-1272
- del Rio LA, Pastori GM, Palma JM, Sandalio LM, Sevilla F, Corpas FJ, Jimenez A, Lopez-Huertas, E, Hernandez JA** (1998a) The activated oxygen role of peroxisomes in senescence. *Plant Physiol* 116, 1195-1200
- del Rio LA, Palma JM, Sandalio LM, Corpas FJ, Pastori GM, Bueno P, Lopez-Huertas,** (1996) Peroxisomes as a source of superoxide and hydrogen peroxide in stressed plants. *Biochem. Soc. Trans.* 24, 434-438
- del Rio LA, Sandalio LM, Corpas FJ, Lopez-Huertas E, Palma JM and Pastori GM** (1998b) Activated oxygen-mediated metabolic functions of leaf peroxisomes. *Physiol Plant* 104, 673-680
- del Rio LA, Sandalio LM, Palma JM, Bueno P and Corpas FJ** (1992) Metabolism of oxygen radicals in peroxisomes and cellular implications. *Free Radic Biol Med* 13, 557-580
- Diefenbach J, Kindl H** (2000) The membrane-bound DnaJ protein located at the cytosolic site of glyoxysomes specifically binds the cytosolic isoform 1 of Hsp70 but not other Hsp70 species. *Eur J Biochem* 267, 746-754
- Donaldson RP, Yanik TO, Kwak Y, Balakrishnan S** (2003) Protein Oxidation in Peroxisomes, [abstracts.aspb.org/pb2003/public/P30/0731.html](http://abstracts.aspb.org/pb2003/public/P30/0731.html)
- Douce R, Heldt HW** (2000) Photorespiration. In *Photosynthesis: Physiology and metabolism*, pp 115-136. Eds: Leegood RC, Sharkey RD, von Cammerer S. Kluwer Academic Publishers, Dordrecht, The Netherlands
- Eastmond PJ, Hooks MA, Williams D, Lange P, Bechtold N, Sarrobert C, Nussaume L, Graham IA** (2000) Promoter trapping of a novel medium-chain acyl-CoA oxidase, which is induced transcriptionally during *Arabidopsis* seed germination. *J Biol Chem* 275, 34375-34381
- Egland PG, Pelletier DA, Dispensa M, Gibson J, Harwood CS** (1997) A cluster of bacterial genes for anaerobic benzene ring biodegradation. *Proc Natl Acad Sci USA* 94, 6484-6489
- Eilers T, Schwarz G, Brinkmann H, Witt C, Richter T, Nieder J, Koch B, Hille R, Hansch R, Mendel RR** (2001) Identification and biochemical characterization of *Arabidopsis thaliana* sulfite oxidase. A new player in plant sulfur metabolism. *J Biol Chem* 276, 46989-46994
- Emanuelsson O, Eloffson A, von Heijne G, Cristobal S** (2003) *In silico* prediction of the peroxisomal proteome in fungi, plants and animals. *J Mol Biol* 330, 443-456



- Emanuelsson O, Nielsen H, Brunak S, von Heijne G** (2000) Predicting subcellular localization of proteins based on their N-terminal amino acid sequence. *J Mol Biol* 300, 1005-1016
- Erdmann R, Blobel G** (1996) Identification of Pex13p a peroxisomal membrane receptor for the PTS1 recognition factor. *J Cell Biol* 135, 111-121.
- Ettinger WF, Harada JJ** (1990) Translational or post-translational processes affect differentially the accumulation of isocitrate lyase and malate synthase proteins and enzyme activities in embryos and seedlings of *Brassica napus*. *Arch Biochem Biophys* 281, 139-143
- Expert-Bezancou N, Rabilloud T, Vuillard L, Goldberg ME** (2003) Physical-chemical features of non-detergent sulfobetaines active as protein-folding helpers. *Biophys Chem* 100, 469-479
- Fang TK, Donaldson RP, Vigil EL** (1987) Electron transport in purified glyoxysomal membranes from castor-bean endosperm. *Planta* 172, 1-13
- Fernandez E, Fernandez M, Moreno F, Rodicio R** (1993) Transcriptional regulation of the isocitrate lyase encoding gene in *Saccharomyces cerevisiae*. *FEBS Lett* 333, 238-242
- Finnessy, JJ Trelease RN and Randall DD** (1994) Glyoxysomal isocitrate lyase is a phosphoprotein. *Plant Physiol* 105 (Suppl), 92
- Finnie C, Melchior S, Roepstorff P, Svensson B** (2002) Proteome analysis of grain filling and seed maturation in barley. *Plant Physiol* 129, 1308-1319
- Foyer CH, Noctor G** (1999) Leaves in the dark see the light. *Science* 284, 599-601.
- Froehlich JE, Wilkerson CG, Ray WK, McAndrew RS, Osteryoung KW, Gage DA, Phinney BS** (2003) Proteomic study of the *Arabidopsis thaliana* chloroplastic envelope membrane utilizing alternatives to traditional two-dimensional electrophoresis. *J Proteome Res* 2, 413-25.
- Froman BE, Edwards PC, Bursch AG, Dehesh K** (2000) ACX3, a novel medium-chain acyl-coenzyme A oxidase from *Arabidopsis*. *Plant Physiol* 123, 733-742
- Fukao Y, Hayashi M, Hara-Nishimura I, Nishimura M** (2003) Novel glyoxysomal protein kinase, GPK1, identified by proteomic analysis of glyoxysomes in etiolated cotyledons of *Arabidopsis thaliana*. *Plant Cell Physiol* 44, 1002-1012
- Fukao Y, Hayashi M, Nishimura M** (2002) Proteomic analysis of leaf peroxisomal proteins in greening cotyledons of *Arabidopsis thaliana*. *Plant Cell Physiol* 43, 689-696
- Fukamatsu Y, Yabe N, Hasunuma K** (2003) *Arabidopsis* NDK1 is a component of ROS signaling by interacting with three catalases. *Plant Cell Physiol* 44, 982-989
- Fulda M, Shockey J, Werber M, Wolter FP, Heinz E** (2002) Two long-chain acyl-CoA synthetases from *Arabidopsis thaliana* involved in peroxisomal fatty acid beta-oxidation. *Plant J* 32, 93-103
- Gallardo K, Job C, Groot SPC, Puype M, Demol H, Vandekerckhove J, Job D** (2001) Proteomic analysis of *Arabidopsis* seed germination and priming. *Plant Physiol* 126, 835-848
- Gerhardt B** (1986). Basic metabolic function of the higher plant peroxisomes. *Physiol Vég* 24, 397-410
- Gerhardt B** (1992) Fatty acid degradation in plants. *Prog Lipid Res* 31, 417-446
- Gerhardt B** (1993) Catabolism of fatty acids (alpha- and beta-oxidation). In *Lipid metabolism in plants*, pp 527-565. Ed Moore TS Jr. CRC press, Boca Raton, FA
- Ghosh MK, Hajra AK** (1986) A rapid method for the isolation of peroxisomes from rat liver. *Anal Biochem* 159, 169-174
- Gietl C, Faber KN, van der Klei IJ, Veenhuis M** (1994) Mutational analysis of the N-terminal topogenic signal of watermelon glyoxysomal malate dehydrogenase using the heterologous host *Hansenula polymorpha*. *Proc Natl Acad Sci USA* 91, 3151-3155

- Giuliano G, Al-Babili S, von Lintig J** (2003) Carotenoid oxygenases: cleave it or leave it. *Trends Plant Sci* 8, 145-149.
- Givan CV** (1980) Aminotransferases in higher plants. In *The Biochemistry of Plants*, Vol 5, pp 329-357. Ed Miflin BJ. Academic Press, New York, NY
- Glover JR, Andrews DW, Subramani S, Rachubinski RA** (1994) Mutagenesis of the amino targeting signal of *Saccharomyces cerevisiae* 3-ketoacyl-CoA thiolase reveals conserved amino acids required for import into peroxisomes *in vivo*. *J Biol Chem* 269, 7558-7563
- Godavari HR, Badour SS, Waygood ER** (1973) Isocitrate lyase in green leaves. *Plant Physiol* 51, 863-867
- Godovac-Zimmermann J, Brown LR** (2001) Perspectives for mass spectrometry and functional proteomics. *Mass Spectrom Rev* 20, 1-57
- Gomez SM, Nishio JN, Faull KF, Whitelegge JP** (2002) The chloroplast grana proteome defined by intact mass measurements from liquid chromatography mass spectrometry. *Mol Cell Proteomics* 1, 46-59
- Georg A** (2000) Advances in 2D gel techniques. In *Proteomics: A Trends Guide*, pp 3-6. Eds Blackstock W, Mann M. Elsevier Science, London, UK
- Georg A, Boguth G, Obermaier C, Weiss W** (1998) Two-dimensional electrophoresis of proteins in an immobilized pH 4-12 gradient. *Electrophoresis* 19, 1516-1519
- Georg A, Dunn M** (2001) Two-dimensional polyacrylamide gel electrophoresis for proteome analysis. In *Proteomics*, pp 43-63. Eds Pennington SR, Dunn MJ. BIOS Scientific Publishers, Oxford, UK
- Georg A, Obermaier C, Boguth G, Csordas A, Diaz J-J, Madjar J-J** (1997) Very alkaline immobilized pH gradients for two-dimensional electrophoresis of ribosomal and nuclear proteins. *Electrophoresis* 18, 328-337
- Georg A, Obermaier C, Boguth G, Weiss W** (1999) Recent developments in two-dimensional gel electrophoresis with immobilized pH gradients: Wide pH gradients up to pH 12, longer separation distances and simplified procedures. *Electrophoresis* 20, 712-717
- Gould SG, Keller GA, Subramani S** (1987) Identification of a peroxisomal targeting signal at the carboxy terminus of firefly luciferase. *J Cell Biol* 105, 2923-2931
- Gould SJ, Keller GA, Hosken N, Wilkinson J, Subramani S** (1989) A conserved tripeptide sorts proteins to peroxisomes. *J Cell Biol* 108, 1657-1664
- Greenler JM, Becker WM** (1990) Organ specificity and light regulation of NADH-dependent hydroxypyruvate reductase transcript abundance. *Plant Physiol* 94, 1484-1487
- Greenler JM, Sloan JS, Schwartz BW, Becker WM** (1989) Isolation, characterization and sequence analysis of a full-length cDNA clone encoding NADH-dependent hydroxypyruvate reductase from cucumber. *Plant Mol Biol* 113, 139-150
- Gühnemann-Schäfer K, Kindl H** (1995) The leaf peroxisomal form (MFP IV) of multifunctional protein functioning in fatty-acid beta-oxidation. *Planta* 196, 642-646
- Gurvitz A, Hamilton B, Ruis H, Hartig A** (2001) Peroxisomal degradation of trans-unsaturated fatty acids in the yeast *Saccharomyces cerevisiae*. *J Biol Chem* 276, 895-903
- Halliwell B, Gutteridge JMC** (1989) *Free radicals in Biology and Medicine*. Clarendon Press, Oxford, UK.
- Haslbeck M** (2002) sHsps and their role in the chaperone network. *Cell Mol Life Sci* 59, 1649-1657
- Hayashi H, De Bellis L, Ciurli A, Kondo M, Hayashi M, Nishimura M** (1999) A novel acyl-CoA oxidase that can oxidize short-chain acyl-CoA in plant peroxisomes. *J Biol Chem* 274, 12715-12721
- Hayashi H, De Bellis L, Hayashi Y, Nito K, Kato A, Hayashi M, Hara-Nishimura I, Nishimura M** (2002) Molecular characterization of an *Arabidopsis* acyl-coenzyme A synthetase localized on glyoxysomal membranes. *Plant Physiol* 130, 2019-2026

- Hayashi H, Suga T, Ninobe S (1975) Studies on peroxisomes. V. Effect of ethyl p-chlorophenoxyisobutyrate on the centrifugal behavior of rat liver peroxisomes. *J Biochem* 77, 1199-1204
- Hayashi M, Aoki M, Kato A, Kondo M, Nishimura M (1996a) Transport of chimeric proteins that contain a carboxy-terminal targeting signal into plant microbodies. *Plant J* 10, 225-234
- Hayashi M, Aoki M, Kato A, Nishimura M (1997) Changes in targeting efficiencies of proteins to plant microbodies caused by amino acid substitutions in the carboxyl-terminal tripeptide. *Plant Cell Physiol* 38, 759-768
- Hayashi M, Toriyama K, Kondo M, Nishimura M (1998) 2,4-Dichlorophenoxybutyric acid-resistant mutants of *Arabidopsis* have defects in glyoxysomal fatty acid beta-oxidation. *Plant Cell* 10, 183-195
- Hayashi M, Tsugeki R, Kondo M, Mori H, Nishimura M (1996b) Pumpkin hydroxypyruvate reductases with and without a putative C-terminal signal for targeting to microbodies may be produced by alternative splicing. *Plant Mol Biol* 30, 183-189
- Heazlewood JL, Howell KA, Millar AH. (2003) Mitochondrial complex I from *Arabidopsis* and rice: orthologs of mammalian and fungal components coupled with plant-specific subunits. *Biochim Biophys Acta*. 1604,159-69
- Heber U, Krause GH (1980) What is the physiological role of photorespiration? *Trends Biochem Sci* 5, 32-34
- Herbert B, Galvani M, Hamdan M, Olivieri E, MacCarthy J, Pedersen S, Righetti PG. (2001) Reduction and alkylation of proteins in preparation of two-dimensional map analysis: why, when, and how? *Electrophoresis* 22:2046-57
- Heupel R, Heldt HW (1994) Protein organization in the matrix of leaf peroxisomes. A multi-enzyme complex involved in photorespiratory metabolism. *Eur J Biochem* 220, 165-172
- Heupel R, Markgraf T, Robinson DG, Heldt HW (1991) Compartmentation studies on spinach leaf peroxisomes. Evidence for channeling of photorespiratory metabolites in peroxisomes devoid of intact boundary membrane. *Plant Physiol* 96, 971-979
- Hooks M (2002) Molecular biology, enzymology, and physiology of beta-oxidation In: *Plant Peroxisomes: Biochemistry, Cell Biology and Biotechnological Applications*, pp 19-55. Eds Baker A, Graham IA. Kluwer Academic Publishers, Dordrecht, The Netherlands
- Hooks MA, Kellas F, Graham IA (1999) Long-chain acyl-CoA oxidases of *Arabidopsis*. *Plant J* 20, 1-13
- Horn DM, Zubarev RA, McLafferty FW (2000) Automated *de novo* sequencing of proteins by tandem high-resolution mass spectrometry. *Proc Natl Acad Sci USA* 97, 10313-10317
- Howitz KT, McCarty RE (1985a) Kinetic characteristics of the chloroplast envelope glycolate transporter. *Biochem* 24, 2645-2652
- Howitz KT, McCarty RE (1985b) Substrate specificity of the pea chloroplast glycolate transporter. *Biochem* 24, 3645-3650
- Howitz KT, McCarty RE (1986) D-Glycerate transport by the pea chloroplast glycolate carrier. *Plant Physiol* 80, 390-395
- Howitz KT, McCarty RE (1988) Measurement of proton-linked transport activities in pyranine loaded chloroplast inner envelope vesicles. *Plant Physiol* 86, 999-1001
- Howitz KT, McCarty RE (1991) Solubilization, partial purification, and reconstitution of the glycolate/glycerate transporter from chloroplast inner envelope membranes. *Plant Physiol* 96, 1060-1069
- Hoyt JC, Reeves HC (1992) Phosphorylation of *Acinetobacter* isocitrate lyase. *Biochem Biophys Res Commun* 182, 367-371
- Huang AHC, Trelease RN, Moore TS Jr (1983) *Plant Peroxisomes*. Academic Press, New York, NY

- Hubbard MJ, Cohen P** (1993) On target with a new mechanism for the regulation of protein phosphorylation. *Trends Biochem Sci* 18, 172-177
- Huber LA, Pfaller K, Vietor I** (2003) Organelle proteomics: implications for subcellular fractionation in proteomics. *Circ Res* 92, 962-968.
- Hunt L and Fletcher JS** (1977) Intracellular location of isocitrate lyase in leaf tissue. *Plant Sci Lett* 10, 243-247
- Hutton D and Stumpf PK** (1969) Characterization of the beta-oxidation system from maturing and germinating castor bean seeds. *Plant Physiol* 44, 508-516
- Igarashi D, Miwa T, Seki M, Kobayashi M, Kato T, Tabata S, Shinozaki K, Ohsumi C** (2003) Identification of photorespiratory glutamate:glyoxylate aminotransferase (GGAT) gene in *Arabidopsis*. *Plant J* 33, 975-987
- Ireland RI, Joy KW** (1983) Purification and properties of an asparagine aminotransferase from *Pisum sativum* leaves. *Arch Biochem Biophys* 223, 291-296
- Isaya G, Kalousek F, Fenton WA, Rosenberg LE** (1991) Cleavage of precursors by the mitochondrial processing peptidase requires a compatible mature protein or an intermediate octapeptide. *J Cell Biol* 113, 65-76
- Ishikawa T, Yoshimura K, Sakai K, Tamoi M, Takeda T, Shigeoka S** (1998) Molecular characterization and physiological role of a glyoxysome-bound ascorbate peroxidase from spinach. *Plant Cell Physiol* 39, 23-34
- Janssen B-J** (1995) A cDNA clone for isocitrate lyase from tomato. *Plant Physiol.* 108, 1339
- Jensen ON** (2000) Modification-specific proteomics: systematic strategies for analysing post-translationally modified proteins. In *Proteomics: A Trends Guide*, pp 36-41. Eds Blackstock W, Mann M. Elsevier Science, London, UK
- Jimenez A, Hernandez JA, Del Rio LA, Sevilla F** (1997) Evidence for the presence of the ascorbate-glutathione cycle in mitochondria and peroxisomes of pea leaves. *Plant Physiol* 114, 275-284
- Johnson TW, Shen G, Zybailov B, Kolling D, Reategui R, Beauparlant S, Vassiliev IR, Bryant DA, Jones AD, Golbeck JH, Chitnis PR** (2000) Recruitment of a foreign quinone into the A(1) site of photosystem I. I. Genetic and physiological characterization of phylloquinone biosynthetic pathway mutants in *Synechocystis* sp. PCC6803. *J Biol Chem* 275, 8523-8530
- Jornvall H, Persson B, Krook M, Atrian S, Gonzalez-Duarte R, Jeffery J, Ghosh D** (1995) Short-chain dehydrogenases/reductases (SDR). *Biochem* 34, 6003-6013
- Kamada T, Nito K, Hayashi H, Mano S, Hayashi M, Nishimura M** (2003) Functional differentiation of peroxisomes revealed by expression profiles of peroxisomal genes in *Arabidopsis thaliana*. *Plant Cell Physiol* 44, 1275-1289
- Karas M, Hillenkamp F** (1988) Laser desorption ionization of proteins with molecular masses exceeding 10,000 daltons. *Anal Chem* 60, 2299-2301
- Karpichev IV, Small GM** (2000) Evidence for a novel pathway for the targeting of a *Saccharomyces cerevisiae* peroxisomal protein belonging to the isomerase/hydratase family. *J Cell Sci* 113, 533-544
- Kato A, Hayashi M, Kondo M, Nishimura M** (1996) Targeting and processing of a chimeric protein with the N-terminal presequence of the precursor to glyoxysomal citrate synthase. *Plant Cell* 8, 1601-1611
- Kato A, Hayashi M, Mori H, Nishimura M** (1995) Molecular characterization of a glyoxysomal citrate synthase that is synthesized as a precursor of higher molecular mass in pumpkin. *Plant Mol Biol* 27, 377-390
- Kim KK, Kim R, Kim SH** (1998) Crystal structure of a small heat-shock protein. *Nature* 394, 595-599
- Kindl H, Kruse C** (1983) Biosynthesis of glyoxysomal proteins. *Methods Enzymol* 96, 700-715

- Kleff S, Sander S, Mielke G., Eising R** (1997) The predominant protein in peroxisomal cores of sunflower cotyledons is a catalase that differs in primary structure from the catalase in the peroxisomal matrix. *Eur J Biochem* 245, 402-410
- Kliebenstein DJ, Monde RA, Last RL** (1998) Superoxide dismutase in *Arabidopsis*: an eclectic enzyme family with disparate regulation and protein localization. *Plant Physiol* 118, 637-650
- Koeller W and Kindl H** (1977) Glyoxylate cycle enzymes of the glyoxysomal membrane from cucumber cotyledons. *Arch Biochem Biophys* 181, 236-248
- Koster KL, Reisdorph N, Ramsay JL** (2003) Changing desiccation tolerance of pea embryo protoplasts during germination. *J Exp Bot* 54, 1607-1614
- Kovacs WJ, Faust PL, Keller G-A, Krisans SK** (2001) Purification of brain peroxisomes and localization of 3-hydroxy-3-methylglutaryl coenzyme A reductase. *Eur J Biochem* 268, 4850-4859
- Kragler F, Lametschwandtner G, Christmann J, Hartig A, Harada JJ** (1998) Identification and analysis of the plant peroxisomal targeting signal 1 receptor NtPEX5. *Proc Natl Acad Sci USA* 95, 13336-13341
- Krishna RG, Wold F** (1993) Post-translational modification of proteins. *Adv Enzymol Relat Areas Mol Biol* 67, 265-298
- Kruft V, Eubel H, Jansch L, Werhahn W, Braun H-P** (2001) Proteomic approach to identify novel mitochondrial proteins in *Arabidopsis*. *Plant Physiol* 127, 1694-1710
- Laemmli UK** (1970) Cleavage of structural proteins during the assembly of the head of bacteriophage T4. *Nature* 227, 680-685
- Lazarow PB, Fujiki Y** (1985) Biogenesis of peroxisomes. *Annu Rev Cell Biol* 1, 489-530
- Leimgruber RM, Malone JP, Radabaugh MR, LaPorte ML, Violand BN and Monahan JB** (2002) Development of improved cell lysis, solubilization and imaging approaches for proteomic analyses. *Proteomics* 2, 135-144
- Liepmann AH, Olsen LJ** (2001) Peroxisomal alanine:glyoxylate aminotransferase (AGT1) is a photorespiratory enzyme with multiple substrates in *Arabidopsis thaliana*. *Plant J* 25, 1-14
- Liepmann AH, Olsen, LJ** (2003) Alanine aminotransferase homologs catalyze the glutamate:glyoxylate aminotransferase reaction in peroxisomes of *Arabidopsis*. *Plant Physiol* 131, 215-227
- Loomis WF, Shaulsky G, Wang N** (1997) Histidine kinases in signal transduction pathways of eukaryotes. *J Cell Sci* 110, 1141-1145
- Lopez-Boado YS, Herrero P, Fernandez T, Fernandez R, Moreno F** (1988) Glucose-stimulated phosphorylation of yeast isocitrate lyase *in vivo*. *J Gen Microbiol* 134, 2499-2505
- Lopez-Huertas E, Sandalio LM, Del Rio LA** (1995) Integral membrane polypeptides of pea leaf peroxisomes: characterization and response to plant stress. *Plant Physiol Biochem* 33, 295-302
- Lopez-Huertas E, Sandalio LM, Del Rio LA** (1996) Superoxide generation in peroxisomal membranes: Characterization of redox proteins involved-Biochem. Soc. Trans. 24, 195S *Plant Physiol Biochem* 33, 295-302
- Lopez-Huertas E, Sandalio LM, Gomez M, Del Rio LA** (1997) Superoxide generation in peroxisomal membranes: Evidence for participation of the 18-kDa integral membrane polipeptide. *Free Radic Res.* 26, 497-506
- Lorimer GH, Andrews TJ** (1982) The C<sub>2</sub> chemo- and photorespiratory carbon oxidation cycle. In *The Biochemistry of Plants Vol 8*, pp 329-374. Eds Hatch MD, Boardman NK. Academic Press, New York, NY
- Low D, Brandle K, Nover L, Forreiter C** (2000) Cytosolic heat-stress proteins Hsp17.7 class I and Hsp17.3 class II of tomato act as molecular chaperones *in vivo*. *Planta* 211, 575-582
- Lowry OH, Rosebrough NJ, Farr AL, Randall RJ** (1951) Protein measurement with the folin phenol reagent. *J Biol Chem* 193, 265-275

- Majoul T, Bancel E, Triboi E, Ben Hamida J, Branlard G** (2004) Proteomic analysis of the effect of heat stress on hexaploid wheat grain: characterization of heat-responsive proteins from non-prolamins fraction. *Proteomics* 4, 505-513
- Mann M, Hendrickson RC, Pandey A** (2001) Analysis of proteins and proteomes by mass spectrometry. *Annu Rev Biochem* 70, 437-473
- Mann M, Jensen, ON** (2003) Proteomic analysis of post-translational modifications. *Nat Biotechnol* 21, 255-261
- Mann M, Wilm M** (1994) Error-tolerant identification of peptides in sequence databases by peptide sequence tags. *Anal Chem* 66, 4390-4399
- Mano S, Hayashi M, Kondo M, Nishimura M** (1997) Hydroxypyruvate reductase with a carboxy-terminal targeting signal to microbodies is expressed in Arabidopsis. *Plant Cell Physiol* 38, 449-455
- Mano S, Hayashi M, Nishimura M** (1999) Light regulates alternative splicing of hydroxypyruvate reductase in pumpkin. *Plant J* 17, 309-320
- Marzioch M, Erdmann R, Veenhuis M, Kunau WH** (1994) PAS7 encodes a novel yeast member of the WD-40 protein family essential for import of 3-oxoacyl-CoA thiolase, a PTS2-containing protein, into peroxisomes. *EMBO J* 13, 4908-4918
- Mekhedov S, Martinez de Ilarduya O, Ohlrogge J** (2000) Toward a functional catalog of the plant genome. A survey of genes for lipid biosynthesis. *Plant Physiol* 122, 389-402
- Mettler IJ, Beevers H** (1980) Oxidation of NADH in glyoxysomes by a malate-aspartate shuttle. *Plant Physiol* 66, 555-560
- Millar AH, Heazlewood JL** (2003) Genomic and proteomic analysis of mitochondrial carrier proteins in Arabidopsis. *Plant Physiol* 131, 443-453
- Millar AH, Sweetlove LJ, Giege P, Leaver CJ** (2001) Analysis of the Arabidopsis mitochondrial proteome. *Plant Physiol* 127, 1711-1727
- Mittova V, Tal M, Volokita M, Guy M** (2003) Up-regulation of the leaf mitochondrial and peroxisomal antioxidative systems in response to salt-induced oxidative stress in the wild salt-tolerant tomato species *Lycopersicon pennellii*. *Plant Cell Environ* 26, 845-856
- Molloy MP** (2000) Two-dimensional electrophoresis of membrane proteins using immobilized pH gradients. *Anal Biochem* 280, 1-10
- Mori H and Nishimura M** (1989) Glyoxysomal malate synthase is specifically degraded in microbodies during greening of pumpkin cotyledons. *FEBS Lett* 244, 163-166
- Musante L, Candiano G, Ghiggeri GM** (1998) Resolution of fibronectin and other uncharacterized proteins by two-dimensional polyacrylamide electrophoresis with thiourea. *J Chromatogr B Biomed Sci Appl.* 705, 351-356
- Nakamura T, Meyer C, Sano H** (2002) Molecular cloning and characterization of plant genes encoding novel peroxisomal molybdoenzymes of the sulphite oxidase family. *J Exp Bot* 53, 1833-1836
- Nakamura T, Yokota S, Muramoto Y, Tsutsui K, Oguri Y, Fukui K, Takabe T** (1997) Expression of a betaine aldehyde dehydrogenase gene in rice, a glycinebetaine nonaccumulator, and possible localization of its protein in peroxisomes. *Plant J* 11, 1115-1120
- Nakamura Y, Tolbert NE** (1983) Serine:glyoxylate, alanine:glyoxylate, and glutamate:glyoxylate aminotransferase reactions in peroxisomes from spinach leaves. *J Biol Chem* 258, 7631-7638
- Neuhoff V, Arold N, Taube D, Ehrhardt W** (1988) Improved staining of proteins in polyacrylamide gels including isoelectric focusing gels with clear background at nanogram sensitivity using Coomassie Brilliant Blue G-250 and R-250. *Electrophoresis* 9, 255-262
- Nishimura M, Takeuchi Y, De Bellis L, Hara-Nishimura I** (1993) Leaf peroxisomes are directly transformed to glyoxysomes during senescence of pumpkin cotyledons. *Protoplasma* 175, 131-137

- Noctor G, Foyer CH** (1998) Ascorbate and glutathione: Keeping active oxygen under control. *Annu Rev Plant Physiol Plant Mol Biol* 49, 249-279
- Oda Y, Nagasu T, Chait BT** (2001) Enrichment analysis of phosphorylated proteins as a tool for probing the phosphoproteome. *Nat Biotechnol* 19, 379-382
- Ogren WL** (1984) Photorespiration: Pathways, regulation, and modification. *Annu Rev Plant Physiol* 35, 415-442
- O'Farrell PH** (1975) High resolution two-dimensional electrophoresis of proteins. *J. Biol. Chem.* 250, 4007-4021
- Okinaka Y, Yang CH, Herman E, Kinney A, Keen NT.** (2002) The P34 syringolide elicitor receptor interacts with a soybean photorespiration enzyme, NADH-dependent hydroxypyruvate reductase. *Mol Plant Microbe Interact.* 15,1213-8
- Palma JM, Pastori GM, Bueno P, Distefano S, Del Rio LA** (1997) Purification and properties of cytosolic copper, zinc superoxide dismutase from watermelon (*Citrullus vulgaris* Schrad.) cotyledons. *Free Radic Res* 26, 83-91.
- Pastori GM, Del Rio LA** (1997) Natural Senescence of Pea Leaves (An Activated Oxygen-Mediated Function for Peroxisomes). *Plant Physiol* 113, 411-418
- Pastori GM, Distefano S, Palma JM, del Rio LA** (1996) Purification and characterization of peroxisomal and mitochondrial Mn-superoxide dismutases from watermelon cotyledons. *Biochem Soc Trans* 24 (Suppl), 196
- Patterson SD, Aebersold R, Goodlett DR** (2001) Mass spectrometry-based methods for protein identification and phosphorylation site analysis. In *Proteomics*, PP 87-130. Eds Pennington SR, Dunn MJ. BIOS Scientific Publishers, Oxford, UK
- Peltier J-B, Emanuelsson O, Kalume DE, Ytterberg J, Friso G, Rudella A, Liberles DA, Söderberg L, Roepstorff P, von Heijne G, van Wijk KJ** (2002) Central functions of the lumenal and peripheral thylakoid proteome of Arabidopsis determined by experimentation and genome-wide prediction. *Plant Cell* 14, 211-236
- Peltier J-B, Ytterberg J, Liberles DA, Roepstorff P, van Wijk K** (2001) Identification of a 350-kDa ClpP protease complex with 10 different Clp isoforms in chloroplasts of *Arabidopsis thaliana*. *J Biol Chem* 276, 16318-16327
- Perez-Bueno ML, Rahoutei J, Sajnani C, Garcia-Luque I, Baron M** (2004) Proteomic analysis of the oxygen-evolving complex of photosystem II under biotec stress: Studies on *Nicotiana benthamiana* infected with tobamoviruses. *Proteomics* 4, 418-25
- Perkins DN, Pappin DJ, Creasy DM, Cottrell JS** (1999) Probability-based protein identification by searching sequence databases using mass spectrometry data. *Electrophoresis* 18, 3551-3567
- Poirier Y** (2002) Polyhydroxyalkanoate synthesis in plant peroxisomes. In *Plant Peroxisomes: Biochemistry, Cell Biology and Biotechnological Applications*, pp 465-496. Eds Baker A, Graham IA. Kluwer Academic Publishers, Dordrecht, The Netherlands
- Polidoros AN, Scandalios JG** (1998) Circadian expression of the maize catalase Cat3 gene is highly conserved among diverse maize genotypes with structurally different promoters. *Genetics* 149, 405-15
- Posewitz M, Tempst P** (1999) Immobilized Gallium(III) affinity chromatography of phosphopeptides. *Anal Chem* 71, 2883-2892
- Pratt JM, Petty J, Riba-Garcia I, Robertson DHL, Gaskell SJ, Oliver SG, Beynon RJ** (2002) Dynamics of protein turnover, a missing dimension in proteomics. *Mol Cell Proteomics* 1, 579-591
- Preisig-Müller R, Gühnemann-Schäfer K, Kindl H** (1994) Domains of the tetrafunctional protein acting in glyoxysomal fatty acid beta-oxidation. Demonstration of epimerase and isomerase activities on a peptide lacking hydratase activity. *J Biol Chem* 269, 20475-20481
- Prime TA, Sherrier DJ, Mahon P, Packman LC, Dupree P** (2000) A proteomic analysis of organelles from *Arabidopsis thaliana*. *Electrophoresis* 21, 3488-3499

- Rabilloud T** (1998) Use of thiourea to increase the solubility of membrane proteins in two-dimensional electrophoresis. *Electrophoresis* 19, 758-760
- Randall PJ, Bouma D** (1973) Zinc deficiency, carbonic anhydrase, and photosynthesis in leaves of spinach. *Plant Physiol.* 52, 229-239
- Rehling P, Marzioch M, Niesen F, Wittke E, Veenhuis M, Kunau WH** (1996) The import receptor for the peroxisomal targeting signal 2 (PTS2) in *Saccharomyces cerevisiae* is encoded by the PAS7 gene. *EMBO J* 15, 2901-2913
- Reumann S** (1993) Funktionelle und strukturelle Untersuchungen zur Kompartimentierung des Stoffwechsels von Peroxisomen aus Spinatblättern. Diploma thesis, Göttingen University, Göttingen
- Reumann S** (1996) Nachweis, Charakterisierung und Aufreinigung eines Porins pflanzlicher Peroxisomen. PhD Dissertation, Göttingen University, Göttingen
- Reumann S** (2000) The structural properties of plant peroxisomes and their metabolic significance. *Biol Chem* 381, 639-648
- Reumann S** (2002) The photorespiratory pathway of leaf peroxisomes. In *Plant Peroxisomes: Biochemistry, Cell Biology and Biotechnological Applications*, pp 141-189. Eds Baker A, Graham IA. Kluwer Academic Publishers, Dordrecht, The Netherlands
- Reumann S:** Specification of peroxisome targeting signals type 1 and type 2 of plant peroxisomes by bioinformatics analyses. *Plant Physiol*, *in press*
- Reumann S, Ma C, Lemke S, Babujee L:** AraPerox: a database of Arabidopsis proteins from plant peroxisomes. *Plant Physiol*, *submitted*
- Reumann S, Maier E, Benz R, Heldt HW** (1995) The membrane of leaf peroxisomes contains a porin-like channel. *J Biol Chem* 270, 17559-17565
- Reumann S, Maier E, Benz R, Heldt HW** (1996) A specific porin is involved in the malate shuttle of leaf peroxisomes. *Biochem Soc Trans* 24, 754-757
- Reumann S, Maier E, Heldt HW, Benz R** (1998) Permeability properties of the specific porin of spinach leaf peroxisomes. *Eur J Biochem* 251, 359-366
- Rittstieg C** (2001) Proteomics-Untersuchungen zur Identifizierung von unbekanntem Matrixproteinen aus Blattperoxisomen von *Spinacia oleracea* L. Diploma thesis, Göttingen University, Göttingen
- Robertson EF, Hoyt JC, Reeves HC** (1988) Evidence of histidine phosphorylation in isocitrate lyase from *Escherichia coli*. *J Biol Chem* 263, 2477-2482
- Robertson EF, Reeves HC** (1989) Phosphorylation of isocitrate lyase in *Escherichia coli*. *Biochimie* 71, 1065-1070
- Romero-Puertas MC, McCarthy I, Sandalio LM, Palma JM, Corpas FJ, Gomez M, del Rio LA** (1999) Cadmium toxicity and oxidative metabolism of pea leaf peroxisomes. *Free Radic Res* 31 (Suppl), 25-31
- Rylot E, Larson T** (2002) Futile cycling through beta-oxidation as a barrier to increased yields of novel oils In *Plant Peroxisomes: Biochemistry, Cell Biology and Biotechnological Applications*, pp. 445-463. Eds Baker A, Graham IA. Kluwer Academic Publishers, Dordrecht, The Netherlands
- Sanchez J-C, Rouge V, Pisteur M, Ravier F, Tonella L, Moosmayer M, Wilkins MR, Hochstrasser DF** (1997) Improved and simplified sample application using reswelling of dry immobilized pH gradients. *Electrophoresis* 18, 324-327
- Sanders PM, Lee PY, Biesgen C, Boone JD, Beals TP, Weiler EW, Goldberg RB** (2000) The *Arabidopsis* DELAYED DEHISCENCE1 gene encodes an enzyme in the jasmonic acid synthesis pathway. *Plant Cell* 12, 1041-1061
- Santoni V, Doumas P, Rouquie D, Mansion M, Rabilloud T, Rossignol M** (1999) Large scale characterization of plant plasma membrane proteins. *Biochimie* 81, 655-661
- Schaller F, Hennig P, Weiler EW** (1998) 12-Oxophytodienoate-10,11-reductase: occurrence of two isoenzymes of different specificity against stereoisomers of 12-oxophytodienoic acid *Plant Physiol* 118, 1345-51.



- Scharf KD, Siddique M, Vierling E** (2001) The expanding family of *Arabidopsis thaliana* small heat stress proteins and a new family of proteins containing alpha-crystallin domains (Acid proteins). *Cell Stress Chaperones* 6, 225-237
- Schockey JM, Fulda MS, Browse J** (2003) *Arabidopsis* contains a large superfamily of acyl-activating enzymes. Phylogenetic and biochemical analysis reveals a new class of acyl-coenzyme A synthetases. *Plant Physiol* 132, 1065-1076
- Schubert M, Petersson UA, Haas BJ, Funk C, Schröder WP, Kieselbach T** (2002) Proteome map of the chloroplast lumen of *Arabidopsis thaliana*. *J Biol Chem* 277, 8354-8365
- Schulenberg B, Aggeler R, Beechem JM, Capaldi RA, Patton WF** (2003) Analysis of steady-state protein phosphorylation in mitochondria using a novel fluorescent phosphosensor dye *J Biol Chem* 278, 27251-27255
- Schultz CJ, Coruzzi GM** (1995) The aspartate aminotransferase gene family of *Arabidopsis* encodes isoenzymes localized to three distinct subcellular compartments. *Plant J* 7, 61-75
- Sharkey TD** (1988) Estimating the rate of photorespiration in leaves. *Physiol Plant* 73, 147-152
- Sharma V, Suvarna K, Meganathan R, Hudspeth ME** (1992) Menaquinone (vitamin K2) biosynthesis: nucleotide sequence and expression of the *menB* gene from *Escherichia coli*. *J Bacteriol* 174, 5057-5062
- Shevchenko A, Wilm M, Vorm O, Mann M** (1996) Mass spectrometric sequencing of proteins from silver-stained polyacrylamide gels. *Anal Chem* 68, 850-858
- Shockey JM, Fulda MS, Browse JA** (2002) *Arabidopsis* contains nine long-chain acyl-coenzyme A synthetase genes that participate in fatty acid and glycerolipid metabolism. *Plant Physiol* 129, 1710-1722
- Shockey JM, Fulda MS, Browse J** (2003) *Arabidopsis* contains a large superfamily of acyl-activating enzymes. Phylogenetic and biochemical analysis reveals a new class of acyl-coenzyme A synthetases. *Plant Physiol* 132: 1065-1076
- Srivalli B, Khanna-Chopra R** (2001) Induction of new isoforms of superoxide dismutase and catalase enzymes in the flag leaf of wheat during monocarpic senescence. *Biochem Biophys Res Commun* 288, 1037-1042
- Stintzi A, Browse J** (2000) The *Arabidopsis* male-sterile mutant, *opr3*, lacks the 12-oxophytodienoic acid reductase required for jasmonate synthesis. *Proc Natl Acad Sci USA* 97, 10625-10630
- Stitt M** (1984) Fumarase. In *Methods of Enzymatic Analyses Vol 4*, pp 359-362. Ed Bergmeyer HU. Verlag Chemie, Weinheim, Deutschland.
- Strassner J, Schaller F, Frick UB, Howe GA, Weiler EW, Amrhein N, Macheroux P, Schaller A** (2002) Characterization and cDNA-microarray expression analysis of 12-oxophytodienoate reductases reveals differential roles for octadecanoid biosynthesis in the local versus the systemic wound response. *Plant J* 32, 585-601
- Subramani S** (1993) Protein import into peroxisomes and biogenesis of the organelle. *Annu Rev Cell Biol* 9, 445-478
- Sun W, Van Montagu M, Verbruggen N** (2002) Small heat shock proteins and stress tolerance in plants. *Biochim Biophys Acta* 1577, 1-9
- Swinkels BW, Gould SJ, Bodnar AG, Rachubinski RA, Subramani S** (1991) A novel, cleavable peroxisomal targeting signal at the amino-terminus of the rat 3-ketoacyl-CoA thiolase. *EMBO J* 10, 3255-3262
- Swinkels BW, Gould SJ, Subramani S** (1992) Targeting efficiencies of various permutations of the consensus C-terminal tripeptide peroxisomal targeting signal. *FEBS Lett* 305, 133-136
- Taler D, Galperin M, Benjamin I, Cohen Y, Kenigsbuch D** (2004) Plant eR genes that encode Photorespiratory enzymes confer resistance against disease. *Plant Cell* 16, 172-184

- Tastet C, Lescuyer P, Diemer H, Luche S, van Dorsselaer A, Rabilloud T.** (2003) A versatile electrophoresis system for the analysis of high- and low-molecular-weight proteins. *Electrophoresis* 24, 787-94.
- Thiellement H, Bahrman N, Damerval C, Plomion C, Rossignol M, Santoni V, de Vienne D, Zivy M** (1999) Proteomics for genetic and physiological studies in plants. *Electrophoresis* 20, 2013-2026
- Thomas JD, van Bogelen R** (2000) Experimentalism in proteomics. In *Proteomics: A Trends Guide*, pp 7-11. Eds Blackstock W, Mann M. Elsevier Science, London, UK
- Titus DE, Hondred D, Becker WM** (1983) Purification and characterization of hydroxypyruvate reductase from cucumber cotyledons. *Plant Physiol* 72, 402-408
- Tolbert NE** (1971) Microbodies-peroxisomes and glyoxysomes. *Annu Rev Plant Physiol* 21, 45-74
- Tolbert NE** (1980) Photorespiration. In *The Biochemistry of Plants Vol 2*, pp 487-523. Ed Davies DD. Academic Press, New York, NY
- Tolbert NE, Oeser A, Kisaki T, Hageman RH, Yamazaki RK** (1968) Peroxisomes from spinach leaves containing enzymes related to glycolate metabolism. *J Biol Chem* 243, 5179-5184
- Tugal HB, Pool M, Baker A** (1999) Arabidopsis 22-kilodalton peroxisomal membrane protein. Nucleotide sequence analysis and biochemical characterization. *Plant Physiol* 120, 309-320
- Van der Leij I, Franse MM, Elgersma Y, Distel B, Tabak HF** (1993) PAS10 is a tetratricopeptide-repeat protein that is essential for the import of most matrix proteins into peroxisomes of *Saccharomyces cerevisiae*. *Proc Natl Acad Sci USA* 90, 11782-11786
- Vicentini F, Matile P** (1993) Gerontosomes, a multifunctional type of peroxisomes in senescent leaves. *J Plant Physiol* 142, 50-56
- Vuillard L, Madern D, Franzetti B, Rabilloud T** (1995) Halophilic protein stabilization by the mild solubilizing agents nondetergent sulfobetaines. *Anal Biochem* 230, 290-294
- Wang J, Zhang H, Allen RD.** (1999) Overexpression of an Arabidopsis peroxisomal ascorbate peroxidase gene in tobacco increases protection against oxidative stress. *Plant Cell Physiol* 40, 725-32
- Waterham HR, Titorenko VI, Haima P, Cregg JM, Harder W, Veenhuis M** (1994) The *Hansenula polymorpha* *PER1* gene is essential for peroxisome biogenesis and encodes a peroxisomal matrix protein with both carboxy- and amino-terminal targeting signals. *J Cell Biol* 127, 737-749
- Wessel D, Fluegge UI** (1984) A method for the quantitative recovery of protein in dilute solution in the presence of detergents and lipids. *Anal Biochem* 138, 141-143
- Willekens H, Chamnongpol S, Davey M, Schraudner M, Langebartels C, van Montagu M, Inze D, van Camp W** (1997) Catalase is a sink for H<sub>2</sub>O<sub>2</sub> and is indispensable for stress defense in C<sub>3</sub> plants. *EMBO J* 16, 4806-4816
- Wimmer B, Lottspeich F, van der Klei I, Veenhuis M, Gietl C** (1997) The glyoxysomal and plastid molecular chaperones (70-kDa heat shock protein) of watermelon cotyledons are encoded by a single gene. *Proc Natl Acad Sci USA* 94, 13624-13629
- Winter H, Robinson DG, Heldt HW** (1994) Subcellular volumes and metabolite concentrations in spinach leaves. *Planta* 193, 530-535
- Wirtz W** (1983) Einige Aspekte zur Regulation der CO<sub>2</sub>-Fixierung während der photosynthetischen Induktion. PhD Dissertation, Göttingen University, Göttingen
- Wu CC, Yates R** (2003) The application of mass spectrometry to membrane proteomics. *Nat Biotechnol* 21, 262-267
- Xiao L, Koster KL** (2001) Desiccation tolerance of protoplasts isolated from pea embryos. *J Exp Bot* 52, 2105-2114
- Yamaguchi K, Mori H, Nishimura M** (1995) A novel isoenzyme of ascorbate peroxidase localized on glyoxysomal and leaf peroxisomal membranes in pumpkin. *Plant Cell Physiol* 36, 1157-1162

- Yang T, Poovaiah BW** (2002) Hydrogen peroxide homeostasis: activation of plant catalase by calcium/calmodulin. *Proc Natl Acad Sci USA* 99, 4097-4102
- Yang Y-P, Randall DD and Trelease RN** (1988) Phosphorylation of glyoxysomal malate synthase from castor oil seeds *Ricinus communis* L. *FEBS Lett* 234, 275-279
- Yates III JR** (1998) Database searching using mass-spectrometry data. *Electrophoresis* 19, 893-900
- Yates JR** (2000) Mass spectrometry from genomics to proteomics. *Trends Genet* 16, 5-8
- Yoshihara T, Hamamoto T, Munakata R, Tajiri R, Ohsumi M, Yokota S** (2001) Localization of cytosolic NADP-dependent isocitrate dehydrogenase in the peroxisomes of rat liver cells: biochemical and immunocytochemical studies. *J Histochem Cytochem* 49, 1123-1131
- Yoshimura K, Yabuta Y, Ishikawa T, Shigeoka S.** (2000) Expression of spinach ascorbate peroxidase isoenzymes in response to oxidative stresses. *Plant Physiol.* 123:223-34.
- Young JC, Barral JM, Hartl UF** (2003) More than folding: localized functions of cytosolic chaperones. *Trends Biochem Sci* 28, 541-547
- Yu C, Huang AHC** (1986) Conversion of serine to glycerate in intact spinach leaf peroxisomes: Role of malate dehydrogenase. *Arch Biochem Biophys* 245, 125-133
- Zelitch I** (1988) Synthesis of glycolate from pyruvate via isocitrate lyase by tobacco leaves in light. *Plant Physiol* 86, 463-468
- Zhong HH, McClung CR** (1996) The circadian clock gates expression of two *Arabidopsis* catalase genes to distinct and opposite circadian phases. *Mol Gen Genet* 251, 196-203
- Zhong HH, Young JC, Pease EA, Hangartner RP, McClung CR** (1994) Interactions between light and the circadian clock in the regulation of *CAT2* expression in *Arabidopsis*. *Plant Physiol* 104, 889-898
- Zolman BK, Monroe-Augustus M, Thompson B, Hawes JW, Krukenberg KA, Matsuda SPT, Bartel B** (2001) *chy1*, an *Arabidopsis* mutant with impaired beta-oxidation, is defective in a peroxisomal beta-hydroxyisobutyryl-CoA hydrolase. *J Biol Chem* 276, 31037-31046

## ACKNOWLEDGEMENT

I would like to express my sincere thanks to Prof. Dr. H. W. Heldt for giving me the opportunity to work in his department and for his most invaluable suggestions during the course of this study.

I am deeply indebted to my supervisor, Dr. Sigrun Reumann, for her encouragement, advice, mentoring, and research support throughout my doctoral studies. I also truly appreciate her patience and tolerance during my numerous mishaps.

I am extremely thankful to Prof. Dr. Ivo Feussner for his invaluable suggestions, encouragement and help and also for accepting to be on my doctoral committee as the co-referent.

I extend my sincere thanks to a long list of people who helped with the mass spectrometric analysis. I thank Dr. Virginie Wurtz, at the laboratory of Dr. Alain Van Dorselaer, Strasbourg, France who performed mass spectrometric analysis for spinach proteins reported in this study. The Arabidopsis samples were analyzed at the laboratory of Dr. Hartmut Kratzin, Max-Planck-Institut für Experimentelle Medizin, Goettingen, Germany. I thank him and his team for the same.

I am fortunate to have the opportunity to work with a group of energetic people in the lab. I have enjoyed every moment that we have worked together and I sincerely thank them. I shall remember Gabriele Ertl for her excellent help during the isolation of peroxisomes and also for the sheer joy of her company. Gabi and I have had the most stimulating discussions on several topics including 'A possible effect of the lunar cycle on leaf peroxisomes'. I thank Changle Ma, Caroline Meyer and Franziska Lueder for their help to finish this dissertation. I also thank the former members of the lab Alex Crauel, Clemens Rittstieg, Sven Teiwes and Monika Raabe. I also thank Jens Georg for his help with isolation of peroxisomes.

I sincerely appreciate the collective encouragement and support of every member at our department to finish this dissertation. I thank Dr. Anke Sirrenberg for always lending a listening ear to all my problems and for her whole-hearted support. I reserve my very special thanks to Dr. Katharina Pawlowski, for all her help, support and invaluable discussions. My brief stint at her office will remain in my memory for a very long time to come. I thank Dr. Gertrud Lohaus for her helpful suggestions and also for 'enlightening' me on the 'Tannenbaum'. I thank Dr. Ellen Hornung for her useful suggestions and also for her most generous and affectionate display of culinary skills. I also wish to express my thanks to Dr. Dieter Heineke, Dr. Martin Fulda and Dr. K. P. Heise. I would like to express my thanks to Andrea Nickel for her sunny disposition. I thank Gerd Mader for his technical wisdom, especially during my several disastrous encounters with computers. I take this

opportunity to sincerely thank all my former and present colleagues at the Albrecht von Haller Institute für Pflanzenbiochemie, for their kind help, support and cooperation whenever required. I want to especially thank Dr. Olga Voitsekhovskaja and Caroline Farke. My sincere thanks are due also to our gardeners Uwe Wedemeyer and Suzanne Mester.

I have been very fortunate to have friends who have given me comfort, help and advice whenever I needed them. I especially thank Preeti Gopikrishna, Madhumati Sevanna and Muthukumaran. I also wish to thank Dr. Venkatesh Balakrishnan for his help.

This dissertation is dedicated to my parents, Akhilandeswari and Babujee, who have given me all their love and unconditional support and let me freely do whatever I want. Along the way, my sister Vandana and brother-in-law Ganesh have shared their caring thoughts. Without them, there is no way I could possibly have accomplished this.

## Lebenslauf

### Lavanya Babujee

- 11-08-1974: geboren in Chennai (Madras), Indien  
Staatsangehörigkeit : indisch
- 1979-1989: Besuch der Mittelschule in Chennai
- 1989-1991: Besuch des Gymnasiums in Chennai; Schulabschluß: Abitur
- 1991-1994 : Studium an der Universität Madras, Chennai  
Bachelor of Science (Botany)
- 1994-1996 : Studium an der Universität Madras, Chennai  
Master of Science (Botany)
- 1996-1997 : Studium an der Universität Madras, Chennai  
Master of Philosophy (Botany) über  
"Assessment of the stability of rice blast fungus *Magnaporthe grisea*  
in Kerala rice fields by DNA fingerprinting and plant inoculations"
- 1997-2000 : Junior Research Fellow, Universität Madras, Chennai  
Project title : "Pyramiding of genes for rice blast resistance in rice"
- Seit ab Sep. 2000 : Doktorandin an der Abteilung für Biochemie der Pflanze des  
Albrecht-von-Haller-Instituts für Pflanzenwissenschaften der  
Universität zu Göttingen unter der Anleitung von Prof. Dr. H.-W.  
Heldt